mRNA LOCALISATION AND CELL POLARITY IN THE *DROSOPHILA* EMBRYO

Julian Richard Hughes

University College London

and

Developmental Genetics Laboratory, Cancer Research UK, London

Supervisor: Dr. David Ish-Horowicz FRS

A thesis submitted for the degree of Doctor of Philosophy

University of London

September 2004

ProQuest LLC
789 East Eisenhower Parkway
P.O. Box 1346
Ann Arbor, MI 48106-1346

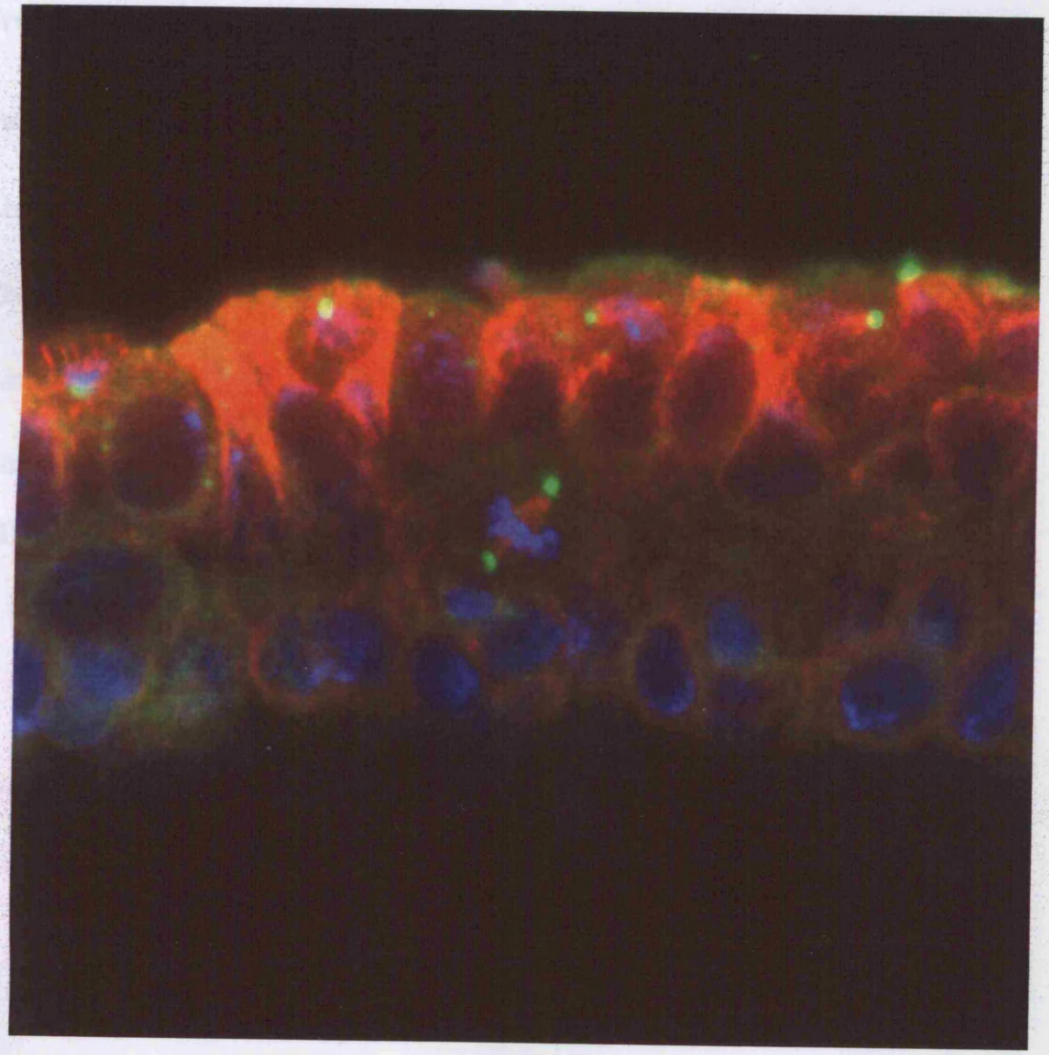

Table of contents

Abstract

Asymmetric localisation of mRNA transcripts to specific sites within the cytoplasm is a widely employed mechanism for targeting of proteins and generating cell polarity. The mechanism and function of mRNA localisation has been extensively studied in *Drosophila melanogaster*, where, for example, the Egalitarian/Bicaudal-D/dynein complex mediates transport of mRNA transcripts, towards microtubule minus-ends, during oogenesis and in syncytial blastoderm embryos. However, it is not known whether the Egalitarian/Bicaudal-D/dynein mRNA transport machinery is required to localise mRNAs in somatic cell types in the *Drosophila* embryo.

In this thesis, I show that the Egalitarian/Bicaudal-D/dynein complex is active in embryonic epithelial cells and neuroblasts and mediates asymmetric localisation of *inscuteable, wingless* and *crumbs*, but not *miranda,* mRNA transcripts, indicating that this is a general mechanism for mRNA localisation in *Drosophila.* I provide preliminary evidence that γ-Tubulin mediates asymmetric *miranda* localisation.

I have also explored the role of mRNA localisation in protein targeting in epithelial cells and neuroblasts, and find that asymmetric localisation of *inscuteable* and *wingless*, but not *crumbs,* mRNA transcripts is required to enhance the targeting of their protein products. I find that asymmetric localisation of *wingless* mRNA and protein is not required to support Wingless function in the embryo, although, Inscuteable activity is significantly reduced when *inscuteable* mRNA localisation is disrupted, and neuroblasts display defects in apico-basal polarity and metaphase spindle length. In conclusion, mRNA localisation acts to enhance protein targeting and activity in somatic cell types in the *Drosophila* embryo.

Preface

This thesis is my own work. The experiments described in this thesis were carried out in the Developmental Genetics Laboratory of the Imperial Cancer Research Fund, now known as Cancer Research UK, London Research Institute.

I cannot give enough thanks to Simon Bullock, who supervised me throughout my PhD. I will be forever grateful for his encouragement, patience and mentoring.

I thank David Ish-Horowicz for giving me the opportunity to work in his lab and for all his help and support when I needed it. I am also grateful for all the valuable discussion and assistance given to me by David and other members, past and present, of the Ish-Horowicz, Lewis and McNeill Labs. To Antonin Flament for his friendship and guidance, and Mark Wainwright for teaching me the finer points of fly culture. There are also many who have made my time at Cancer Research UK incredibly enjoyable and from whom I have learned a lot about science, life and myself: Alex, Nico, François, Barbara, Carolina, Aphrodite, Gavin, Neil, Joe, Liz, Sheena, Manolis, Hideta, Christine, Trevor, Chetana, Chris, Inbal, Rhian, Michael.

I thank those who have collaborated with me, provided me with reagents and given helpful advice: Jürgen Knoblich, Bill Chia, Murni Tio, Fumio Matsuzaki and Ulli Tepass.

I am eternally grateful for the support of all my family and friends, Mum, Dad, Sarah, Marc and my fiancée Julie.

Julian Hughes

List of Figures

page

List of Tables

page

CHAPTER 1: INTRODUCTION

The relationship between cell polarity and cell function is a fundamental question of developmental and cell biology. Most cells manifest polarity to some degree, with one side being different from the other. However, this is not always morphologically apparent, as cell polarity is often in the form of asymmetrically distributed sub-cellular components.

In metazoans, the development from a single cell to an adult organism requires the regulated division of cells, their differentiation into various cell types, and the organisation of these cells into tissues. Cell polarisation is required for accurate control of all these processes. The mechanisms that create cell asymmetries have been extensively studied in the fruit fly, *Drosophila melanogaster*. These molecular pathways are highly conserved throughout evolution, making *Drosophila* an excellent model system to understand how cell polarity is established (Wodarz, 2002).

In *Drosophila*, the asymmetric accumulation, or localisation, of maternal proteins and messenger ribonucleic acids (mRNAs) to specific regions within the oocyte is required for patterning of the embryonic body axes. As a result, much work has focussed on the mechanisms of mRNA localisation during *Drosophila* oogenesis. Localised mRNA transcripts have also been observed in the *Drosophila* embryo, although in many of these cases, the mechanisms underpinning and the developmental functions of mRNA localisation are poorly understood.

This thesis describes my studies into the mechanisms and function of mRNA transcript localisation in somatic cell types in the *Drosophila* embryo. Specifically, I

investigate the mRNA transport machinery that mediates mRNA localisation to the apical cytoplasm in embryonic neuroblasts and epithelial cells, and test the requirement for mRNA localisation in asymmetric protein targeting and activity in these cells.

In this introduction, I firstly describe mechanisms and functions of mRNA localisation in different organisms, focussing on the information obtained from studies during *Drosophila* oogenesis and early embryogenesis. Secondly, I detail the events and factors controlling apico-basal polarity and asymmetric cell division in *Drosophila* neuroblasts.

1.1 Mechanisms and function of mRNA localisation during development

1.1.1 mRNA localisation is a widespread occurrence

mRNA localisation is the accumulation of mRNA transcripts to specific regions of the cytoplasmic and is an evolutionarily conserved mechanism for creating cellular asymmetries and polarity. More than 90 examples of localised mRNAs have been described in organisms such as plants, yeast, insects, fish, ascidians and mammals (reviewed in (Bashirullah et al., 1998). Asymmetric mRNA localisation can be employed to rapidly target protein production to sites of activity and to restrict these proteins from regions where they may be detrimental to the cell. This is particularly useful in large cells, where polarised accumulation of mRNAs can quickly establish protein localisation to regions far from the sites of transcription. In addition, asymmetric enrichment of mRNAs can produce high concentrations of localised determinants that act to induce specific cell fates (reviewed in Jansen, 2001).

1.1.1.1 Saccharomyces cerevisiae.

There are several examples of localised mRNAs in the yeast, *S. cerevisiae*. For example, *ASH1* mRNA transcripts localise specifically to the daughter cell upon division, which is required for segregation of the Ash1p transcriptional repressor to that daughter cell (Long et al., 1997; Takizawa et al., 1997). Ash1p mediates mating type switching by controlling expression of daughter-specific genes (Bobola et al., 1996; Sil and Herskowitz, 1996). Other transcripts, including *Atm1p* mRNAs localise to mitochondrion-bound yeast polysomes (Corral-Debrinski et al., 2000), although the function of *Atm1p* mRNA localisation is unknown.

1.1.1.2 Vertebrates.

Many different mRNAs have been found to localise asymmetrically in vertebrate cells. In chicken embryonic fibroblasts, *β-actin* mRNA has been shown to localise to the leading edge of the lamellopodia (Lawrence and Singer, 1986). This is required for remodelling of the actin cytoskeleton at the leading edge, as disruption of *β-actin* mRNA localisation leads to inhibition of cell motility (Kislauskis et al., 1997; Shestakova et al., 2001). In fibroblasts, *metallothionein-1* transcripts are enriched in the perinuclear region, which facilitates efficient import of Metallothionein-1 protein into the nucleus (Levadoux et al., 1999).

Some transcripts are found to localise to intracellular organelles, including mRNAs encoding secreted, lysosomal and membrane proteins, which are targeted to the endoplasmic reticulum (ER) (Pfeiffer and Rothman, 1987). Similarly, transcripts encoding the Acetyl Choline Receptor are localised to neuromuscular junctions and *vimentin, vinculin* and *desmin* mRNAs are found at the structural elements called

costameres in cultured myofibrils (Fontaine and Changeux, 1989; Morris and Fulton, 1994). *c-myc* mRNA transcripts are found enriched at cytoskeletal-bound polysomes in fibroblasts (Hesketh et al., 1991).

mRNA localisation is also observed in several cell types of the nervous system in mammals. In oligodendrocytes, *Myelin Basic Protein* mRNA localises to the processes at the periphery of the cell at the sites of membrane compaction and myelinisation (Ainger et al., 1993). Several mRNAs are specifically localised in the mammalian nervous system, such as *tau* (Litman et al., 1993) and *TropomyosinV* (Hannan et al., 1995). However, the significance of this mRNA localisation is unknown.

In the zebrafish, *Brachydanio rerio*, mRNA localisation is involved in germline differentiation. *vasa* mRNA transcripts are localised to the cleavage furrow at the 2-4-cell stage and segregate specifically to the germ-line. From the 8-cell to the 1000-cell stage, *vasa* transcripts remain specifically in the presumptive primordial germ cells and are localised to the assembling germplasm. Subsequently, *vasa* transcripts are found in all primordial germ cells (Knaut et al., 2000; Yoon et al., 1997).

1.1.1.3 Xenopus laevis

The vertebrate species most studied with respect to mRNA localisation is *X. laevis*, where the first examples of mRNAs exhibiting an asymmetric distribution were described (Rebagliati et al., 1985). In the *Xenopus* oocyte, maternally deposited cytoplasmic mRNAs are asymmetrically localised in the early embryo, and encode determinants that specify the body axes. For example, *Vg1* mRNA transcripts localise to the vegetal pole. The proteins encoded by mRNAs localised in the

germplasm in the vegetal pole (*Xcat2* (the *Xenopus nanos* homologue) *Xlsirts*, *Xdazl*) are likely to play a role in determination of germ-cell fate. Other vegetally localised transcripts, including *Vg1* and XWnt11 (encoding extracellular signalling molecules), and *vegT* (encoding a transcription factor) regulate axis formation (reviewed in (Bashirullah et al., 1998).

1.1.2 mRNA localisation during *Drosophila* oogenesis

mRNA transcript localisation has been investigated most extensively in *D. melanogaster*. In particular, studies during oogenesis have provided much information on the mechanisms and function of mRNA localisation. Recent work has shown that some of these mechanisms are conserved between different tissues and function to localise mRNA transcripts in *Drosophila* embryos (Bullock and Ish-Horowicz, 2001). Here, I describe oogenesis in *Drosophila* and the information gained from studies on mRNA localisation during these stages of development.

1.1.2.1 The early egg chamber and the onset of oogenesis

(Reviewed in (Spradling, 1993). A *Drosophila* ovary consists of a cluster of about 16 ovarioles, which form chains of developing egg chambers progressing through 14 morphologically defined developmental stages in an anterior to posterior direction. At the anterior tip of the ovariole is the germarium. The germarium contains the oogonial stem cells, which divide asymmetrically to produce a stem cell and a committed cell, the cystoblast. Each cystoblast divides four times with incomplete cytokinesis to form 16 cystocyte cells, which are interconnected by cytoplasmic bridges that run through specialised actin-based structures called ring canals. One of the 16 cystocytes becomes the future oocyte. The oocyte is initially apparent very early in oogenesis, when the synaptonemal complex (a marker for meiosis) becomes asymmetrically localised to the oocyte. The remaining 15 cystocytes become nurse

cells, whose function is to synthesise and transport proteins and mRNAs that are required for the development of the oocyte. Many of these molecules will also be needed during early zygotic development.

1.1.2.2 Oogenesis stages 1-6: mRNA accumulation in the oocyte

During stages 1-6, the nurse cells and oocyte grow to 40 times their original size. Most of this increase in oocyte size is due to transfer of material from the nurse cells into the oocyte. Many mRNA transcripts are transported to and accumulate within the oocyte at these stages (Figure 1.1, 1.2A) including, *bicoid (bcd)* (Figure 1.1A; (St Johnston et al., 1989), *Bicaudal-D* (*BicD*) (Suter et al., 1989), *Bicaudal-C* (*BicC*) (Mahone et al., 1995), *egalitarian (egl)* (Mach and Lehmann, 1997), *gurken (grk)* (Figure 1.1D; (Neuman-Silberberg and Schupbach, 1993), *female sterile (1) K10* (*fs(1)K10;* referred to as *K10* in this thesis); (Cheung et al., 1992; Serano et al., 1994), *oo18 RNA-binding protein (orb)* (Lantz et al., 1992), and *oskar* (*osk*) (Figure 1.1B; (Ephrussi et al., 1991; Kim-Ha et al., 1991). At these stages, mRNAs appear throughout the oocyte cytoplasm, but with slightly higher concentrations present at the posterior cortex, the site of the microtubule organising centre (MTOC).

There is only one MTOC in the 16-cell egg chamber complex. It is localised in the oocyte, and microtubule arrays connect all 16 cells through the ring canals. Since the MTOC nucleates the minus-ends of microtubules, the microtubule-based cytoskeleton that connects the 16 cells is polarised. At this stage, the MTOC is at the posterior end of the oocyte (Figure 1.2A; reviewed in (Cooley and Theurkauf, 1994). This gives the first indication of the importance of a polarised microtubule network for mRNA transport and localisation during oogenesis (Figure 1.1, 1.2A).

Figure 1.1 Drosophila oogenesis and mRNA localisation in the oocyte.

Schematic representation of oocyte development and the four major mRNA localisation pathways during *Drosophila* oogenesis (adapted from (Lasko, 1999). **(A-D)** Localisation patterns of **(A)** *bcd* **(B)** *osk* **(C)** *nos, cyclin B* and **(D)** *grk* at various stages of oogenesis. The genes required for the localisation of these mRNAs, at different stages of oogenesis, are detailed above egg chambers. Additional information about these pathways and *trans*-acting factors can be found in the Introduction, Chapter 1 and Lasko, 1999. The anterior-posterior axis is indicated above **(A)**. Numbers below each egg chamber refer to the stage of oogenesis; G refers to the germarium (King, 1970). Different cell types within the egg chamber are labelled in **(A)**: oocyte (oo), nurse cells (nc) and follicle cells (fc).

Figure 1.1

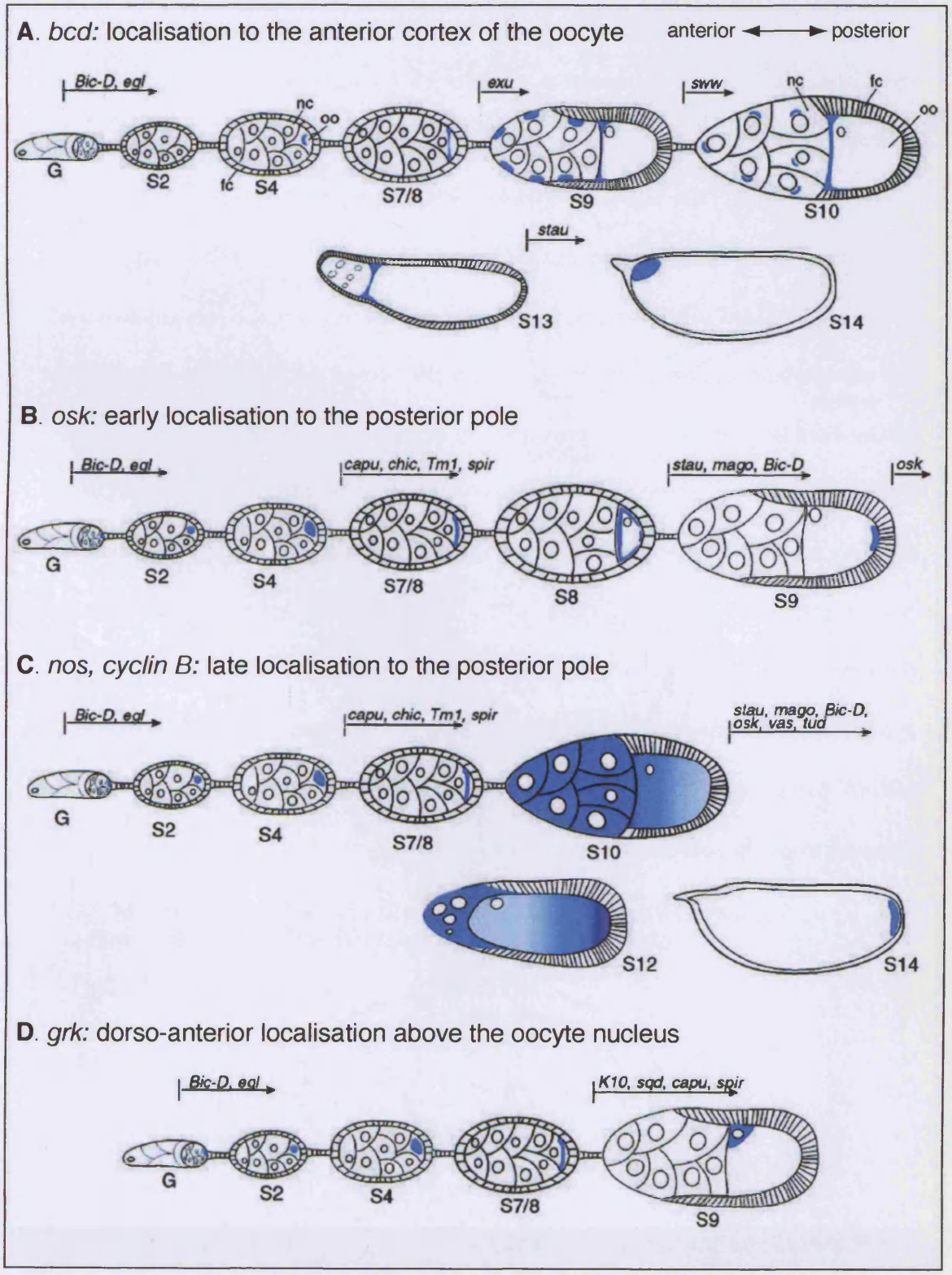

Adapted from Lasko, 1999

Figure 1.2 mRNA transport during *Drosophila* oogenesis: organisation of the microtubule cytoskeleton and nurse cell dumping.

(A) During early stages of oogenesis, microtubule minus-ends are concentrated at the posterior of the oocyte, while plus-ends extend toward the anterior and into the nurse cells. At this stage, the Egl/BicD/dynein mRNA transport machinery mediates the transport of many mRNAs, from the nurse cells, towards the microtubule minus-ends in the oocyte (also shown in Figure 1.1). **(B)** At mid-oogenesis, a reorganisation of the microtubule cytoskeleton occurs within the oocyte such that the microtubule minus-ends are anteriorly anchored and the plus-ends are located at the posterior. The oocyte nucleus migrates to the dorso-anterior corner of the oocyte, and several mRNAs localise to specific positions within the oocyte. *bcd* mRNA is shown in orange, *grk* mRNA in pink, and *osk* mRNA in green. **(C)** At late stages of oogenesis, the nurse cells transfer their contents into the oocyte (nurse cell dumping). Rapid cytoplasmic streaming (arrows) and localisation of some specific factors such as *nos* mRNA (blue) takes place. The anterior-posterior axis is indicated below **(C)**. Adapted from (Johnstone and Lasko, 2001).

Figure 1.2

A. Early Oogenesis: Egl/BicD/dynein-dependent transport of mRNAs, towards microtubule minus-ends, from the nurse cells to the developing oocyte.

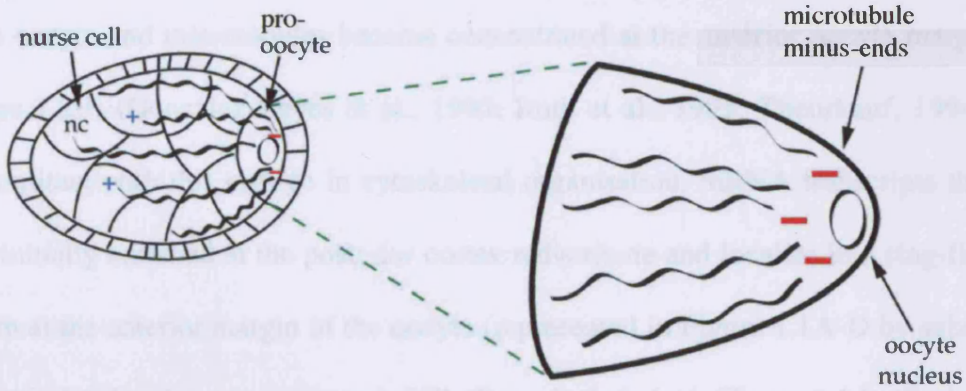

B. Mid-Oogenesis: Reorganisation of the microtubule cytoskeleton, concomitant with localisation of *bcd, osk* and *grk* mRNAs.

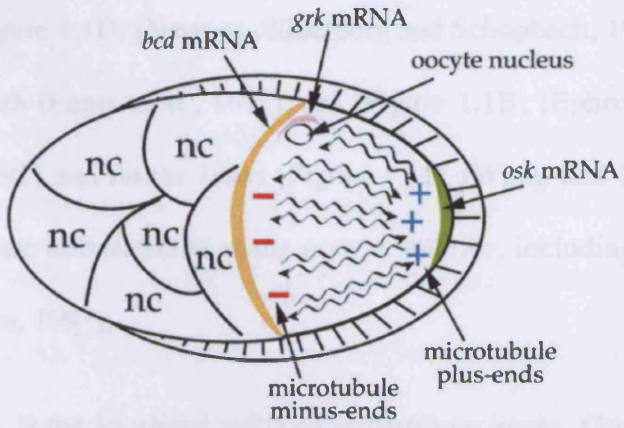

C. Late Oogenesis: Dumping of nurse cell contents into the oocyte and posterior localisation of several mRNAs, including *nos*.

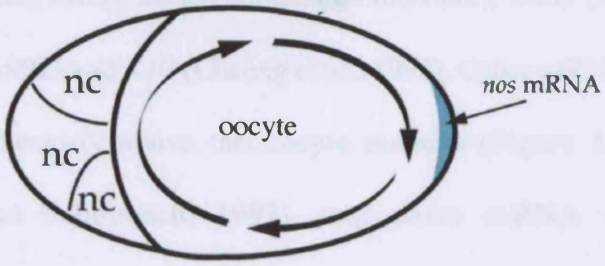

anterior ⟷ posterior

Adapted from Johnstone and Lasko, 2001

1.1.2.3 Oogenesis stages 7-9: asymmetric mRNA localisation in the oocyte

At stage 7, signalling between the follicle cells and the oocyte results in a reorganisation of the cytoskeleton, such that the MTOC disappears from the posterior of the oocyte and microtubules become concentrated at the anterior oocyte margin (Figure 1.2B; (Gonzalez-Reyes et al., 1995; Roth et al., 1995; Theurkauf, 1994). Concomitant with this change in cytoskeletal organisation, mRNA transcripts that were initially enriched at the posterior cortex redistribute and localise in a ring-like pattern at the anterior margin of the oocyte (represented in Figure 1.1A-D by subtle change in localisation pattern at stage 7/8). These include *bcd*, (Figure 1.1A; (Berleth et al., 1988), *BicD* (Suter et al., 1989), *BicC* (Mahone et al., 1995), *egl* (Mach and Lehmann, 1997), *grk* (Figure 1.1D; (Neuman-Silberberg and Schupbach, 1993), *K10* (Cheung et al., 1992), *orb* (Lantz et al., 1992), *osk* (Figure 1.1B; (Ephrussi et al., 1991; Kim-Ha et al., 1991) and *nanos (nos)* (Figure 1.1C; (Wang and Lehmann, 1991). Several proteins are also detected at the oocyte anterior, including Egl and BicD (Mach and Lehmann, 1997).

Between stages 8 and 9, some localised mRNAs redistribute again. One class of mRNAs relocalise in a general anterior cortical pattern. These include *bcd* (Figure 1.1A, 1.2B; (Berleth et al., 1988), *BicC* (Mahone et al., 1995), *BicD* (Suter et al., 1989), *orb* (Lantz et al., 1992) and *K10* (Cheung et al., 1992). Other mRNAs, such as *grk*, relocalise dorso-anteriorly above the oocyte nucleus (Figure 1.1D, 1.2B; (Neuman-Silberberg and Schupbach, 1993), and some mRNA transcripts progressively relocalise to the posterior cortex, for example, *osk* (Figure 1.1B, 1.2B; (Ephrussi et al., 1991; Kim-Ha et al., 1991).

1.1.2.4 Oogenesis stages 9-14

During stages 9-12, some localized transcripts such as *BicD* (Suter et al., 1989), *BicC* (Mahone et al., 1995), *orb* (Lantz et al., 1992), *egl* (Mach and Lehmann, 1997) and *nos* (Figure 1.1C; (Wang and Lehmann, 1991) become uniformly distributed throughout the oocyte cytoplasm. *nos* transcripts are synthesised in the nurse cells between stages 9-11 (Figure 1.1C), and after a period of bulk cytoplasmic transport into the oocyte ('nurse cell dumping'; Figure 1.2C), *nos* transcripts accumulate specifically at the posterior pole at the end of oogenesis (Figure 1.1C, 1.2C; (Wang and Lehmann, 1991). *osk* mRNAs also localise posteriorly (Figure 1.1B; (Ephrussi et al., 1991; Kim-Ha et al., 1991). The anterior localisation pattern of *bcd* transcripts is maintained (Figure 1.1A; (Berleth et al., 1988; St Johnston et al., 1989).

Patterning of the early embryo along the anterior-posterior (A-P) axis is initiated by the anterior localisation of *bcd* mRNA, and the posterior localisation of *nos* and *osk* mRNAs. After fertilisation, *bcd, nos* and *osk* mRNAs are translated at the sites of mRNA localisation. Bcd and Nos proteins then diffuse through the embryo, establishing gradients of Bcd and Nos transcription factor activity along the A-P axis. The highest concentrations of Bcd protein activity anteriorly result in the formation of head structures, whilst Nos activity at the posterior pole specifies abdominal structures. Similarly, Osk protein activity at the posterior of the embryo is required for formation of posterior structures, such as the abdominal region and the primordial germ cells (reviewed in St Johnston and Nusslein-Volhard, 1992; (Bashirullah et al., 1998; St Johnston and Nusslein-Volhard, 1992).

1.1.3 mRNA localisation in *Drosophila* embryos

1.1.3.1 Early zygotic development

Upon fertilisation, 13 rapid synchronous mitotic divisions (cycles) occur without cytokinesis, resulting in around 6000 nuclei sharing a common, maternally inherited cytoplasm (reviewed in (Foe et al., 1993; Sullivan and Theurkauf, 1995). By cycle 10, nuclei have migrated to the periphery of the embryo, but cell membranes between them have not completely formed (Figure 1.3A,B). This is termed the syncytial blastoderm embryo. From cycle 10 onwards, the cytoplasm progressively clears of yolk and the embryo can be divided into several distinct domains along the apico-basal axis (Figure 1.3C). The nuclei are arranged just beneath the plasma membrane and a thin layer of cytoplasm, the apical cytoplasm. The basal cytoplasm and a yolk mass are below the nuclei, within the embryo. Most microtubules are found in the apical cytoplasm, where their minus-ends are nucleated by apically located centrosomes. Most microtubule plus-ends are found in the basal cytoplasm or the yolk (Figure 1.3C; (Foe et al., 1993).

A 14^{th} cell cycle takes place and invaginations of the embryonic membrane surround each nuclei, cellularising the blastoderm and establishing an epithelium of columnar cells (Figure 1.3D; (Mazumdar and Mazumdar, 2002). This is termed the cellular blastoderm (3 h after egg lay at 25°C; embryonic stage 5 of (Campos-Ortega and Hartenstein, 1985). Shortly after cellularisation is complete, the layer of blastoderm cells then undergoes the complex morphogenetic movements of gastrulation, which gives rise to the formation of multiple cell layers and tissues (Figure 1.3E; 3.5h after egg lay at 25°C; embryonic stage 7 of (Campos-Ortega and Hartenstein, 1985).

Subsequent patterning of the *Drosophila* embryo involves the setting up of repeated elements, or metamers, along the A-P axis. A cascade of zygotically expressed genes, control the segmental pattern of the embryo (reviewed in (Akam, 1987; Pankratz and Jackle, 1993). The embryo is divided into 16 segments that are initially 4 epithelial cells wide, expanding to 8 epithelial cells after one round of mitotic division. This segmented embryo will give rise to a segmented larva after hatching (20 h after fertilisation at 25°C). The larva is visibly divided into 3 thoracic and 8 abdominal segments. Each of the 8 abdominal segments possesses a belt of cuticle protrusions, or denticles, on the ventral face of the larva. These larval denticle belts are a readout of the segmentation process and have been used as a visible marker in screens for genes controlling segmentation (Nusslein-Volhard and Wieschaus, 1980).

1.1.3.2 *Asymmetrically localising mRNAs in the* Drosophila *embryo*

The pair-rule genes initially establish a repeating, segmented pattern in the embryo. The pair-rule genes encode transcription factors that are expressed, by transcriptional control, in partially overlapping stripes along the A-P axis of the syncytial blastoderm embryo (Pankratz and Jackle, 1993). mRNA transcripts for almost all the pair-rule genes, including *hairy (h)*, *fushi-tarazu (ftz)* and *even-skipped (eve)*, accumulate specifically in the apical cytoplasm above the layer of peripheral nuclei (Hafen et al., 1984; Ingham et al., 1985; Macdonald et al., 1986). Recent studies have found that pair-rule mRNAs target their protein products apically, in close proximity to the nuclei. In turn, this augments nuclear pair-rule protein levels and modulates their activity, increasing the reliability of the embryonic segmentation process (Bullock et al., 2004).

Figure 1.3 Early stages of *Drosophila* embryogenesis.

(A-F) Early stages of zygotic development. Adapted from Lawrence, 1992. As indicated above embryos, syncytial stages are represented as number of cell cycles after fertilisation in **(A-C)** or as embryonic stages according to (Campos-Ortega and Hartenstein, 1985) in **(D-F)**. **(A)** Following fertilisation, nuclei undergo 14 rapid, synchronous cell cycles. During cycle 7, nuclei begin to migrate towards the cortex (arrows), indicating the initial polarisation of the embryo. **(B)** Syncytial blastoderm embryo: nuclei become arranged at the periphery, whilst some remain at the centre of the embryo. **(C)** The cytoplasm progressively clears of yolk and nuclei are asymmetrically organised within a shared cytoplasm. There is a thin apical layer of cytoplasm above the nuclei (apical cytoplasm) and a thicker basal layer below the nuclei (basal cytoplasm). As indicated in close up (adapted from (Costa and Schedl, 2001), the centrosomes and microtubule minus-ends are located in the apical cytoplasm, whereas plus-ends probe the basal cytoplasm and yolk. **(D)** Cellular blastoderm: membranes invaginate and grow down, eventually surrounding the nuclei. The blastoderm nuclei elongate during this process. Membranes grow into the basal cytoplasm and fuse, cellularising the blastoderm and forming a columnar epithelium (see close up). **(E)** Embryo begins to undergo gastrulation movements, leading to the formation of distinct tissue types, such as ectoderm as mesoderm. **(F)** Embryo during germ band extension at stage 8/9. At this stage of development, neuroblasts are singled out from the neuroepithelium (or neuroectoderm) and migrate basally by delaminating into the sub-ectodermal space between the neuroepithelium and the mesoderm.

Figure 1.3

A. Nuclear migration
cycle 7, ~128 nuclei

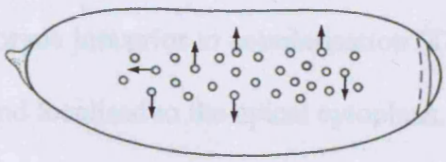

B. Syncytial blastoderm
cycle 10, ~1500 nuclei

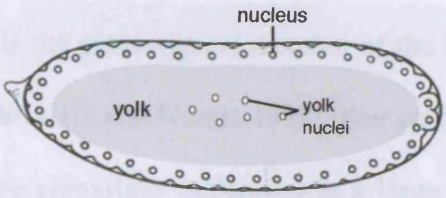

C. Syncytial blastoderm

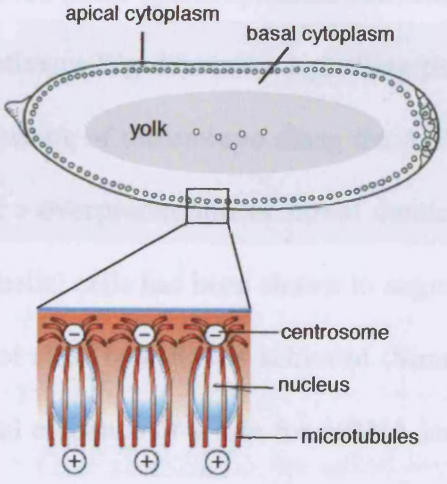

D. Cellular blastoderm - Stage 5

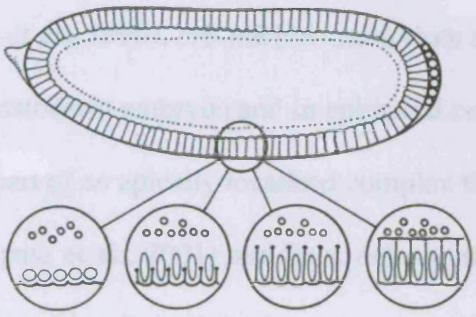

E. Gastrula - Stage 6-7

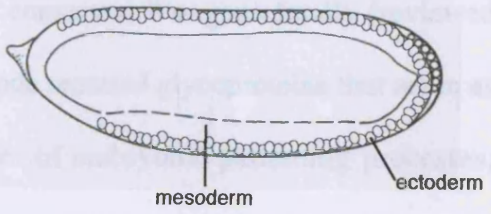

F. Stage 8-9
Onset of neuroblast delamination

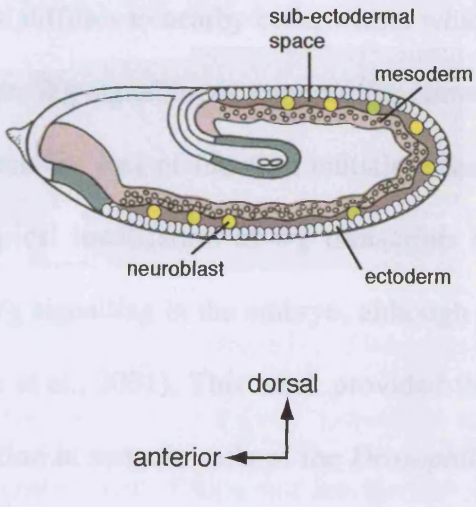

mRNA transcripts of other zygotically expressed genes are also found localised to the apical cytoplasm in blastoderm embryos and epithelial cells, including *crumbs (crb)* (Tepass et al., 1990) and *wingless (wg)* (Baker, 1987; Baker, 1988). *crb,* which encodes an apical transmembrane protein, is initially expressed in blastoderm embryos just prior to cellularisation (Tepass et al., 1990). *crb* mRNA transcripts are found localised to the apical cytoplasm in blastoderm embryos and in epithelial cells following cellularisation. Crb protein forms part of an apically localised complex that controls epithelial polarity (reviewed in (Tepass et al., 2001) and thus, *crb* mutants have disrupted epithelial organisation together with cell death in these tissues, which leads to the absence of larval cuticle (Tepass et al., 1990).

wg is the proto-typical member of the highly conserved *Wnt* gene family (reviewed in (Wodarz and Nusse, 1998). *Wnt* genes encode secreted glycoproteins that serve as major signalling molecules in a large number of embryonic patterning processes, including patterning of the *Drosophila* embryo. *wg* is expressed just prior to gastrulation, in one of the epithelial cells in each embryonic segment. Wg protein is secreted at the apical epithelial cell cortex and diffuses to nearby cells, within which it activates Wg-dependent signalling pathways. Wg signalling is required for correct patterning of the embryo along the A-P axis and *wg* loss-of-function mutations lead to the overproduction of larval denticle. Apical localisation of *wg* transcripts in epithelial cells has been shown to augment Wg signalling in the embryo, although it is not clear how this is achieved (Simmonds et al., 2001). This work provided the initial evidence of a role for mRNA localisation in somatic cells of the *Drosophila* embryo.

Asymmetric mRNA localisation also occurs in neuroblasts, the stem cell-like precursors of the *Drosophila* central nervous system (described in section 1.3). Neuroblasts undergo asymmetric divisions along the apico-basal axis to produce daughters with different fates. *inscuteable* (*insc*) is a key regulator of polarity in the neuroblast, and Insc protein and *insc* mRNA transcripts localise apically in these cells (Knirr et al., 1997; Li et al., 1997). *insc* transcripts also localise apically in epithelial cells of the procephalic neurogenic region (PNR; (Knoblich et al., 1999), also termed Mitotic Domain 9 (Foe, 1989), which are located in the head region of the embryo and give rise to the brain (Campos-Ortega, 1997). This thesis describes the mechanism and function of *insc* mRNA localisation in neuroblasts and PNR epithelial cells (Chapter 2, 3).

Asymmetric localisation of *bazooka (baz)*, *miranda (mira)* and *prospero (pros)* mRNA transcripts in neuroblasts has also been described, and are found localised to the apical cytoplasm (Broadus et al., 1998; Kuchinke et al., 1998; Li et al., 1997; Schuldt et al., 1998). *pros* transcripts are subsequently relocated to the basal side of the neuroblast during mitosis, which is required for sufficient Pros activity in the basal daughter cell upon cytokinesis (Broadus and Doe, 1997; Li et al., 1997; Schuldt et al., 1998; Shen et al., 1998). The mechanism and function of apical *pros, baz* and *mira* mRNA localisation has not been studied.

Asymmetric localisation is not observed for all mRNAs expressed in *Drosophila* embryos. For example, in cycle 14 blastoderm embryos, *gap* gene transcripts are uniformly distributed in the apical and basal cytoplasm (Davis and Ish-Horowicz, 1991; Hafen et al., 1984; Ingham et al., 1985; Pankratz et al., 1990). In neuroblasts, *par6* transcripts are also unlocalised (Petronczki and Knoblich, 2001). Therefore,

asymmetric localisation is specific to particular mRNA transcripts, suggesting that it has functional significance in these cases.

1.2 Mechanisms of mRNA localisation

How is localisation of mRNAs to specific sites within the cytoplasm achieved? Here I describe the three major mechanisms by which mRNAs are asymmetrically localised within cells. First, mRNA transcripts can be recognised by motor complexes that mediate transport along cytoskeletal filaments. Second, mRNAs at the correct regions of the cytoplasm are stabilised, whereas unlocalised transcripts are degraded throughout the rest of the cytoplasm. Third, mRNA transcripts become associated with anchorage complexes that retain mRNAs at the correct location within the cell (Figure 1.4).

1.2.1 Active, directed transport of mRNAs

Active, directed transport of mRNAs is by far the most extensively studied. This mechanism requires a functional cytoskeleton and the activity of motor proteins that move mRNAs along these cytoskeletal filaments (Figure 1.4A; (Jansen, 2001). This is a three-step process. The localising mRNA initially assembles with mRNA-binding proteins that recognise mRNA targeting signals within the transcript. The resulting ribonucleoprotein (RNP) complex then binds to motor proteins, and directed, transport occurs along the cytoskeleton. Finally, mRNAs are anchored by specific anchorage complexes, which prevent diffusion away from the site of localisation (Figure 1.4, section 1.2.3).

Figure 1.4 Mechanisms of mRNA localisation.

mRNA transcripts (red) are transcribed and then exit the nucleus (shown in left panel) along with specific hnRNP proteins. In the cytoplasm, additional *trans*-acting factors mediate asymmetric localisation of mRNAs to specific regions. This can occur via one of three mechanisms. **(A)** Active, directed transport along components of the cytoskeleton: mRNA transcripts are transported along microtubules (blue arrows) by dynein or kinesin based motor complexes (green); or Myosin motor complexes mediate transport of mRNAs along actin filaments, perhaps at the cell cortex (purple arrow). **(B)** mRNA transcripts may simply diffuse and become anchored at specific sites. Anchorage is also known to occur following active transport. **(C)** Selective degradation of mRNAs throughout the cytoplasm achieves asymmetric localisation at sites where the degradation machinery (yellow) is inactive or not present. (Right panel) mRNA localisation can be maintained by anchorage complexes or by continuous active transport by motors. Adapted from (Lipshitz and Smibert, 2000).

Figure 1.4

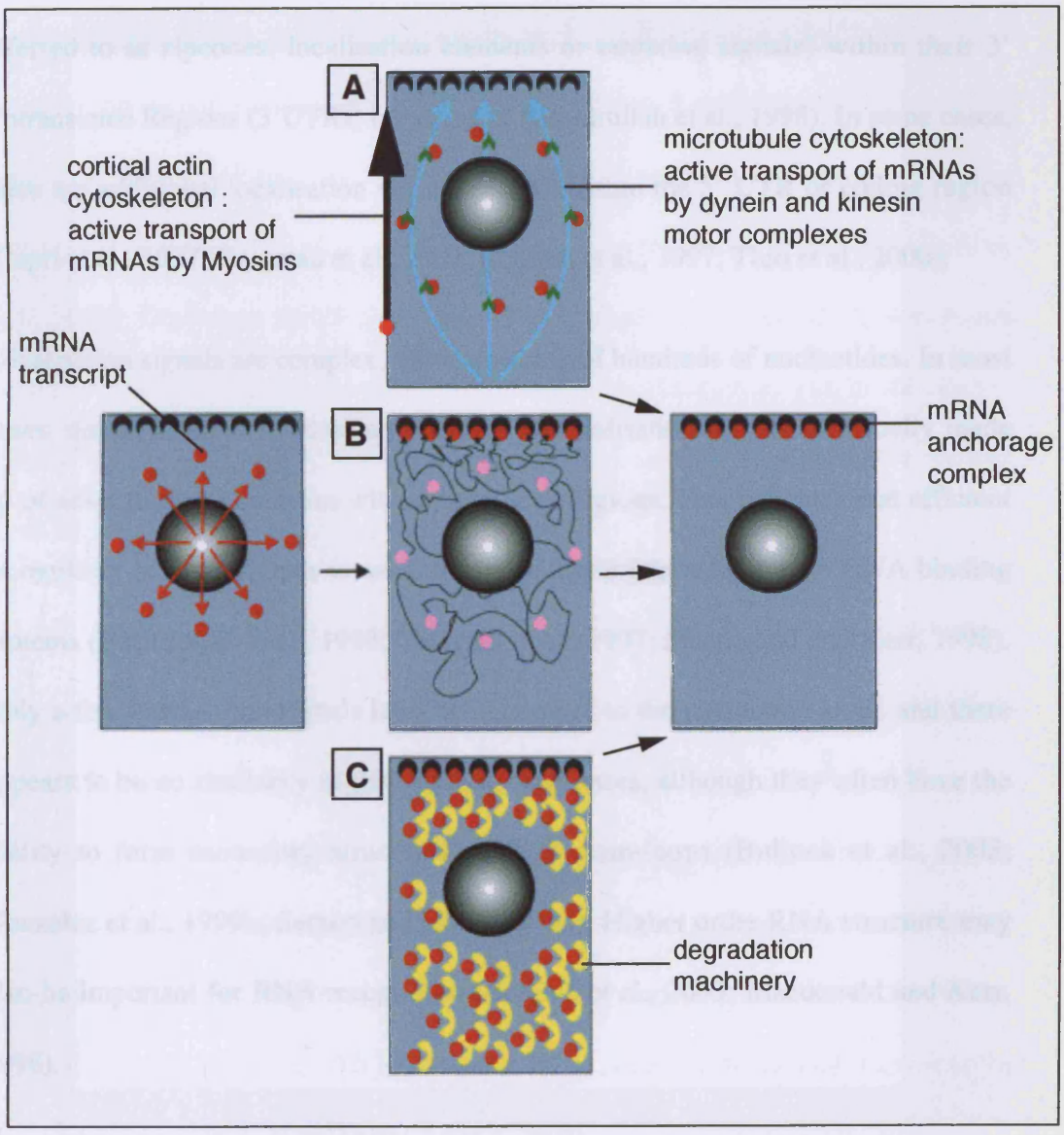

Adapted from Lipshitz and Smibert, 2000

1.2.1.1 cis-*acting mRNA localisation signals*

In general, localising mRNAs are characterised by the presence of specific signals within the transcript that allow them to be recognised by the correct transport complexes. All localising transcripts studied to date contain localisation signals (also referred to as zipcodes, localisation elements or targeting signals) within their 3' Untranslated Regions (3'UTRs; reviewed in (Bashirullah et al., 1998). In some cases, there are additional localisation signals present within the 5' UTR or coding region (Capri et al., 1997; Gautreau et al., 1997; Prakash et al., 1997; Thio et al., 2000).

Localisation signals are complex, often spanning of hundreds of nucleotides. In most cases, not all of these residues are required as localisation signals are usually made up of several short sequences within these large regions. This indicates that efficient recognition of these signals is mediated by multiple interactions with RNA binding proteins (Bashirullah et al., 1998; Gautreau et al., 1997; Macdonald and Kerr, 1998). Only a few localisation signals have been mapped to the nucleotide level, and there appears to be no similarity in their primary sequences, although they often have the ability to form secondary structures such as stem-loops (Bullock et al., 2003; Gonzalez et al., 1999b; Serano and Cohen, 1995). Higher order RNA structure may also be important for RNA recognition (Bullock et al., 2003; Macdonald and Kerr, 1998).

1.2.1.2 Nuclear factors

Specific RNA binding proteins direct the accumulation of localising transcripts to the correct cytoplasmic regions by interpreting the information contained within localisation signals. Data from studies in different systems has indicated that recognition of localising mRNAs first occurs in the nucleus by heterogeneous

nuclear RNPs (hnRNPs). Thus, a number of nuclear proteins have been implicated in active mRNA transport, indicating that nuclear history of a mRNA transcript is coupled to its cytoplasmic localisation (Gu et al., 2002; Lall et al., 1999; Norvell et al., 1999; Ross et al., 1997). For example, the *Xenopus* homologue of the zipcode binding protein (ZBP), called Vera (Deshler et al., 1998), can bind *Vg1* mRNA. ZBP binds to the localisation signal (zipcode) of localising *β-actin* transcripts in Chick embryo fibroblasts (Ross et al., 1997). ZBP contains nuclear localisation and export motifs, suggesting that its role in mRNA localisation begins in the nucleus (Deshler et al., 1998; Oleynikov and Singer, 2003). In *Drosophila*, the hnRNP A homologue Squid, is able to bind and mediate dorso-anterior localisation of *grk* in the oocyte (Norvell et al., 1999). *ASH1* mRNA localisation in *S. cerevisiae* requires the nuclear RNA binding protein, Loc1p (Long et al., 2001).

1.2.1.3 mRNA transport along microtubules I: dynein and kinesin motor complexes

After export of the hnRNP-mRNA complex from the nucleus, hnRNPs that are specific for mRNA localisation either stay associated with the mRNA, or they are replaced by cytoplasmic mRNA binding proteins. Adaptor molecules then act to link the RNA-RNP complex to specific motor proteins, before movement along cytoskeletal filaments (Figure 1.4A). Two classes of cytoskeletal networks have been implicated in the transport of RNA cargoes: actin microfilaments and microtubules (reviewed in (Lopez de Heredia and Jansen, 2004).

Microtubules are central to mRNA localisation in oligodendrocytes (Carson et al., 1998), neurons (Job and Eberwine, 2001), *Xenopus* and *Drosophila* oocytes and embryos (Tekotte and Davis, 2002). The role of microtubules in mRNA localisation has been studied in detail during *Drosophila* oogenesis, where stage-specific changes

in microtubule organisation correlates with transcript localisation (Figure 1.2; (Theurkauf, 1994). Here, microtubule-based transport depends on the activity of two types of motor proteins that mediate polar movement to opposite microtubule ends. Cytoplasmic dynein is minus-end directed, while Kinesin family members are mostly plus-end directed (reviewed in (Goldstein, 2001; Karki and Holzbaur, 1999).

Kinesin is a multisubunit complex. The Kinesin Heavy Chain (Khc) is the force generating subunit of Kinesin I (conventional kinesin). Kinesin I is a heterotetramer composed of two Khc subunits and two Kinesin light chains (Klc), which bind to cargo (Goldstein, 2001). In the oocyte, Khc is reported to be specific for transport towards the posterior pole, where it mediates the localisation of *osk* mRNA (Brendza et al., 2000). However, it is unknown whether kinesin I mediates transport of the *osk* transcript. It has been proposed that at the time of posterior *osk* accumulation, microtubule minus-ends are found at the entire oocyte cortex, except at the posterior. Thus, by association with kinesin, *osk* may be restricted from unwanted sites, ensuring accumulation at the posterior pole (Cha et al., 2002).

Cytoplasmic dynein has been implicated in transport of many intracellular cargoes, including chromosomes, mitotic spindles and vesicles (Karki and Holzbaur, 1999). Dynein is a multisubunit complex consisting of two heavy chains (Dhc), which form the motor heads, as well as multiple intermediate chains (Dic) and light chains (Dlc). All cellular functions of dynein depend on interaction with the dynactin complex, which includes $p150^{Glued}$, p50 Dynamitin (Dmn) and Lissencephaly-1 (Lis1). Lis1 is involved in linking dynein to its cargo and improving motor processivity (King, 2000; Smith et al., 2000; Tai et al., 2002). Dmn appears to negatively regulate the dynein motor in *Drosophila* (Januschke et al., 2002). In mammals, overexpression of

Dmn causes dynactin to dissociate from Dynein (Echeverri et al., 1996; Eckley et al., 1999), which has been shown to inhibit dynein mediated processes in tissue culture and *in vivo* in transgenic mice (Burkhardt et al., 1997; LaMonte et al., 2002).

In *Drosophila*, a function for cytoplasmic dynein in minus-end directed mRNA transport is well established. At mid-oogenesis microtubule minus-ends accumulate at the oocyte anterior, concomitant with localisation of *bcd* and other mRNAs to this region. Disruption of dynein function in mid-stage oocytes impairs *bcd* localisation. Anterior localisation of *bcd* also requires kinesin, which may represent the recycling of free cytoplasmic dynein to the plus-ends for recruitment of more mRNA cargo (Duncan and Warrior, 2002; Januschke et al., 2002).

Localisation of *bcd* requires a well characterised signal within the *bcd* 3'UTR (MacDonald, 1990; Macdonald and Struhl, 1988). A multiprotein complex that binds to the *bcd* 3'UTR has recently been purified (Arn et al., 2003), and contains three RNA binding proteins, the kinesin family member Nod and Swallow (Sww). The RNA binding protein, Exuperantia, is required for localisation but not maintenance of anterior *bcd* localisation (Figure 1.1; (St Johnston et al., 1989, Macdonald, 1991 #837). Sww is essential for *bcd* localisation during late stages of oogenesis (Figure 1.1; (St Johnston et al., 1989; Stephenson et al., 1988). Sww interacts with the light chains of cytoplasmic dynein, suggestive of dynein-dependent movement of *bcd* to the oocyte anterior (Schnorrer et al., 2000). Maintenance of *bcd* at late stages of oogenesis requires Staufen (Stau; Figure 1.1A; section 1.2.3.1).

The mammalian homologue of Stau (mStau) has recently been implicated in dendritic mRNA localisation in neurons as it is found within moving RNP particles

in dendrites. Transport of these RNP particles appears to be dependent on kinesin-like proteins (Kohrmann et al., 1999; Mallardo et al., 2003).

1.2.1.4 *mRNA transport along microtubules II: The Egl/BicD/dynein mRNA transport complex in* Drosophila

Null mutations for *egalitarian (egl)* and *Bicaudal-D (BicD)* lead to failure to specify an oocyte, causing all 16 cells of the cyst to become nurse cells (Mach and Lehmann, 1997; Ran et al., 1994; Suter and Steward, 1991; Theurkauf et al., 1993). Weak mutant alleles of both *egl* and *BicD*, which overcome the block in oogenesis, fail to localise mRNAs in the early oocyte between stages 1-6 (Figure 1.1, 1.2A). Mutations in dynein motor components also disrupt mRNA accumulation to the early oocyte and oocyte differentiation (McGrail and Hays, 1997).

Egl, BicD and dynein have recently been shown to be components of a motor complex that mediates transport of mRNAs from nurse cells to the early oocyte (Bullock and Ish-Horowicz, 2001), and pair-rule and *wg* mRNAs towards microtubule minus-ends during *Drosophila* embryogenesis (Bullock and Ish-Horowicz, 2001; Wilkie and Davis, 2001). mRNAs that are known to accumulate in the early oocyte at stages 1-6, such as *bcd*, *grk* and *K10*, are found to localise to the apical cytoplasm when injected into syncytial blastoderm embryos, indicating that Egl/BicD/dynein mRNA transport machinery is conserved between these developmental stages (Bullock and Ish-Horowicz, 2001). Furthermore, endogenous Egl and BicD proteins specifically associate with injected RNAs that contain mRNA localisation signals (Bullock and Ish-Horowicz, 2001), which in turn are able to modulate the kinetics and efficiency of Egl/BicD/dynein-mediated mRNA transport (Bullock et al., 2003).

The exact functions of Egl and BicD are unclear. They are possibly required to act as adaptors, linking the mRNA molecule to the motor complex or they may modulate the kinetics of the motor-RNP complex. BicD contains multiple heptad-repeat domains, which may mediate oligomerisation or interactions with other proteins (Suter et al., 1989; Wharton and Struhl, 1989). BicD is conserved in a variety of species from *Caenorhabditis elegans* to human, and mammalian BicD homologues have been implicated in dynein-dependent vesicle trafficking (Hoogenraad et al., 2001; Hoogenraad et al., 2003).

Egl contains a domain shared with 3'-5' exonucleases (RNase D domain; (Moser et al., 1997) suggesting that Egl is a nucleic acid-interacting protein. However, mutating 5 conserved catalytic residues in the RNase D domain, that are essential for exonuclease activity in other proteins (Bernad et al., 1989), does not block oogenesis (Navarro et al., 2004) or inhibit mRNA localisation in blastoderm embryos (Simon Bullock and Mark Wainwright, personal communication). This data suggests that exonuclease activity is not required for Egl function. However, the entire RNase D domain is required for Egl activity, as removal of this domain blocks oogenesis, indicating that Egl has additional roles during oogenesis that are independent of mRNA transport (Navarro et al., 2004).

Egl and BicD proteins can be co-immunoprecipitated from oocyte extracts and they co-localise at microtubule minus-ends in oocytes and blastoderm embryos. This indicates that there is a physical interaction between these two proteins, although it is not known if this link is direct (Bullock and Ish-Horowicz, 2001; Mach and Lehmann, 1997; Oh and Steward, 2001). Egl is able to interact directly with Dlc (Navarro et al., 2004), thereby providing a link between Egl-BicD and the dynein

motor complex. In *egl* and *BicD* mutants, the synaptonemal complex does not localise asymmetrically into the oocyte (Huynh and St Johnston, 2000; Mach and Lehmann, 1997). Neither the interaction between Egl and Dlc, nor microtubule-based transport in general are required for initial asymmetry, of the synaptonemal complex, between the oocyte and the nurse cells, suggesting that Egl may have additional activities that are independent of microtubules, such as mRNA translational control (Bolivar et al., 2001; Huynh and St Johnston, 2000; Navarro et al., 2004).

1.2.1.5 Actin filament-based transport: movement by myosins

Transport of mRNAs along actin filaments by Myosin motor proteins can occur along cytoplasmic actin or cortical actin (Figure 1.4A) and has been extensively studied in chick embryo fibroblasts and yeast. The localisation of *β-actin* mRNA to the leading edge of migrating chick embryo fibroblasts is myosin-II dependent (Latham et al., 2001) and is sensitive to the actin-depolymerising drug Cytochalasin-D (Sundell and Singer, 1991). Inhibiting the transport of ZBP-GFP containing particles with the myosin ATPase inhibitor BDM (2,3-butanedione-2-monoxime) provides further evidence for myosin-based transport of ZBP1/*β-actin* mRNA along actin filaments (Oleynikov and Singer, 2003).

In *S. cerevisiae*, a myosin-V, She1p (also called Myo4p) associates with localised mRNAs via two proteins, She2p (an RNA binding protein) and She3p (an adaptor that links the myosin motor to She2p). This She-protein complex is involved in the localisation of 22 mRNA transcripts, including *ASH1* (Shepard et al., 2003), although in this case it is not fully understood whether actin is involved in transport or anchorage of *ASH1* transcripts.

Actin filaments are required for Stau-dependent *pros* mRNA localisation to the basal cell cortex of *Drosophila* neuroblasts (Shen et al., 1998). Basal *pros* localisation requires the adaptor protein Miranda (described below) and the activity of the myosin motors, Zipper (Type II myosin; (Barros et al., 2003) and Jaguar (Type VI myosin; (Petritsch et al., 2003), which translocates *pros* transcripts basally along cortical actin.

1.2.2 Localised stabilisation of mRNA transcripts

A second mechanism for mRNA localisation is general degradation of the bulk unlocalised transcript, coupled with stabilisation of mRNA transcripts at the sites of localisation (Figure 1.4C). In the early *Drosophila* embryo, the maternally deposited pool of *heat-shock protein 83* (*hsp83*) mRNA is degraded throughout the cytoplasm, except at the posterior pole of the embryo (Ding et al., 1993), resulting in a concentrated pool of *hsp83* transcript in the posterior cytoplasm. Most notably, enrichment of *nos* mRNA at the posterior pole of the oocyte requires anchorage posteriorly, but also degradation of the unlocalised *nos* transcript throughout the rest of the cytoplasm (Figure 1.1C, 1.2C; (Bergsten and Gavis, 1999).

1.2.3 Anchorage of mRNA transcripts

1.2.3.1 Anchored mRNAs and known anchorage factors

Very little is known about how mRNAs are retained once they have been localised. mRNAs may be anchored by specific anchorage factors, localised with cytoskeleton-associated ribosomes, or maintained by constant motor-dependent transport. Anchorage can occur after active transport of mRNAs, but may also retain randomly diffusing mRNAs at specific sites (Figure 1.4B).

The cortical actin cytoskeleton appears to play a major role in mRNA anchoring. mRNA anchorage was first demonstrated in *Xenopus* oocytes, where transported *vg1* transcripts are subsequently anchored at the cortical actin cytoskeleton (Yisraeli et al., 1990). Anchorage of *β-actin* transcripts in chick embryo fibroblasts is also dependent on cortical actin (Sundell and Singer, 1991). Studies in *Drosophila* oocytes have shown that the actin-binding proteins, Moesin, Tropomyosin, Homer and Bifocal, are required for organisation of the cortical actin network that anchors *osk* mRNAs posteriorly (Babu et al., 2004; Erdelyi et al., 1995; Jankovics et al., 2002). Cytoplasmic diffusion and mRNA anchorage is sufficient for some steps of short-range localisation of injected *osk* mRNA (Glotzer et al., 1997). Interestingly, localised synthesis of Osk protein is also required to keep *osk* at the posterior pole (Rongo et al., 1995). The capture of the *ASH1* transcript at the bud tip also involves ASH1 translation (Gonzalez et al., 1999a).

Posterior *nos* localisation in the *Drosophila* oocyte is also achieved by local entrapment (Bergsten and Gavis, 1999; Gavis and Lehmann, 1992). However, only 10% of *nos* mRNA is enriched at the posterior cortex (Bergsten and Gavis, 1999). Localisation of *nos* occurs at late stages of oogenesis (Figure 1.1C, 1.2C), and results from a combination of mRNA diffusion and localised anchorage at the posterior. Live imaging of *nos* movement and localisation has provided further evidence that cortical actin is an essential component for mRNA localisation in *Drosophila* (Forrest and Gavis, 2003).

Stau, a ds-RNA-binding protein (St Johnston et al., 1992), is involved in transport and anchorage of mRNA transcripts (Broadus et al., 1998; Li et al., 1997; Matsuzaki et al., 1998; Schuldt et al., 1998; St Johnston et al., 1991). *stau* mutant mothers

produce embryos with defects in embryonic patterning (Schupbach and Wieschaus, 1986). *stau* mutant oocytes exhibit partially delocalised *bcd* mRNA (Berleth et al., 1988; St Johnston et al., 1989), and *osk* mRNA fails to relocate to the posterior after stage 9 (Ephrussi et al., 1991) (Figure 1.1). Anchorage of *bcd* mRNA at the anterior cortex of *Drosophila* oocytes is mediated by Stau (St Johnston et al., 1991) as well as specific mRNA anchorage signals within the *bcd 3'UTR* (Ferrandon et al., 1994). Recently, Sww and the γ-Tubulin Ring Complex (γ-TuRC), which is a microtubule-associated component of the centrosome (section 1.2.4.1), have also been implicated in anchorage of *bcd* anteriorly (Schnorrer et al., 2002).

1.2.4 Translational control

In *Drosophila*, regulation of translation represents an important aspect of mRNA localisation (reviewed in (Johnstone and Lasko, 2001). If mRNA transport is to control the sites of protein synthesis then the mRNA transcript must not be translated whilst in transit. In fact, ectopic or premature translation of localising *osk* mRNA results in developmental defects in the *Drosophila* embryo (Kim-Ha et al., 1995). Little is known about the mechanisms of translational control of localising mRNAs. Polyadenylation of localised mRNAs appears to be important in activating translation of mRNA transcripts, such as localised *bcd* mRNAs (Salles et al., 1994). Inhibition of translation is likely to involve proteins that bind to specific translational control sequences within localising transcripts. For example, translational repression of localising *osk* transcripts requires both signals within the 3'UTR, which are bound by a translational control factor called Bruno (Lasko, 1999). However, a detailed understanding of how translational repression and derepression is achieved is still lacking, especially outside of *Drosophila*.

1.2.4.1 Centrosomes and mRNA anchorage

Centrosomes of animal cells are the major microtubule nucleating centres and are responsible for anchorage of microtubule minus-ends (reviewed in (Moritz and Agard, 2001). They are composed of two centrioles, both located at the core of the centrosome. The centrioles are surrounded by a pericentriolar matrix (PCM), which is the main site for nucleation of cytoplasmic and spindle microtubules. Microtubule nucleation by the PCM requires the γ-TuRC, which is comprised of γ-Tubulin molecules together with several other factors. γ-TuRCs are mainly cytoplasmic and are also found located within the PCM throughout the cell cycle. Within the PCM, γ-TuRCs are concentrated at microtubule minus-ends (Wiese and Zheng, 2000).

Very little is known about the mechanism and function of mRNA localisation to centrosomes. The localisation of *cyclin B1* mRNA to spindles and centrosomes in *Xenopus* eggs (Groisman et al., 2000) was the first described example of mRNA localisation to centrosomes. This appears to be important in localised synthesis of Cyclin B1 at the mitotic spindle. The protein components involved in the localisation of mRNAs to centrosomes are largely unknown. To date, the γ-TuRC is the only centrosome-associated factor implicated in mRNA localisation (Schnorrer, 2000).

The involvement of centrosomes in mRNA sorting has also been described in the embryo of the mollusc, *Ilyanassa obsoleta*. Localising mRNAs associate with centrosomes during mitosis and are subsequently distributed asymmetrically between daughter cells. How intrinsic differences between the two centrosomes are recognised by localising mRNAs remains unclear. During cell division, localising mRNAs move from the centrosome to the cell cortex of one daughter cell, suggesting that the centrosomes act as an assembly site for delivery of mRNAs to the cell

cortex. Asymmetric inheritance of mRNAs after mitotic division is required to generate distinct cell types in the *I. obsoleta* embryo (Lambert and Nagy, 2002).

1.3 Asymmetric cell division and the *Drosophila* neuroblast

1.3.1 Introduction

An important question in cellular and developmental biology is how a cell divides to produce daughter cells with different fates. Diverse organisms, from bacteria to humans, have evolved means by which to create multiple cell types. One method of generating daughter cells with distinct identities is that two identical daughter cells encounter different environments. An alternative mechanism is asymmetric cell division. Asymmetric cell division is the unequal inheritance of cell determinants, or regulatory proteins, during mitosis that activate differential gene expression in each of the daughter cells. Cell polarisation is required for accurate control of this process.

The significance of asymmetric cell division for the development of a multicellular organism is widely recognised. Of particular importance is the asymmetric nature of stem cell division: Stem cells must generate daughter cells that are committed to differentiation, while others maintain their stem cell properties. It is becoming increasingly evident that asymmetric cell divisions are involved in the process of neurogenesis in a wide range of organisms from insects to vertebrates. Most of the insight into this process comes from studies in *Drosophila* and *C. elegans*, although the underlying principles are very similar between these and other organisms.

Asymmetric cell divisions are widely employed during *C. elegans* and *Drosophila* development (reviewed in (Doe and Bowerman, 2001; Knoblich, 2001). In *C.*

elegans, early development is a series of asymmetric cell divisions. For example, the one cell embryo divides along the A-P axis to produce a large anterior blastomere (AB) and a smaller posterior blastomere (P_1). The AB and P_1 cells end up generating different tissues in the developing embryo (Lyczak et al., 2002; Schneider and Bowerman, 2003; Sulston et al., 1983). In *Drosophila*, asymmetric cell divisions have been described in the developing muscle, gut, malphighian tubules and nervous system. In particular, much work has focussed on asymmetric divisions of neuroblasts in the central nervous system (CNS) and sensory organ precursors in the peripheral nervous system (Bardin et al., 2004; Jan and Jan, 2001). In this introduction, I will discuss the principles of asymmetric cell division gained from studies on the *Drosophila* neuroblast.

1.3.2 The *Drosophila* neuroblast

The *Drosophila* embryonic CNS consists of repeats of a basic building block, the hemineuromere, which is comprised of ~300 neurons. The majority of these neurons develop from precursor cells that have stem cell-like properties, called neuroblasts. There are ~30 neuroblasts in each hemineuromere (Bossing et al., 1996; Schmidt et al., 1997). Neuroblasts of the ventral neurogenic region, which give rise to the ventral nerve cord, are initially specified within the apico-basally polarised neuroectodermal epithelium (Figure 1.3F, 1.5A) by a cascade of regulatory events involving both cell intrinsic and cell extrinsic signals (reviewed in (Skeath, 1999).

Commencing soon after gastrulation, neuroblasts exit the neuroepithelium by delaminating basally towards the interior of the embryo (Figure 1.5B; 4 h after egg lay at 25°C; embryonic stage 7 of (Campos-Ortega and Hartenstein, 1985). They

come to rest within the subectodermal zone, between the neuroepithelium and the mesoderm (Figure 1.3F). Transiently, an apical stalk is left behind the delaminating neuroblast, in between the epithelial cells, which extends to the exterior of the embryo (Figure 1.5B). Not all neuroblasts delaminate at the same time; delamination occurs in a series of 3 waves over 3 hours (described in (Campos-Ortega, 1993).

Shortly after delamination, the neuroblasts undergo repeated rounds of asymmetric cell division, in a stem cell like fashion along the apico-basal axis, budding off a series of small ganglion mother cells (GMCs) from the basal cortex (Figure 1.5). During neuroblast division the mitotic spindle rotates by 90°. This ensures that the neuroblast divides apico-basally, perpendicular to the plane of the overlying neuroepithelium (Figure 1.5D, E; (Kaltschmidt et al., 2000).

Each GMC divides once and gives rise to two neurons or glial cells, whereas the apical neuroblast continues to divide asymmetrically (Campos-Ortega, 1993). The neuroblast progeny not only differ in size, but also in developmental fate, exhibiting distinct capacities for cell division and expression of regulatory genes. Interestingly, after each division the neuroblast also begins to express different transcription factor genes. This leads to different gene expression patterns in each GMC, producing of the full repertoire of neurons in each hemisegment (Pearson and Doe, 2003).

1.3.3 Mechanisms controlling polarised asymmetric cell division of neuroblasts

Asymmetric cell division can be categorised into three distinct steps. Firstly, before division, an axis of polarity is established and coordinated with the body axes. Second, the mitotic spindle must be correctly oriented along this axis of polarity.

Third, cell fate determinants are distributed asymmetrically in response to the axis of polarity, ensuring segregation into specific daughter cells upon cytokinesis. Thus, different concentrations of these determinants in the two daughter cells leads to the establishment of distinct cell fates. Below, I describe the mechanisms involved in asymmetric cell division in *Drosophila* neuroblasts.

1.3.3.1 Establishment of apico-basal polarity in neuroblasts

The initial apico-basal polarity of neuroblasts is inherited in part from the epithelial cells that generate them (Schober et al., 1999; Wodarz et al., 1999). Epithelial cells are polarised along the apico-basal axis, which is initially apparent by the formation of zonula adherens (ZA). The ZA is a belt like adherens junction, at the apex of the cell, which connects epithelial cells to their neighbours (Figure 1.5A). In epithelial cells, several proteins are localised apically of the ZA, in the sub-apical region. These include the multi-PDZ domain protein, Bazooka (Baz; Par3 in *C. elegans*), the single-PDZ domain containing protein DmPar6 (referred to as Par6), and an atypical protein kinase C. This is referred to as the aPKC Par/aPKC complex (Figure 1.5A). The Par/aPKC complex acts with Crb and Stardust (Sdt) at the sub-apical region, to control apico-basal polarity in epithelial cells (Bachmann et al., 2001; Bilder et al., 2003; Hong et al., 2001; Johnson and Wodarz, 2003; Rolls et al., 2003; Sotillos et al., 2004; Tanentzapf and Tepass, 2003; Tepass et al., 2001).

Figure 1.5 Asymmetric cell division in *Drosophila* neuroblasts.

A time course of delamination and division of a *Drosophila* neuroblast (adapted from (Wodarz and Huttner, 2003). The subcellular localisation of polarity regulators, cell fate determinants and their adaptor proteins is indicated in different colours (see legend). **(A)** Neuroblasts are singled out from an apico-basally polarised epithelial cell layer, the neuroepithelium. The Par/aPKC complex direct apico-basal polarity in epithelial cells, which is evident by apical location of zonula adherens that link these cells together and maintain their polarity. **(B)** The selected neuroblast migrates basally, towards the interior of the embryo. The Par/aPKC complex, along with Insc, Pins and Gαi, is localised to the delamination stalk that extends to the exterior of the embryo. **(C)** The apical localisation of these factors is maintained into interphase, leading to the formation of the apical complex, which directs apico-basal polarity of the neuroblast. At interphase, the Mira complex (red) is also apically localised. **(D, E)** At the onset of mitosis, the mitotic spindle rotates and becomes oriented along the apico-basal axis. Cell fate determinants and their adaptors are relocalised to the basal cortex, underneath the basal spindle pole. **(F)** At anaphase, the centrosomes are different sizes, which leads to the formation of an asymmetric mitotic spindle with large apical, and smaller basal, astral microtubules. Consequently, the cleavage plane is asymmetrically positioned. The localisation of apical complex components is lost at anaphase/telophase. **(G)** This leads to the formation of a larger apical neuroblast and a smaller GMC. Mira and Numb complexes are segregated into the GMC. Mira is degraded, releasing Pros to control gene expression specifically in the GMC nucleus.

Figure 1.5

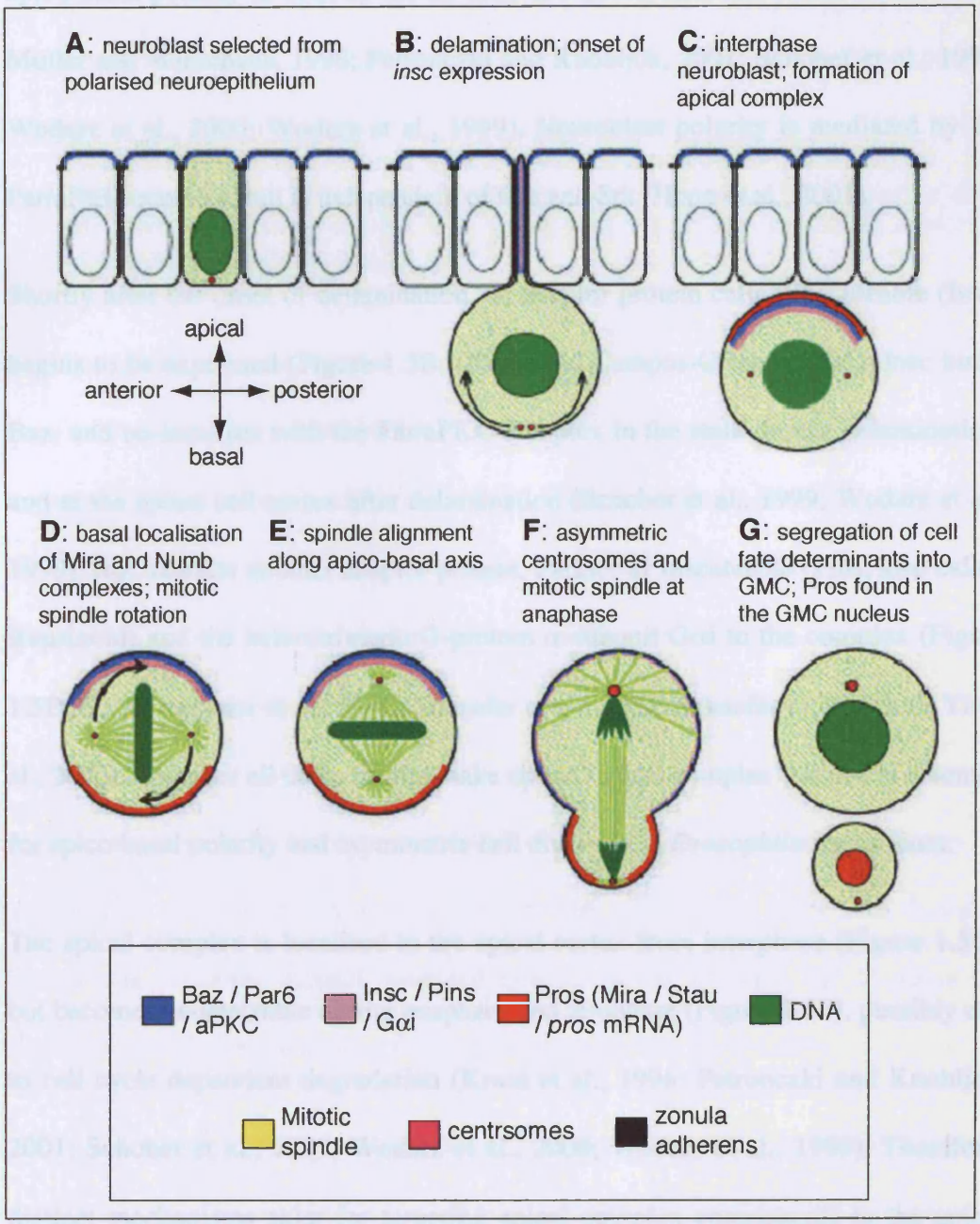

Adapted from Wodarz and Huttner, 2003

Upon delamination, ZA connections are broken and the neuroblast adopts a spherical shape. A newly delaminated neuroblast maintains the apical enrichment of the Par/aPKC complex proteins (Figure 1.5B) Thus, mutations in these genes disrupts apico-basal polarity in both epithelial cells and neuroblasts (Kuchinke et al., 1998; Muller and Wieschaus, 1996; Petronczki and Knoblich, 2001; Schober et al., 1999; Wodarz et al., 2000; Wodarz et al., 1999). Neuroblast polarity is mediated by the Par/aPKC complex, but is independent of Crb and Sdt (Hong et al., 2001).

Shortly after the onset of delamination, an adaptor protein called Inscuteable (Insc) begins to be expressed (Figure 1.5B; (Kraut and Campos-Ortega, 1996). Insc binds Baz, and co-localises with the Par/aPKC complex in the stalk during delamination, and at the apical cell cortex after delamination (Schober et al., 1999; Wodarz et al., 1999). Insc recruits another adaptor protein, Partner of Inscuteable (Pins, also called Rapsinoid) and the heterotrimeric G-protein α-subunit Gαi to the complex (Figure 1.5B, C; (Parmentier et al., 2000; Schaefer et al., 2001; Schaefer et al., 2000; Yu et al., 2000). Together all these factors make up the 'apical complex', which is essential for apico-basal polarity and asymmetric cell divisions in *Drosophila* neuroblasts.

The apical complex is localised to the apical cortex from interphase (Figure 1.5C), but becomes undetectable during anaphase and telophase (Figure 1.5F), possibly due to cell cycle dependent degradation (Kraut et al., 1996; Petronczki and Knoblich, 2001; Schober et al., 1999; Wodarz et al., 2000; Wodarz et al., 1999). Therefore, distinct mechanisms exist for targeting apical complex components to the apical cortex during interphase: an epithelial cell-linked mechanism in newly delaminated neuroblasts and an additional mechanism that follows each cell division.

The epithelial cell linked mechanism involves the tumour suppressor genes *discs-large (dlg), lethal giant larvae (lgl)* and *scribble (scrib)* which are required for targeting of Par/aPKC complex proteins in epithelial cells (section 1.3.2.3; (Bilder et al., 2000). However, it is unclear how apical complex proteins are correctly localised after mitosis in neuroblasts. Studies on cultured neuroblasts *in vitro* indicate that this requires actin microfilaments and microtubules (Broadus and Doe, 1997). Other factors that participate in the specification or 'memory' of the apical cortex after each cell cycle remain to be elucidated.

All the apical complex members are interdependent for apical localisation in the neuroblast. Loss of one member leads to the delocalisation of all other members to varying degrees (Cai et al., 2003; Rolls et al., 2003; Schaefer et al., 2001; Schaefer et al., 2000; Schober et al., 1999; Wodarz et al., 1999; Yu et al., 2000). The mitotic kinase Cdc2, is also required for maintenance of the apical complex, indicating a link between cell polarity and cell cycle regulation (Tio et al., 2001). This interdependence for apical localisation may reflect the transition from contact mediated polarity by ZA in epithelial cells to cell autonomous polarity in neuroblasts, in which these contacts are lost. Consistent with this, isolated neuroblasts in culture exhibit polarised distributions of proteins and maintain the ability to undergo asymmetric cell divisions (Broadus and Doe, 1997).

All apical complex single mutants have the same phenotype: randomised spindle orientation and failure to segregate cell fate determinants into the GMC reliably (see sections 1.3.2.2/3). This suggests that apical localisation of these proteins is essential for their function. Indeed, apical localisation of Insc, which is mediated by ankyrin-

like repeat domains, is a prerequisite for all aspects of Insc function (Knoblich et al., 1999; Tio et al., 1999).

Heterotrimeric G-proteins, which consist of α-, β- and γ-subunits, are also found to be components of the apical complex. How G-protein signalling can direct apico-basal polarity in the neuroblast is unclear, as the downstream effectors in neuroblasts are unknown. 'Classical' heterotrimeric G-protein signalling cascades are activated by ligand binding to a G-protein coupled seven-transmembrane receptor followed by GDP exchange for GTP on the α-subunit, resulting in dissociation of the G-protein trimer into free α- and βγ-subunits (Hamm, 1998). In many cell types, GTP-bound Gαi releases the βγ-dimer and binds to Adenylyl cyclase at the cell membrane, leading to the production of cyclic AMP. The free βγ dimer activates Phospholipase C, which cleaves PIP_2 to generate the second messengers diacylglycerol and inositol (1,4,5) trisphosphate.

The role for G-protein signalling in asymmetric neuroblast divisions appears to be independent of extracellular signals. For example, neuroblasts can undergo asymmetric division as single cells in culture (Broadus and Doe, 1997). Instead, proteins containing GoLoco domains appear to activate G-proteins (Siderovski et al., 1999). GoLoco domains can bind Gα-subunits and trigger the release of the βγ-dimer, without the need for receptor activation by ligand or GDP/GTP exchange (Kimple et al., 2002). Pins, which contains 3 GoLoco domains, activates Gαi causing the release of the βγ dimer during neuroblast division (Schaefer et al., 2000; Yu et al., 2003; Yu et al., 2000). However, only the βγ dimer appears to activate downstream effectors in neuroblasts (Schaefer et al., 2001).

1.3.3.2 Mitotic spindle positioning and orientation

In *Drosophila* neuroblast division, the mitotic spindle generates asymmetry in two ways. Firstly, correct orientation ensures asymmetric inheritance of cell fate determinants upon cytokinesis. Secondly, asymmetric positioning of the spindle can create daughter cells of different sizes. In the *Drosophila* neuroblast, the apical and basal halves of the mitotic spindle itself are asymmetric (Figure, 1.5F; (Kaltschmidt et al., 2000), leading to the production of a smaller GMC and a larger neuroblast.

In mutants for the apical complex genes, mitotic spindles are randomised and are no longer strictly oriented along the apico-basal axis (Kaltschmidt et al., 2000; Kraut et al., 1996; Kuchinke et al., 1998; Petronczki and Knoblich, 2001; Schober et al., 1999; Wodarz et al., 2000; Wodarz et al., 1999; Yu et al., 2000). Signalling by heterotrimeric G-proteins also plays an important role in spindle orientation. In neuroblasts mutant for the β-subunit Gβ13F, mitotic spindles are not correctly oriented (Schaefer et al., 2001) and similar defects are observed in Gαi and Gγ1 mutant neuroblasts (Izumi et al., 2004; Yu et al., 2003).

How apical complex components act on the mitotic spindle is unclear. Mammalian Par3 can bind the kinesin motor (Nishimura et al., 2004), so Baz may be able to interact with microtubule plus-ends. The human Pins homologue LGN, binds to NuMA, which in turn interacts with dynein (Merdes et al., 1996). Therefore, by their interaction apically with Pins in neuroblasts, heterotrimeric G-protein signalling may regulate spindles through this microtubule-based motor complex. Alternatively, G-proteins may interact with the spindle directly as Gαi has been shown to bind microtubules and alter their polymerisation behaviour (Roychowdhury et al., 1999; Wang et al., 1990).

Insc is the only member of the apical complex that is both necessary and sufficient to orient mitotic spindles along the apico-basal axis. In epithelial cells, ectopically expressed Insc is found to localise apically and directs a 90° spindle reorientation so that epithelial cells begin to divide perpendicular to the plane of the epithelium (Kraut et al., 1996). Epithelial cells normally divide symmetrically along the planar axis, which is controlled by the ZA (Lu et al., 2001). Insc is also expressed in epithelial cells of the PNR, which gives rise to the brain. PNR epithelial cells produce neuroblasts by division along the apico-basal axis, rather than by delamination (Kraut et al., 1996). Together, these results suggest that Insc acts as a switch that mediates apico-basal orientation of mitotic spindles.

The mechanisms by which Insc induces spindle reorientation remain to be elucidated. Insc is localised to the apical cell cortex where it may interact with astral microtubules from the apical spindle pole, inducing rotation of the spindle. Indeed, this would explain why neuroblast spindle orientation is randomised in *insc* mutants, and other mutants for apical complex (see previous paragraph). However, no direct interaction between microtubules and Insc has been demonstrated, and there are no known binding partners for Insc that may provide a link to astral microtubules at the onset of mitosis.

Asymmetry of the mitotic spindle in neuroblasts is important in controlling production of different sized daughter cells. This is achieved by the formation of an asymmetric spindle (Figure 1.5F; (Fuse et al., 2003; Kaltschmidt et al., 2000), which positions the cleavage plane closer to the basal cortex and results in the formation of a smaller basal GMC and a larger neuroblast upon cytokinesis (Figure 1.5G). The spindle poles also differ in size in anaphase/telophase neuroblasts with the apical

centrosome being larger than the basal one (Figure 1.5F; (Kaltschmidt et al., 2000). The apical spindle pole therefore appears to have greater microtubule nucleating activity, as apical astral microtubules are always longer than those at the basal pole (Albertson and Doe, 2003; Fuse et al., 2003). However, astral microtubules appear to be dispensable for spindle asymmetry as unequal neuroblast divisions still occur in *asterless* mutants, in which mitotic spindles lack asters (Giansanti et al., 2001). Insc may also control anchoring of the mitotic spindle at late stages of mitosis, by directing apical localisation of the microtubule binding protein, Cornetto, at anaphase/telophase (Bulgheresi et al., 2001).

Recent studies indicate that two redundant activities of the apical complex control spindle positioning and asymmetry in neuroblasts: One mediated by Pins/Gαi, and the other by the Par/aPKC complex together with Insc (Cai et al., 2003). Thus, symmetric divisions are observed in the majority of neuroblasts where the function of both Baz and Pins is perturbed. Furthermore, symmetric divisions are also observed in Gβ13F mutants, in which the apical localisation of both Pins/Gαi and Par/aPKC/Insc complexes is disrupted (Fuse et al., 2003). It has been proposed that production of unequally sized neuroblasts and GMCs may serve to maintain the stem-cell properties of neuroblasts by minimising the reduction in cell volume (Fuse et al., 2003).

1.3.3.3 Basal localisation of cell fate determinants

Asymmetric cell division is employed to produce daughter cells with distinct fates. This is accomplished by the unequal segregation of cell fate determining proteins and mRNA transcripts into one of the two daughter cells, which in turn leads to differential regulation of daughter cell specific gene expression. In neuroblasts, the

apical complex controls the localisation of determinants and their respective adaptors, which form crescents at the basal cell cortex underlying the basal spindle pole. This is termed "coupling" of basal crescents and basal spindle pole (Kraut et al., 1996), and ensures correct segregation of these determinants into the GMC upon cytokinesis (Figure 1.5).

There are two complexes that are basally localised during mitosis: the 'Miranda complex' and the 'Numb complex' (Figure 1.5D-F; reviewed in (Knoblich, 2001). The 'Miranda complex' contains Miranda (Mira), a cortically associated coiled-coil domain protein, which binds and is required for cortical association of other Mira complex components. These include Prospero (Pros; a homeodomain-containing transcription factor), Stau and *pros* mRNA (which binds Stau via its 3'UTR). This complex is localised apically during interphase and starts to relocate to the basal cortex at prophase. The 'Numb complex' contains Numb and its cortical anchoring protein, Partner of Numb (Pon), which are cytoplasmic at interphase, but become recruited to the basal cortex during mitosis.

In mutants for apical complex components, Mira and Numb complexes either form randomly positioned crescents that do not underlie the basal spindle pole (termed 'uncoupling') or they are uniformly cortical (Kraut et al., 1996). Therefore, the apical complex must specify the apical cortex, thereby providing the spatial cue for localisation of basally localised determinants. The mechanism by which this is controlled is unclear? It is unlikely that apical and basal protein domains are formed by mutual exclusion, as a clear gap exists between the detectable limits of apically and basally localised proteins. The apical complex may control the organisation of the cortical cytoskeleton. Indeed, the actin cytoskeleton is essential for basal

localisation of determinant and their adaptors, but microtubules are dispensable (Broadus and Doe, 1997; Knoblich et al., 1997; Lu et al., 1999). Consistent with this, basal Mira localisation required the unconventional myosin VI motor Jaguar (Jag) and the non-muscle myosin II motor Zipper (Zip) (Barros et al., 2003; Petritsch et al., 2003). Jag actively transports the Mira complex along cortical actin to the basal cortex, whereas Zip appears to 'push' Mira towards the basal cortex.

In addition to the requirement for the apical complex, the tumour suppressor genes *dlg, lgl* and *scrib* also control basal localisation of cell fate determinants without affecting the localisation of apical complex components (Albertson and Doe, 2003; Betschinger et al., 2003; Ohshiro et al., 2000; Peng et al., 2000). These tumour suppressor proteins are localised to the entire neuroblast cortex and may provide a link between apical complex activity and basal cortical localisation. *dlg, lgl* and *scrib* mutants also show symmetric divisions, possibly as a consequence of disrupting the specification and relative sizes of the apical and basal cortical domains (Albertson and Doe, 2003).

To date, *lgl* is the most studied of these three genes with respect to neuroblast division. Lgl protein is initially found at the entire neuroblast cell cortex. However, Lgl binds apical Par6 and is phosphorylated by aPKC, which inhibits cortical localisation of Lgl (Betschinger et al., 2003). Therefore, unphosphorylated, active Lgl localised to the basal cortex may permit specific association of cell determinants basally. Lgl is also able to bind and repress the activity of Zip, perhaps allowing active Zip to associate with the Mira complex apically, prior to basal translocation (Albertson and Doe, 2003; Barros et al., 2003; Ohshiro et al., 2000; Peng et al., 2000; Strand et al., 1995).

As described, many factors are required to control basal localisation of cell fate determinants during mitosis. A surprising phenomenon occurs at anaphase/telophase, whereby basal determinant localisation is restored, leading to correct segregation into the GMC at cytokinesis. This has been termed 'telophase rescue' (Peng et al., 2000) and reveals the existence of an additional mechanism that acts late in mitosis to control basal localisation of cell fate determinants. Mutants for a deletion that uncovers the *snail*, *worniu* and *escargot* genes, which encode snail family transcription factors, exhibit defects in basal localisation that are not rescued at telophase (Ashraf and Ip, 2001; Cai et al., 2001). These three transcription factors act redundantly and are required for *insc* expression in neuroblasts. However, as *insc* mutants also exhibit 'telophase rescue' (Schober et al., 1999) there must be additional targets of the snail family transcription factors that are required this late localisation mechanism.

Upon cytokinesis, the Mira and Numb complexes are segregated into the GMC (Figure 1.5G; reviewed in (Knoblich, 2001). The role for Numb in GMC fate specification has yet to be shown, but may involve repression of Notch signalling, as in *Drosophila* sensory organ precursor cells (Frise et al., 1996; Guo et al., 1996). Mira is segregated and then rapidly degraded in the GMC (Fuerstenberg et al., 1998; Ikeshima-Kataoka et al., 1997; Shen et al., 1997), resulting in the release of Pros/Stau/*pros* mRNA cargo. Pros is a homeodomain containing transcription factor, that enters the GMC nucleus, and activates transcription of GMC specific genes, such as *even-skipped* (Figure 1.5G; (Doe et al., 1991; Hirata et al., 1995; Knoblich et al., 1995; Spana and Doe, 1995; Vaessin et al., 1991). Segregation of *pros* mRNA

transcripts by Stau is required for sufficient Pros levels in the GMC (Broadus et al., 1998).

A number of mRNAs also exhibit polarised, asymmetric distributions in neuroblasts, and their patterns of localisation are often cell cycle-stage specific. For example, *pros* transcripts are apically localised during interphase, before translocation to the basal cortex during mitosis (Broadus et al., 1998; Li et al., 1997; Schuldt et al., 1998; Shen et al., 1998). Several other mRNA transcripts are also localised to the apical cytoplasm during interphase, including *insc, mira* and *baz* mRNA transcripts (Knirr et al., 1997; Kuchinke et al., 1998; Li et al., 1997; Schuldt et al., 1998). However, the mechanism and developmental significance of apical *insc, mira* and *baz* mRNA localisation in neuroblasts is unknown.

In this thesis, I describe my research into the mechanism and function of apically directed mRNA localisation in *Drosophila* embryonic epithelial cells and neuroblasts. In particular, I focus on the mechanisms required for apical localisation of *insc*, *wg*, *crb* and *mira* mRNAs in these cell types and describe my studies into the developmental significance of mRNA localisation in *Drosophila* embryos.

In chapter 2, I describe my studies into whether the Egl/BicD/dynein mRNA localisation machinery is conserved between different tissues in *Drosophila* embryos. To assess the conservation of the Egl/BicD/dynein mRNA localisation machinery, I have investigated the localisation of *insc, crb, wg* and misexpressed *K10* mRNA transcripts by fluorescent *in situ* hybridisation analysis in epithelial cells and neuroblasts in embryos where the function of Egl, BicD or dynein is disrupted.

In Chapter 3, I study the requirement for *insc, crb* and *wg* mRNA localisation in asymmetric targeting and activity of their respective protein products. This chapter focuses on Insc, which directs apico-basal polarisation and augments metaphase spindle length in *Drosophila* neuroblasts. Therefore, I have assessed the localisation of Insc protein, examined apico-basal polarity by immunostaining with polarity markers and measured metaphase spindle lengths in *egl* and *BicD* mutant neuroblasts, in which *insc* mRNA localisation is disrupted.

The function of *wg* and *crb* mRNA localisation was studied by immunostaining for Wg and Crb proteins in *egl* and *BicD* mutants, where localisation of these transcripts is disrupted. Genetic interaction experiments were also performed to determine whether abolishing *wg* or *crb* mRNA localisation resulted in an increased frequency of larval cuticle defects often seen in *wg* and *crb* loss-of-function mutants.

Chapter 4 describes my investigations into the mechanism of *mira* mRNA localisation in *Drosophila* embryos. I have studied this by *mira* RNA injection experiments and *in situ* analyses in wild-type embryos and in mutants for genes known to mediate mRNA localisation in *Drosophila.*

CHAPTER 2: EGALITARIAN, BICAUDAL-D AND DYNEIN MEDIATE APICAL mRNA LOCALISATION IN *DROSOPHILA* EMBRYONIC NEUROBLASTS AND EPITHELIAL CELLS

2.1 Introduction

One of the mechanisms used to transport and localise mRNAs during *Drosophila* development utilises the Egl/BicD/dynein motor complex (described in section 1.2.1.4). This complex is known to transport mRNA transcripts towards the minus-ends of microtubules during oogenesis, when maternal mRNAs translocate from the nurse cells to the oocyte, and in syncytial blastoderm embryos when pair-rule transcripts accumulate apically (Bullock and Ish-Horowicz, 2001; Navarro et al., 2004), and references therein). With an interest to study the generality of this mRNA transport machinery, my project initially focused on whether Egl, BicD and dynein were active and functioning to localise mRNA transcripts in somatic cell types in the *Drosophila* embryo.

I initially examined whether Egl, BicD and dynein were required to localise mRNAs in embryonic neuroblasts and epithelial cells, where a number of mRNA transcripts have been found to localise specifically to the apical cytoplasm. *insc* mRNA transcripts are localised apically in neuroblasts, first in the delamination stalk that extends towards the exterior of the embryo and subsequently to the apical cell cytoplasm during interphase (Knirr et al., 1997; Li et al., 1997). *wg* transcripts are also apically localised in neuroblasts, and *insc, crb* and *wg* mRNAs are all found to localise to the apical cytoplasm in embryonic epithelial cells (Baker, 1987; Baker,

1988; Knoblich et al., 1999; Tepass et al., 1990). However, the mechanism by which *insc, crb and wg* are localised in these cells is unknown.

In this chapter, I describe my investigations into the requirement for the Egl/BicD/dynein mRNA transport machinery in the localisation of *insc*, *wg* and *crb* transcripts in embryonic epithelial cells and neuroblasts.

Figure 2.1 ***insc*** **mRNA transcripts localise apically in neuroblasts and PNR epithelial cells.**

insc **mRNA transcripts localise to the apical cytoplasm in neuroblasts and PNR epithelial cells of wild-type embryos. Apical is up and basal is down in this and all subsequent figures. Arrowheads indicate apical enrichment of** ***insc*** **transcripts.** ***insc*** **transcripts are also detected in basal GMCs (arrow). Scale bar = 20μm.**

Figure 2.1

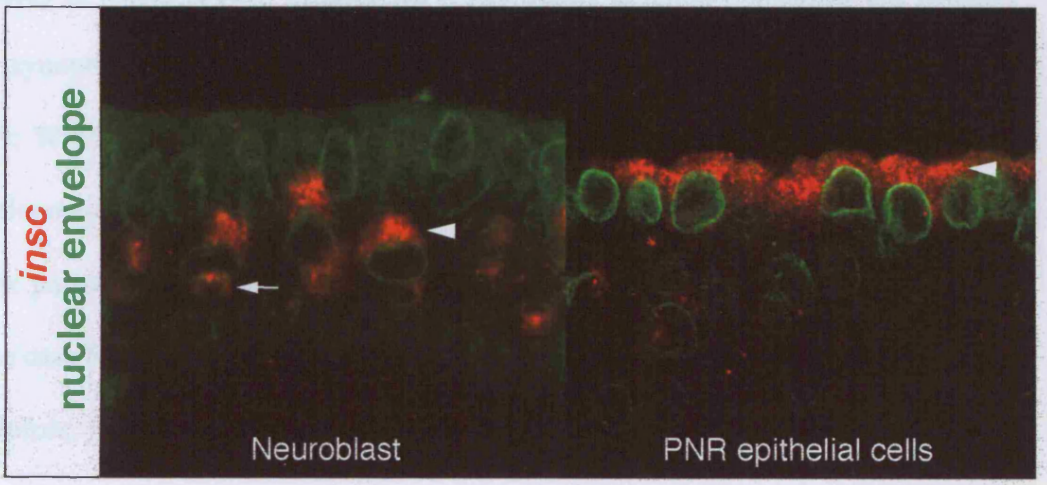

2.2 Results

2.2.1 Injected *insc* transcripts localise apically in the syncytial blastoderm embryo using Egl and BicD

To test if the Egl/BicD/dynein motor complex can mediate apical *insc* mRNA localisation in neuroblasts and epithelial cells of the PNR (Figure 2.1), I made use of an assay in which *in vitro* synthesised fluorescently labelled transcripts are injected into syncytial blastoderm embryos (Bullock and Ish-Horowicz, 2001; Lall et al., 1999; Wilkie and Davis, 2001). Although not normally expressed at this stage of development, the majority of injected full-length *insc* transcripts accumulate apically of the peripheral nuclei within 5 minutes (85% of embryos (n=33); Figure 2.2C), as is the case for injected *h* transcripts (Figure 2.2B; (Bullock and Ish-Horowicz, 2001). Therefore, in a similar manner to injected pair-rule mRNAs, *insc* can be recognised and transported apically by the blastoderm mRNA localisation machinery.

In blastoderm embryos, Egl and BicD proteins are present throughout the cell but enriched at the minus-ends of microtubules (Bullock and Ish-Horowicz, 2001). Injection of *insc* RNA (Figure 2.2D) leads to a further enrichment of Egl (Figure 2.2D') and BicD (Figure 2.2D") proteins at the sites of apical *insc* localisation, showing that injected *insc* transcripts associate with endogenous Egl and BicD. Furthermore, localisation of injected *insc* RNA is inhibited by pre-injection into the basal cytoplasm of antibodies that specifically block the function of Egl and BicD (Bullock and Ish-Horowicz, 2001; Mach and Lehmann, 1997; Suter and Steward, 1991), but is not inhibited by control antibodies (raised against the

Figure 2.2 Egl and BicD mediate localisation of injected *insc* transcripts in the blastoderm embryo.

(A) Diagram of the periphery of a syncytial blastoderm embryo showing arrangement of the nuclei within a shared cytoplasm and the site of RNA injection (arrow). A, apical cytoplasm; N, nuclei; B, basal cytoplasm; Y, yolk. **(B)** Apical localisation of injected *h* transcripts. **(C)** Apical localisation of injected *insc* transcripts. **(D)** Injected *insc* transcripts associate with endogenous Egl **(D')** and BicD **(D")** at sites of apical RNA localisation (100%, number of embryos (n) =17). Arrowheads indicate normal levels of Egl (D') and BicD (D") proteins either side of the domain containing localised injected *insc* transcripts. In this figure, confocal microscope settings have been optimised for visualisation of enriched protein levels associated with injected *insc* mRNA, rather than the distribution of endogenous protein. Pre-injection of blocking antibodies to **(E)** Egl and **(F)** BicD inhibits apical localisation of injected *insc* transcripts (100%, n=28 and 97%, n=33, respectively). **(G)** Pre-injection of control anti-Orb antibody does not significantly inhibit localisation of injected *insc* transcripts (efficient localization in 90%, n=50). Scale bar = 50μm.

Figure 2.2

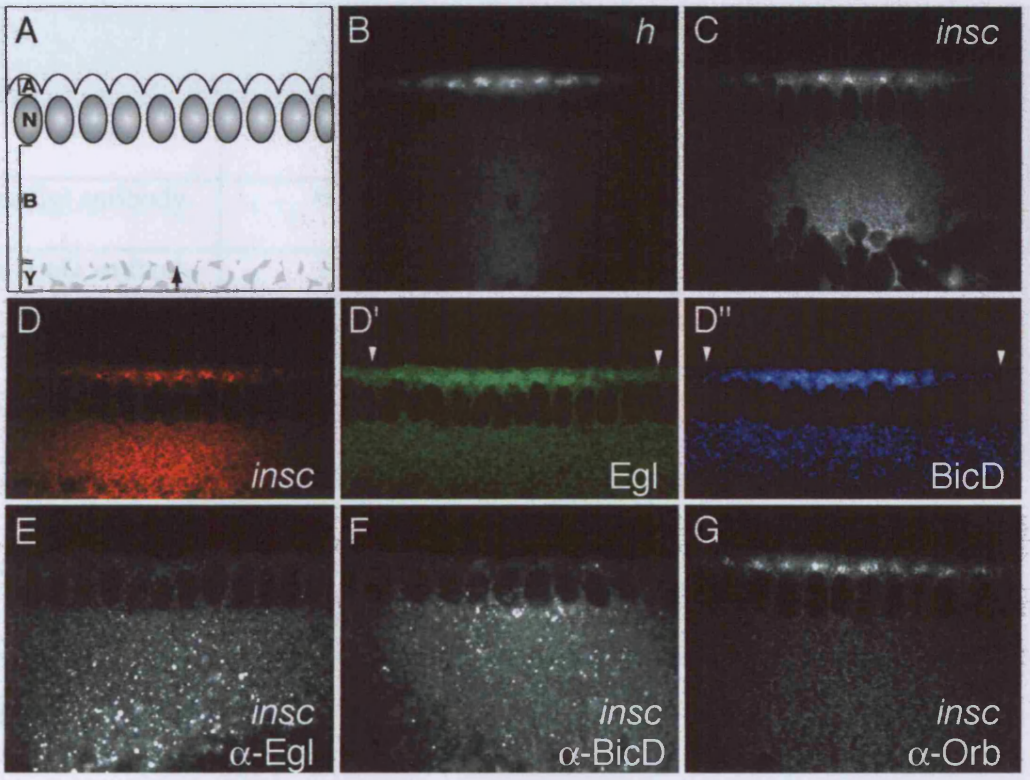
A
A
N
B
Y
B
h
C
insc
D
insc
D'
Egl
D''
BicD
E
insc
α-Egl
F
insc
α-BicD
G
insc
α-Orb

RNA-binding protein Orb) (Figure 2.2G), or injection buffer (Table 2.1). These data indicate that Egl and BicD mediate the localisation of injected *insc* transcripts in blastoderm embryos.

Table 2.1 Localisation of injected *insc* RNA in syncytial blastoderm embryos

none	28	5	0	33
α-Egl antibody	0	0	28	28
α-BicD antibody	1	1	33	35
α-Orb antibody	36	9	5	50
injection buffer	9	1	0	10

n is the total number of embryos scored for injected *insc* RNA localisation.

Strong localisation: majority of injected transcripts apically localised above nuclei.

Weak localisation: most injected RNA in basal cytoplasm, with some localised 'caps' of RNA above the nuclei.

Unlocalised: injected RNA evenly distributed above site of injection.

2.2.2 Apical localisation of *insc* transcripts is mediated by mRNA localisation signals within the *insc* 5' and 3' UTRs

2.2.2.1 Removal of insc *3'UTR*

To further investigate the recognition of the *insc* transcript by the blastoderm localisation machinery, I tested where the *insc* mRNA localisation signal was located within the *insc* transcript. Upon injection, the vast majority of full-length *insc*

transcripts localise to the apical cytoplasm (*insc*; Figures 2.2C, 2.3A and Table 2.1). Apical *insc* localisation is markedly weakened when the *insc3'UTR* is removed with a large proportion of the injected RNAs remaining in the basal cytoplasm (*inscΔ3'UTR*; weak apical localisation in 100% of embryos (n=15); Figure 2.3B). This shows that the *insc* 3'UTR contains part of the *insc* mRNA localisation signal that is required for efficient apical localisation of injected *insc* transcripts in syncytial blastoderm embryo.

Removal of the *insc* 3'UTR has been previously shown to completely abolish apical localisation of *insc* transcripts when misexpressed in neuroblasts and epithelial cells (Tio et al. 1999). However, it is possible that very weak localisation of *insc* transcripts in these cells would not have been detected by standard *in situ* hybridisation techniques.

2.2.2.2 Removal of insc *5' and 3' UTRs*

Transcripts lacking both the 5' and 3' UTRs of *insc* fail to localise apically when injected into the blastoderm embryo (*inscCDS*; 100% of embryos (n=15); Figure 2.3C) and also when misexpressed in epithelial cells and neuroblasts (Knoblich et al., 1999); Figure 2.3D), suggesting that efficient apical localisation of *insc* transcripts is mediated by multiple RNA localisation signals that reside within both the 5' and 3' UTRs.

The comparable localisation efficiencies of truncated *insc* transcripts that are either ectopically expressed or injected into embryos, suggests that injected *insc* RNAs are recognised and transported to the apical cytoplasm in a similar manner to those that are transcribed *in vivo*.

Figure 2.3 ***insc*** **mRNA localisation signals reside within the** ***insc*** **3' and 5' UTRs.**

(A) Apical localisation of injected *insc* transcripts. **(B)** Apical localisation of injected *insc* transcripts lacking the *insc3'UTR (inscΔ3'UTR)* is markedly weakened compared to full-length *insc* transcripts. **(C)** Injected *inscCDS* transcripts, that have both the *insc* 5' and 3' UTRs removed, remain within the basal cytoplasm and do not localise apically. **(D)** *insc* transcripts, produced by misexpression in embryos of the *inscNMyc* transgene (green), which lack both the *insc* 5' and 3' UTRs, do not localise apically in epithelial cells or neuroblasts (100%, n=10 embryos). *UAS-inscNMyc* flies were crossed with *h-Gal4* flies to produce a striped pattern of *inscNMyc* misexpression in stage 8-11 embryos (within brackets). Endogenous *insc* transcripts can be detected either side of the brackets. Nuclear envelope is shown in blue. Brackets also indicate approximate level of epithelial cells at the periphery of the embryo. Dashed circle indicates the location of a representative neuroblast. Scale bar = 50μm (A-C); 30μm (D).

Figure 2.3

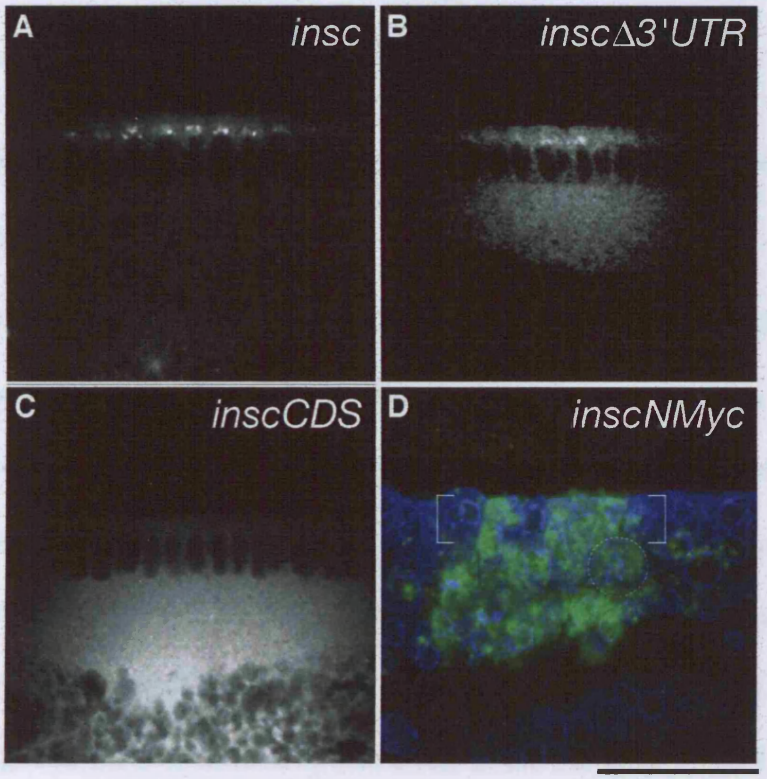

In most cases studied, the localisation of mRNA transcripts is mediated by RNA signals within the UTRs (reviewed in (Bashirullah et al., 1998). This data indicates that this is also the case for *insc* transcripts that are found to localise in *Drosophila.* However, more detailed analysis of both the *insc* 3' and 5' UTRs would be required to precisely map the nucleotides that comprise the *insc* localisation signal. This would lead to a further understanding of the recognition of *insc* transcripts by the Egl/BicD/dynein mRNA transport machinery.

2.2.3 Egl and BicD are apically enriched in delaminating and interphase neuroblasts and epithelial cells

To investigate whether Egl and BicD might transport endogenous *insc* mRNA in neuroblasts, I examined the intracellular distribution of these proteins during neurogenesis. Both proteins are present throughout the cytoplasm but are enriched in the apical cytoplasm of epithelial cells and delaminating and interphase neuroblasts (Figure 2.4). By contrast, Egl and BicD are evenly distributed throughout the neuroblast during the remainder of the cell cycle (Figure 2.4 and Table 2.2). Apical enrichment of Egl and BicD is consistent with a role in the transport of mRNA, and other dynein cargoes, to the apical cytoplasm in interphase neuroblasts and epithelial cells.

The distribution of Egl and BicD correlates with that of *insc* transcripts, which are detected apically in interphase neuroblasts (Li et al., 1997) and PNR epithelial cells (Knoblich et al., 1999), suggesting that these proteins have a role in the apical localisation of *insc* mRNAs.

Figure 2.4 Egl and BicD are apically enriched in neuroblasts and epithelial cells.

Stage 8-10 wild-type embryos stained with anti-Egl and anti-BicD antibodies, and for DNA (blue). Egl and BicD are enriched (arrowheads) in stalks that extend from the exterior of the embryo of delaminating neuroblasts and apically in interphase neuroblasts. Apical enrichment of Egl and BicD is also seen in epithelial cells (arrows). In mitotic neuroblasts at metaphase and anaphase, Egl and BicD are evenly distributed throughout the cytoplasm. Dashed circles indicate the location of representative neuroblasts. 20 neuroblasts were examined for each stage of the cell cycle. Scale bar = 20μm.

Figure 2.4

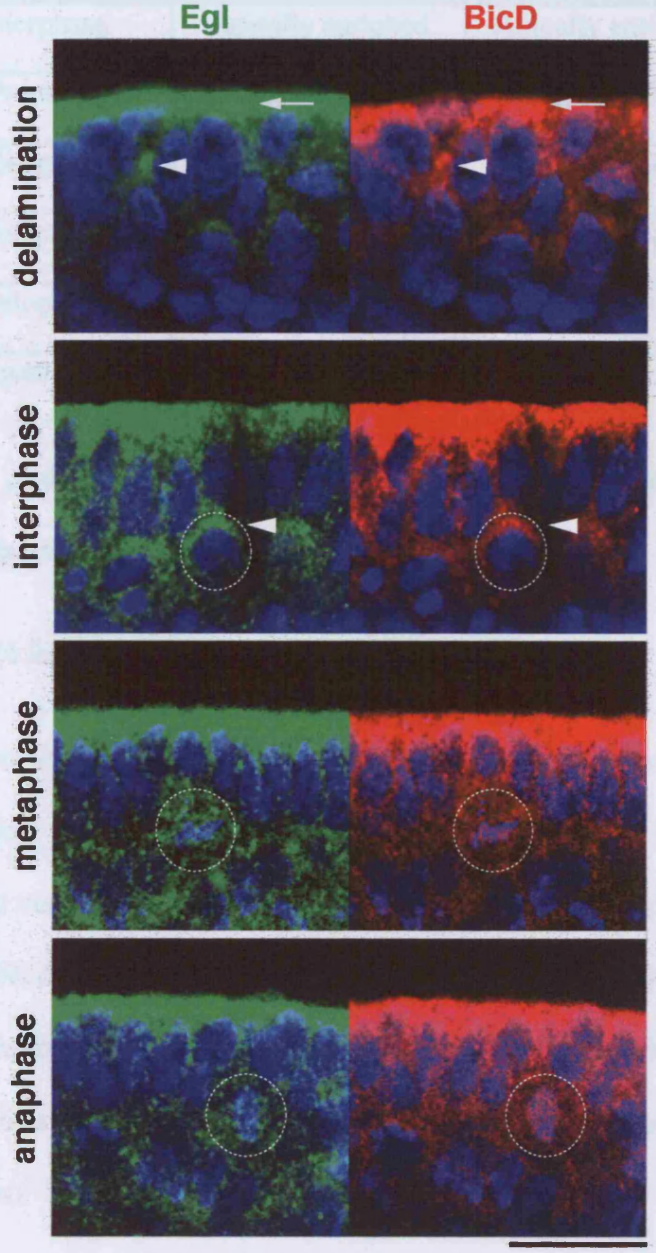

Table 2.2 Distribution of Egl and BicD at different cell cycle stages in wild-type neuroblasts

Interphase	Apically enriched	Apically enriched
Prophase	Evenly distributed	Evenly distributed
Metaphase	Evenly distributed	Evenly distributed
Anaphase	Evenly distributed	Evenly distributed
Telophase	Evenly distributed	Evenly distributed

20 neuroblasts were scored at each stage of the cell cycle.

2.2.4 Egl, BicD and dynein mediate asymmetric *insc* mRNA localisation in neuroblasts and epithelial cells

2.2.4.1 insc *mRNA localisation in neuroblasts requires Egl and BicD*

The requirement for *egl* and *BicD* during neurogenesis cannot be tested using null alleles because they block early stages of oogenesis (Deng and Lin, 2001). I therefore examined *insc* mRNA distribution using mothers mutant for partial loss-of-function *egl* and *BicD* alleles (Navarro et al., 2004; Oh et al., 2000) that retain sufficient activity to complete oogenesis and produce embryos (Bullock et al., 2004); hereafter referred to as *egl* and *BicD* mutant embryos; see Materials and Methods for details of genotypes).

In wild type embryos, *insc* mRNA is apically localised in all interphase neuroblasts (Li et al., 1997), exclusively in 87% and weakly in the rest (n=55; Figure 2.5A, B). By contrast, *insc* transcripts appear to be evenly distributed throughout the cytoplasm in 96% of *egl* mutant neuroblasts (n=50; Figure 2.5A, B). *BicD* mutant embryos

exhibit similar defects, with *insc* transcripts being unlocalised in 59% of neuroblasts and weakly localised in 13% of neuroblasts (n=53; Figure 2.5B). Together with the ability of Egl and BicD to associate with injected *insc* RNA (Figure 2.2), these data argue that Egl and BicD are members of a complex that mediates apical *insc* localisation in neuroblasts directly.

2.2.4.2 insc *mRNA localisation in neuroblasts requires dynein activity*

During oogenesis and in blastoderm embryos, Egl and BicD appear to function as part of the dynein motor complex that transports mRNA cargoes to microtubule minus-ends (Bullock and Ish-Horowicz, 2001; Navarro et al., 2004). Dynein activity depends on the interaction with the dynactin complex, which includes Dmn (see section 1.2.1.3). Dmn appears to negatively regulate the dynein motor in *Drosophila* (Januschke et al., 2002). Overexpression of Dmn in mammals, causes dynactin to dissociate from Dynein (Echeverri et al., 1996; Eckley et al., 1999), and inhibition of dynein mediated processes in tissue culture and *in vivo* in transgenic mice (Burkhardt et al., 1997; LaMonte et al., 2002).

I tested if dynein activity is required to localise *insc* mRNA apically in neuroblasts by overexpressing Dmn, specifically in neuroblasts using the UAS/GAL4 system (Brand and Perrimon, 1993). In these embryos, *insc* mRNA localisation is significantly impaired, with efficient apical accumulation being completely abolished in 22%, and weak in 16% of neuroblasts (n=63; $P<0.01$; Figure 2.5B). Therefore, these results suggest that Egl and BicD mediate dynein-dependent *insc* mRNA localisation in neuroblasts.

insc mRNA localisation phenotypes in *BicD* mutants and Dmn overexpression embryos are only partially penetrant when compared to *egl* mutants, where *insc* localisation is completely abolished (Figure 2.5B). As these are partial loss-of-function mutants, this difference in penetrance is presumably because of residual activity of BicD and dynein in neuroblasts in these embryos, and not due to different requirements for each of these factors in mRNA localisation.

Figure 2.5 Disruption of *insc* mRNA localisation in *egl* and *BicD* mutant and Dynamitin overexpressing neuroblasts.

(A) Examples of different *insc* mRNA distributions in neuroblasts of stage 8-10 wild-type, *egl, BicD* or Dynamitin-overexpressing embryos: localised (*insc* mRNA exclusively at the apical cytoplasm); weak (*insc* transcripts mostly apical but also detected elsewhere in the neuroblast cytoplasm); unlocalised (symmetric cytoplasmic distribution of *insc* transcripts). The frequency at which each type of *insc* mRNA distribution is observed in wild-type, *egl, BicD* or Dynamitin overexpression embryos is shown in **(B)**. Arrow indicates apically localised *insc* transcripts in a wild-type neuroblast. Neuroblasts displaying weak localisation of *insc* mRNA transcripts were distributed randomly throughout the sets of wild-type embryos that were examined and were not found predominantly in a subset of embryos. Scale bar in **(C)** = 20μm.

Figure 2.5

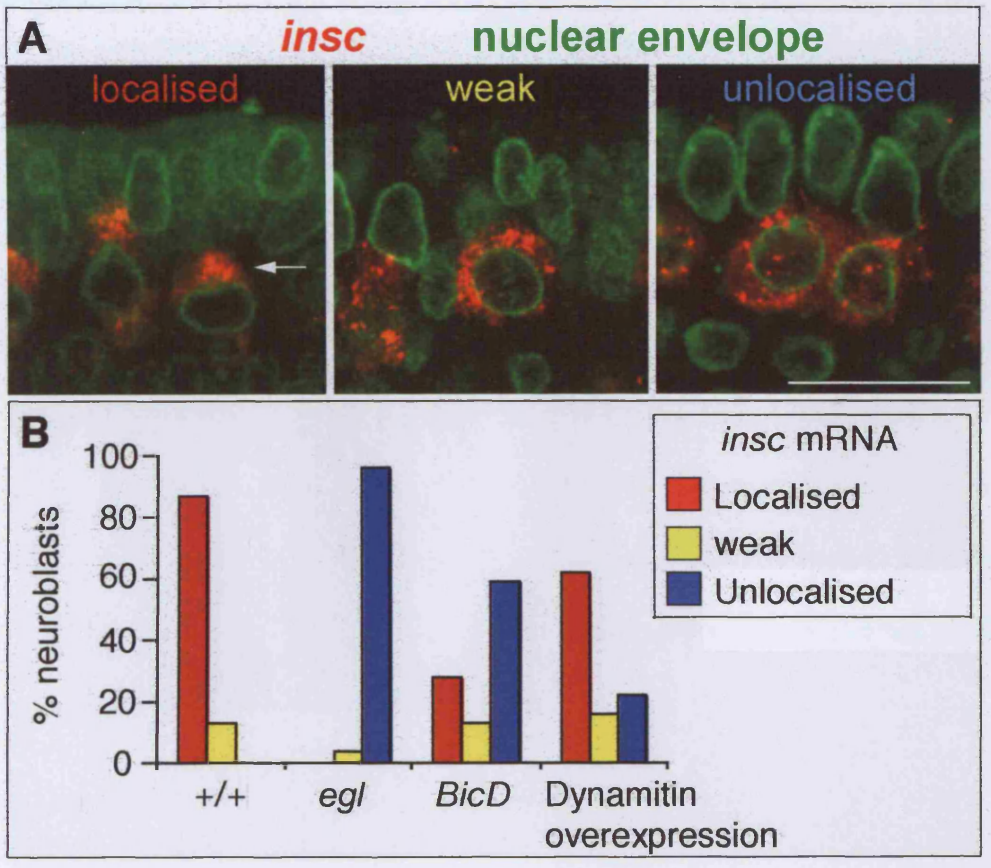
A
insc
nuclear envelope
localised
weak
unlocalised
B
% neuroblasts
100
80
60
40
20
0
+/+
egl
BicD
Dynamitin overexpression
insc mRNA
Localised
weak
Unlocalised

Figure 2.6 Apical *insc* mRNA localisation is disrupted in PNR epithelial cells of *egl* and *BicD* mutant embryos.

(A) Apical localisation of *insc* mRNA transcripts in PNR epithelial cells at the periphery of the embryo (arrowhead) and in the stalk of a delaminating PNR neuroblast (arrow). **(B)** *insc* mRNA localisation is abolished in PNR epithelial cells and neuroblasts of *egl* mutant embryos, with *insc* transcripts distributed evenly throughout the cytoplasm (20/20 embryos). **(C)** *insc* mRNA localisation is disrupted in *BicD* mutant PNR epithelial cells (10/14 embryos), where *insc* transcripts are enriched in the apical cytoplasm but are also detected in more basal cytoplasmic regions (arrowhead). *insc* mRNA localisation is also disrupted in PNR neuroblasts, where *insc* transcripts are detected mostly apically but also elsewhere in the cytoplasm (arrow indicates basal *insc* transcripts in PNR neuroblast). Dashed circles indicate the location of representative neuroblasts. Scale bar = 20μm.

Figure 2.6

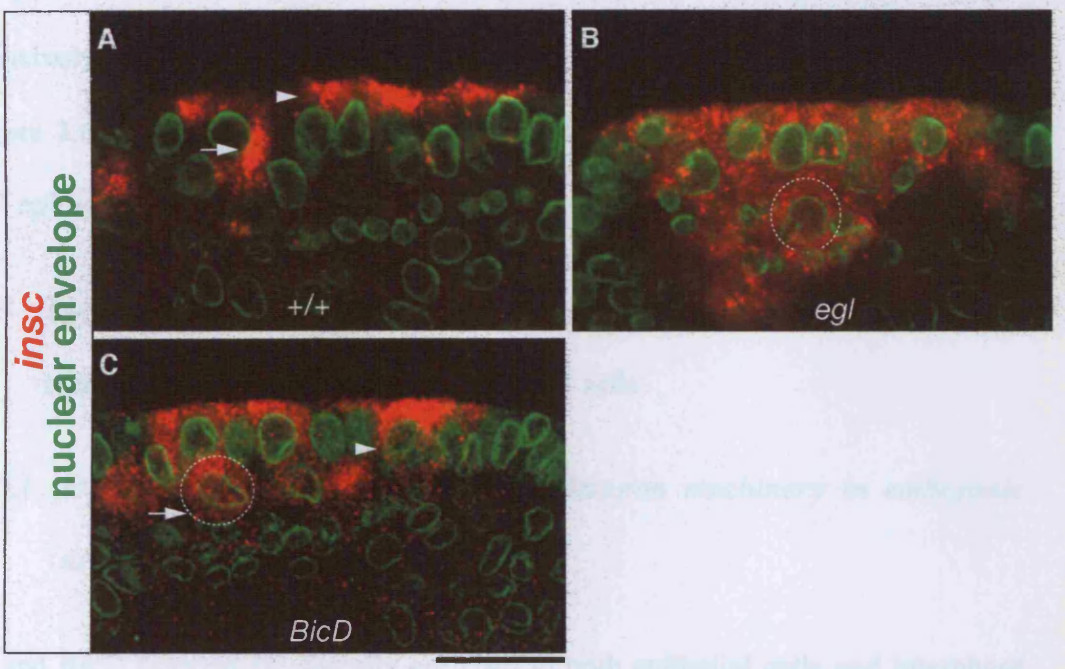

2.2.4.3 insc mRNA localisation in PNR epithelial cells requires Egl and BicD

As in neuroblasts, *insc* mRNA transcripts localise apically in PNR epithelial cells (Knoblich et al., 1999)). *insc* mRNA localisation is completely abolished in *egl* mutant PNR epithelial cells (Figure 2.6B). *BicD* mutant embryos also exhibit disruption of *insc* localisation in the PNR, where *insc* transcripts are no longer exclusively apical, but are also present in basal-lateral regions of the cytoplasm (Figure 2.6C). This suggests that *insc* mRNA transcripts are localised apically in PNR epithelial cells by the Egl/BicD/dynein mRNA transport machinery.

2.2.5 Investigating the apical localisation of *wg, crb* and misexpressed *K10* transcripts in neuroblasts and epithelial cells

2.2.5.1 Evidence for a common mRNA localisation machinery in embryonic neuroblasts and epithelial cells

Egl and BicD proteins are apically enriched in both epithelial cells and interphase neuroblasts (Figure 2.4), suggesting that the Egl/BicD/dynein mRNA machinery is common to both cell types. Indeed, *insc* transcript localisation is disrupted in both neuroblasts and PNR epithelial cells of *egl* and *BicD* mutant embryos (Figure 2.5, 2.6) and full-length *insc* transgenes are found to produce apically localising *insc* transcripts when misexpressed in epithelial cells outside the PNR (Tio et al., 1999). Therefore, to test whether the Egl/BicD/dynein mRNA localisation machinery was active in both neuroblasts and epithelial cells, I examined other mRNA transcripts that localise apically in these cell types.

Figure 2.7 Apical localisation of misexpressed ***K10*** transcripts in neuroblasts and epithelial cells is Egl-dependent.

(A) Apical localisation in neuroblasts of misexpressed ***K10*** transcripts (***hs-K10***), from a heat-shock inducible transgene (arrowhead; 30/30 neuroblasts). Misexpressed ***K10*** transcripts also localize apically in epithelial cells (arrow) (10/10 embryos). **(B)** Apical localisation of misexpressed ***K10*** transcripts is abolished in ***egl*** mutant neuroblasts (30/30 neuroblasts) and epithelial cells (10/10 embryos). Dashed circles indicate the location of representative neuroblasts. Scale bar = 20μm.

Figure 2.7

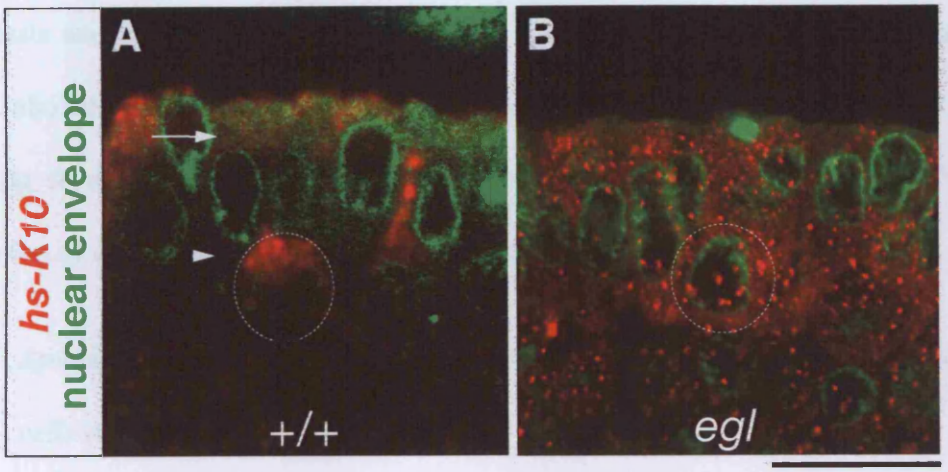

2.2.5.2 *Apical localisation of misexpressed K10 mRNA transcripts in neuroblasts and epithelial cells requires Egl*

K10 transcripts (*fs(1)K10*) contain mRNA localisation signals that can be recognised by the Egl/BicD/dynein mRNA transport machinery to mediate localisation in *Drosophila* oocytes and in blastoderm embryos (Bullock and Ish-Horowicz, 2001; Serano and Cohen, 1995). Misexpressed *K10* transcripts also localise apically in both neuroblasts and epithelial cells (Figure 2.7A). Apical localisation of misexpressed *K10* is abolished in *egl* mutant neuroblasts and epithelial cells (Figure 2.7B), providing further evidence that Egl, BicD and dynein function to mediate the localisation of mRNAs to the apical cytoplasm in neuroblasts and epithelial cells.

2.2.5.3 *Apical localisation of wg mRNA transcripts in neuroblasts and epithelial cells is mediated by Egl and BicD*

I also investigated the localisation of endogenous *wg* transcripts, which localise apically in epithelial cells (Baker, 1987; Baker, 1988) and neuroblasts (Figure 2.8A, E). Apical *wg* localisation is completely abolished in all *wg* expressing neuroblasts of *egl* mutant embryos (n=30; Figure 2.8B, E). *BicD* mutant embryos exhibit similar defects, with *wg* transcripts being unlocalised in 38% of neuroblasts (n=50; Figure 2.8D", E) and weakly localised in 32% of neuroblasts (Figure 2.8D', E). These results indicate that the Egl/BicD/dynein complex mediates apical *wg* localisation in neuroblasts.

Apical localisation of *wg* transcripts is also abolished in epithelial cells of *egl* mutant embryos (Figure 2.8B; 100% of epithelial cells (n=30)). *wg* localisation in disrupted in *BicD* mutant epithelial cells with weak *wg* localisation observed in 90% of

Figure 2.8 Egl and BicD mediate apical localisation of *wg* transcripts in neuroblasts and epithelial cells.

(A) Apical localisation of *wg* mRNA transcripts in wild-type neuroblasts (arrowhead) and epithelial cells (arrow). **(B)** *wg* transcripts localisation is abolished in neuroblasts and epithelial cells of *egl* mutant embryos. **(C)** Apical localisation of injected *wg* transcripts in blastoderm embryos. **(D-D")** Examples of different *wg* mRNA distributions observed in *BicD* mutant neuroblasts and epithelial cells: **(D)** Normal apical localisation of *wg* in neuroblasts (arrowhead) and epithelial cells. **(D')** Weak *wg* mRNA localisation in neuroblasts, where the majority of *wg* transcripts are apical (arrowhead), but are also detected throughout in the neuroblast cytoplasm. **(D")** Unlocalised *wg* mRNA transcripts in neuroblasts, and an example of a *BicD* mutant epithelial cell displaying weak *wg* localisation, where *wg* is detected throughout the cytoplasm (arrow) but is enriched apically (arrowhead). The frequency at which each type of *wg* mRNA distribution is observed in neuroblasts of wild-type, *egl* and *BicD* mutants is shown in **(E)**. Dashed circles indicate the location of representative neuroblasts. Scale bar = 30μm (A, B, D-D"); 50μm (C).

Figure 2.8

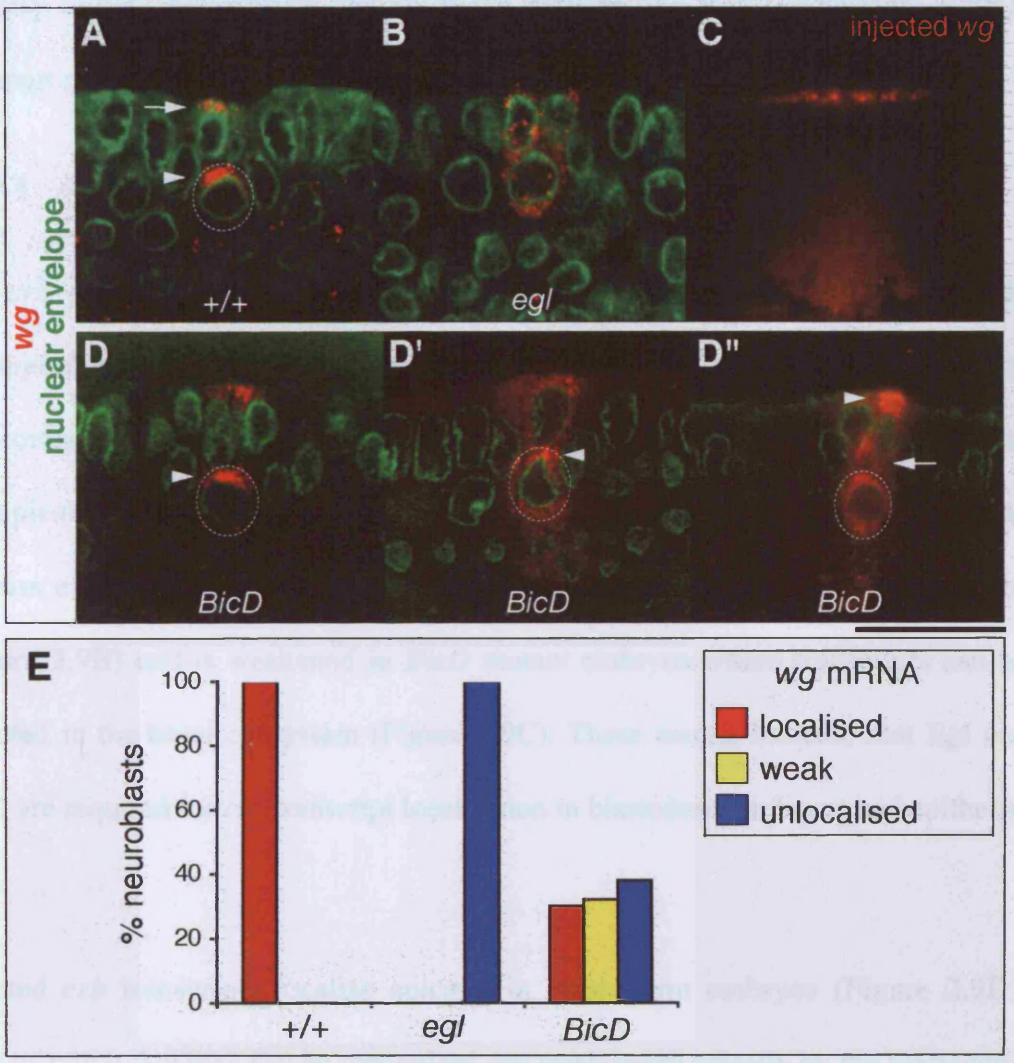
A
B
C
injected wg
wg
nuclear envelope
+/+
egl
D
D'
D"
BicD
BicD
BicD
E
% neuroblasts
100
80
60
40
20
0
+/+
egl
BicD
wg mRNA
localised
weak
unlocalised

epithelial cells (n=50) where transcripts are no longer exclusively in the apical cytoplasm but are detected throughout the cell (Figure 2.8D"). These results are consistent with Egl and dynein-dependent localisation of endogenous and injected *wg* transcripts in blastoderm embryos (Figure 2.8C; (Bullock and Ish-Horowicz, 2001; Wilkie and Davis, 2001) and suggest that *wg* mRNA transcripts are localised apically in both neuroblasts and epithelial cells by the Egl/BicD/dynein mRNA transport machinery.

2.2.5.4 *Apical crb mRNA localisation in epithelial cells requires Egl and BicD*

The *crb* gene is required to maintain apico-basal polarity in epithelial cells in *Drosophila* embryos, which is controlled by localisation of Crb protein to the apical cell cortex (Tepass et al., 2001). *crb* mRNA transcripts are also found to localise to the apical cytoplasm in blastoderm embryos and epithelial cells (Figure 2.9A; (Tepass et al., 1990). *crb* mRNA localisation is abolished in *egl* mutant embryos (Figure 2.9B) and is weakened in *BicD* mutant embryos where transcripts can be detected in the basal cytoplasm (Figure 2.9C). These results indicate that Egl and BicD are required for *crb* transcript localisation in blastoderm embryos and epithelial cells.

Injected *crb* transcripts localise apically in blastoderm embryos (Figure 2.9D), demonstrating that they can be recognised and transported apically by the blastoderm localisation machinery. This provides further evidence that the Egl/BicD/dynein mRNA localisation machinery localises *crb* transcripts apically in epithelial cells.

Figure 2.9 Egl and BicD mediate apical localisation of *crb* mRNA transcripts.

(A) Apical localisation of *crb* transcripts in wild-type embryos. **(B)** *crb* does not localise apically in *egl* mutant embryos and *crb* mRNAs are evenly distributed throughout the cytoplasm (100% of embryos (n=20)). **(C)** *crb* localisation is disrupted in *BicD* mutant embryos and *crb* transcripts are detected in the basal cytoplasm (square brackets) (100% of embryos (n=20)). **(D)** Apical enrichment of injected *crb* RNAs (arrowhead) in blastoderm embryos occurs after 20 min (100% of embryos (n=10)). **(D')** Control, non-localising *pins* RNAs are not enriched in the apical cytoplasm 20 min after injection. A merged image is shown in **(D")**. Scale bar = 50μm.

Figure 2.9

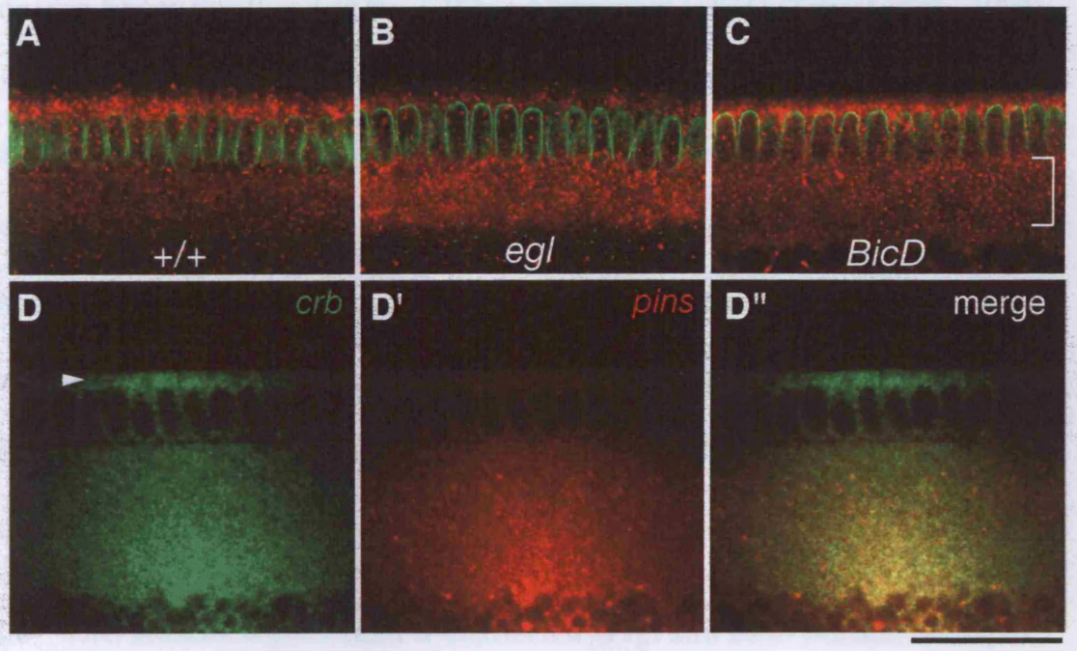

Injected *crb* transcripts localise apically in blastoderm embryos, although this process was delayed and *crb* RNA localisation was only detectable 20 min after injection. Typically, injected pair-rule or *insc* RNAs localise apically within 5 min (Figure 2.2A). This may be because in these experiments, short 1.6Kb RNAs, corresponding to the 3' end of the 7.2Kb *crb* transcript (c4B4; (Tepass et al., 1990); includes entire *crb*3'UTR), were injected into blastoderm embryos. Endogenous *crb* mRNA is localised exclusively to the apical cytoplasm. Thus, there may be other RNA signals within the remainder of the *crb* transcript that are required for fully efficient localisation in the injection assay. Alternatively, following synthesis *in vitro*, this truncated *crb* transcript may not fold into a conformation that can be efficiently recognised by the localisation machinery upon injection into blastoderm embryos.

2.2.6 Microtubule organisation is unaffected in *egl* and *BicD* mutant embryos

The Egl/BicD/dynein complex transports mRNA cargoes along microtubules. It has been suggested previously that defects in mRNA localisation during oogenesis may result from a disruption in microtubule organisation in *egl* and *BicD* null mutant egg chambers (Oh and Steward, 2001; Theurkauf et al., 1993). I tested whether this may account for defects in mRNA localisation observed in the *egl* and *BicD* partial loss-of-function mutants and Dmn overexpressing embryos used in this study, by immunostaining for the microtubule associated protein, End-Binding protein 1 (EB1).

EB1 associates with the microtubule network in cultured mammalian cells (Berrueta et al., 1998). Further studies have shown that EB1 can be detected along the length of

growing microtubules but with an enrichment at their plus-ends, consistent with an involvement of EB1 in microtubule polymerisation in dynamic cells (Berrueta et al., 1998; Nakamura et al., 2001).

In wild-type neuroblasts and epithelial cells, EB1 immunostaining indicates that the microtubule network exhibits a similar distribution to Egl and BicD: microtubules are present throughout the cytoplasm but are enriched in the apical cytoplasm of epithelial cells and delaminating and interphase neuroblasts (Figure 2.10; Table 2.3). The observed defects in mRNA localisation in *egl* and *BicD* mutant embryos are unlikely to be caused by disruption of microtubule organisation, as this appears normal in mutant epithelial cells and delaminating and interphase neuroblasts (Figure 2.10; Table 2.3). Microtubule distribution is also unaffected in interphase neuroblasts that overexpress Dmn (Table 2.3).

Table 2.3 Apical enrichment of microtubules is unaffected in *egl* and *BicD* mutants and Dmn overexpressing neuroblasts

wild-type	100% epithelial cells 100% delamination stalks 100% interphase neuroblasts	10 embryos 50 (5 per embryo) 50
egl mutant	100% epithelial cells 100% delamination stalks 100% interphase neuroblasts	10 embryos 50 (5 per embryo) 50
BicD mutant	100% epithelial cells 100% delamination stalks 100% interphase neuroblasts	10 embryos 50 (5 per embryo) 30
Dmn overexpression	100% interphase neuroblasts	30

Figure 2.10 Apically enriched microtubule distribution in wild-type and *egl* mutant embryos.

Examples of stage 8-10 embryos stained with anti-EB1 antibody to label microtubules (red), and for DNA (blue). In wild-type embryos, microtubules are enriched in stalks that extend from the exterior of the embryo of delaminating neuroblasts and apically in interphase neuroblasts. Apical enrichment of microtubules is also seen in wild-type epithelial cells. Similar microtubule distributions are observed in delamination stalks, neuroblasts and epithelial cells in *egl* mutant embryos. Apically enriched microtubules are indicated in delaminating and interphase neuroblasts (arrowheads) and in epithelial cells (arrows). Dashed circles indicate the location of representative neuroblasts. Scale bar = 25μm.

Figure 2.10

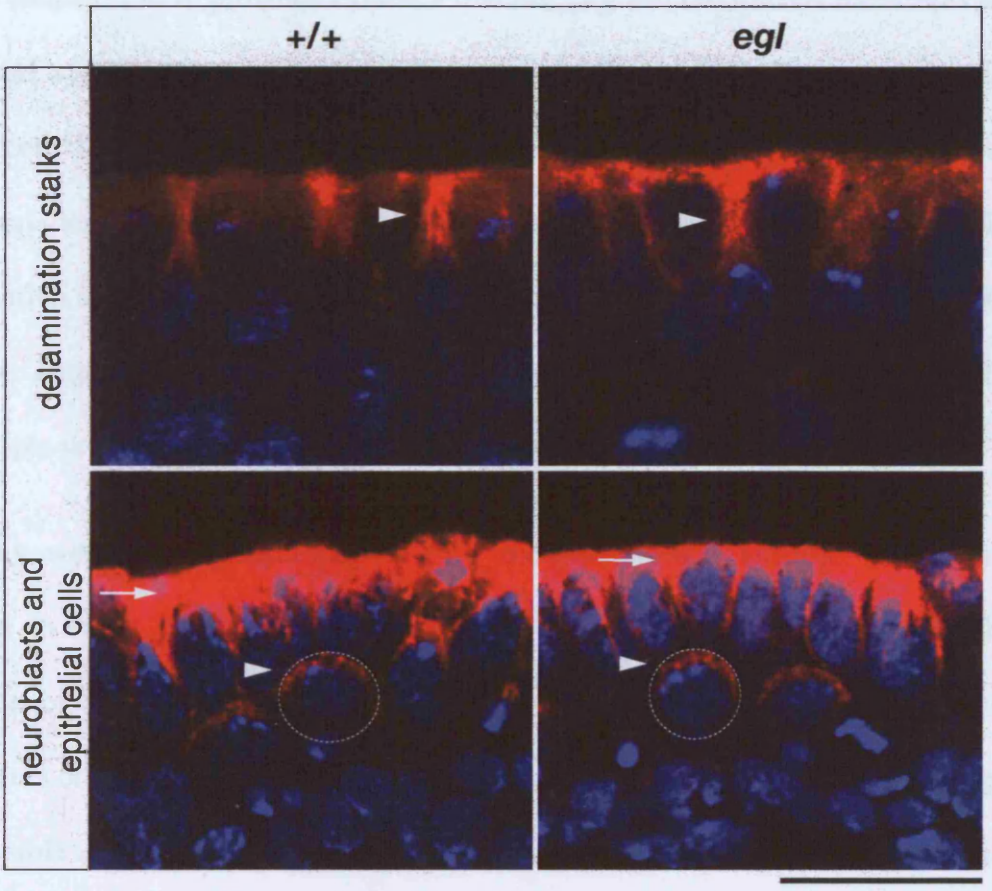
+/+
egl
delamination stalks
neuroblasts and epithelial cells

2.3 Discussion

2.3.1 A conserved machinery for asymmetric mRNA localisation during *Drosophila* embryogenesis

In this chapter, I have provided evidence that *insc*, *wg* and *crb* mRNA transcripts are localised apically in neuroblasts and epithelial cells by Egl, BicD and dynein. Therefore, the Egl/BicD/dynein mRNA transport machinery is conserved between oogenesis and neurogenesis, indicating that this a general mechanism for mRNA localisation in *Drosophila* (this chapter; (Bullock and Ish-Horowicz, 2001), and may also be employed throughout *Drosophila* embryogenesis to transport mRNA transcripts in many different polarised cell types.

insc, *wg* and *crb* transcripts may be able to be localised to specific cytoplasmic regions in other cells types where they are expressed, perhaps supporting the function of their respective protein products. For example, *Drosophila* muscle precursors or myoblasts are polarised in a similar manner to neuroblasts and undergo comparable asymmetric cell divisions, with asymmetrically localised Insc directing the segregation of cell fate determinants into specific daughters (Carmena et al., 1998). Therefore, *insc* transcripts may also be asymmetrically localised by Egl, BicD and dynein in myoblasts.

In addition to the Egl/BicD/dynein complex, studies of cell polarity during oogenesis have identified a large number of proteins required for mRNA localisation. For example, Stau functions in the localisation of *bcd* mRNA in the oocyte (St Johnston et al., 1991) and it has also been found to be required for basal localisation of *pros* transcripts in mitotic neuroblasts (Broadus et al., 1998; Li et al., 1997). Therefore, it

is possible that a number of these factors are utilised during *Drosophila* embryogenesis to mediate asymmetric localisation of many transcripts in different cell types.

In oocytes and blastoderm embryos, Egl and BicD are enriched at the sites of mRNA accumulation (Mach and Lehmann, 1997; Oh and Steward, 2001); (Bullock and Ish-Horowicz, 2001). Egl and BicD are also enriched apically in interphase neuroblasts and epithelial cells (Figure 2.4), presumably as a consequence of apically directed transport of mRNAs and other dynein cargoes. The Egl/BicD/dynein transport machinery may also have an additional role in anchorage of mRNAs apically in these cells. Indeed, some evidence suggests that apically localised dynein heavy chain (Dhc) may anchor pair-rule mRNAs in blastoderm embryos (Renald Delanoue and Ilan Davis, personal communication). Alternatively, maintenance of transcript localisation in these cells might result from sustained minus-end directed transport.

Dhc, Egl and BicD have similar distributions during oogenesis and in blastoderm embryos. However, I have been unable to detect apical enrichment of Dhc or dynein intermediate chain in neuroblasts, and these proteins appear evenly distributed throughout the cytoplasm. This may be because the dynein motor complex is involved in a wide range of cellular processes or the transport of multiple cargoes to different regions of the cytoplasm (Karki and Holzbaur, 1999; King, 2000). Also, high levels of these proteins in the neuroblast cytoplasm may prevent detection of apical dynein enrichment by immunostaining. However, inhibition of *insc* mRNA localisation by overexpression of Dmn (Figure 2.5) is consistent with a role for dynein in apical localisation of mRNA transcripts in neuroblasts.

As described in the introduction (section 1.2.1.2), a number of nuclear proteins have been implicated in active mRNA transport, indicating that 'nuclear history' of a mRNA transcript is coupled to its cytoplasmic localisation (Gu et al., 2002; Lall et al., 1999; Norvell et al., 1999; Ross et al., 1997). In this chapter, I show that *insc*, *wg* and *crb* RNA transcripts, that have been synthesised *in vitro,* are able to localise apically upon injection into the basal cytoplasm in blastoderm embryos. Therefore, transcription in the nucleus does not appear to be absolutely required for apical localisation, and these RNAs are able to associate efficiently with the Egl/BicD/dynein motor complex in the absence of specific nuclear factors.

However, it is possible that association with nuclear factors may increase the efficiency of cytoplasmic transport and localisation of these transcripts, which may explain why some injected RNAs, such as *crb*, localise weakly upon injection into blastoderm embryos (Figure 2.9). This could be tested by incubation of RNAs with nuclear extract prior to injection into blastoderm embryos, together with measurements of their localisation kinetics by tracking of localising RNA particles (Bullock et al., 2003).

The degree of mRNA localisation disruption differs between *egl* and *BicD* mutant embryos. *BicD* mutant neuroblasts and epithelial cells only exhibit partial defects in mRNA localisation in comparison to *egl* mutants, which are likely to be due to residual BicD activity in these embryos rather than distinct roles for Egl and BicD in mRNA localisation.

Disruption of mRNA localisation also differs between cell types in *BicD* mutant embryos. For example, *wg* localisation is affected to a larger degree in neuroblasts

than in epithelial cells. By immunostaining, it appears that there are higher levels of BicD protein present in epithelial cells than in neuroblasts (Figure 2.4). Thus, residual BicD activity may be greater in epithelial cells and could account for the differences in the severity of mRNA localisation defects between these two cell types.

The neuroblast offers a potentially useful system by which to screen for additional components of the Egl/BicD/dynein mRNA localisation machinery. Neuroblasts can be isolated from embryos and cultured *in vitro*, and they maintain their ability to become polarised and undergo asymmetric cell divisions under these conditions (Broadus and Doe, 1997). Therefore, a dsRNA-interference (RNAi) based *in situ* screen could be employed to identify genes required to generate a polarised distribution of *insc* or *wg* transcripts in cultured neuroblasts. In addition, the Egl/BicD/dynein complex may also transport mRNAs in other polarised *Drosophila* cell types that are easier to culture or are more stable *in vitro* to allow adequate time for RNAi-mediated depletion of cellular proteins. A similar screening approach could be taken in these cells to identify novel transport complex components of the Egl/BicD/dynein complex.

It has been shown that the Egl/BicD/dynein mRNA localisation machinery transports mRNAs along a polarised microtubule cytoskeleton during oogenesis and in blastoderm embryos (Bullock and Ish-Horowicz, 2001; Wilkie and Davis, 2001). My results indicate that a polarised microtubule network is present in neuroblasts, where mRNAs are also localised by Egl, BicD and dynein. The general use of this mRNA localisation machinery underlines its importance during *Drosophila* development.

mRNA localisation during oogenesis is required for polarisation of the oocyte and patterning of the embryonic body axes (section 1.1.2). In blastoderm embryos, apical localisation of pair-rule and *wg* mRNAs is required to augment the activity of their protein products (Bullock et al., 2004; Simmonds et al., 2001). The role of mRNA localisation in neuroblasts is less clear, but it may act to focus protein translation to specific regions of the cytoplasm or to enhance the efficiency of protein targeting in these cell types. In the next chapter, I detail my investigations into the functional significance of mRNA localisation in embryonic neuroblasts and epithelial cells.

CHAPTER 3: INVESTIGATING THE FUNCTION OF mRNA LOCALISATION IN *DROSOPHILA* EMBRYONIC NEUROBLASTS AND EPITHELIAL CELLS

3.1 Introduction

mRNA localisation directs mRNA transcripts to specific cytoplasmic regions and in some cases it is necessary for correct targeting of their protein products. For example, the localisation of *β-actin* transcripts is required for remodelling of the actin cytoskeleton at the leading edge of migrating Chick embryo fibroblasts (Kislauskis et al., 1997; Shestakova et al., 2001).

The role of mRNA localisation during *Drosophila* development has been extensively studied for over 15 years. For example, the localisation of *bcd* and *nos* mRNAs, to the anterior and posterior cortex of the oocyte respectively, is required for correct patterning of the embryo along the A-P axis (section 1.1.2.4). Also, recent studies in *Drosophila* blastoderm embryos have shown that pair-rule mRNA localisation augments the activity of their transcription factor products, possibly by targeting them closer to the blastoderm nuclei (Bullock et al., 2004). However, only a handful of studies have focussed on the function of mRNA localisation in smaller, somatic cell types in the *Drosophila* embryo.

mRNA localisation has been previously investigated in the *Drosophila* neuroblast, which offers a useful system to study the function of mRNA localisation, as correct targeting of proteins along the apico-basal axis is crucial for both the establishment of apico-basal polarity and the segregation of cell-fate determinants (reviewed in (Knoblich, 2001). For example the basal localisation of *pros*, by Stau, has been

shown to be important in targeting sufficient levels of Pros to the GMC (Broadus et al., 1998; Li et al., 1997). The significance of *insc* mRNA localisation in neuroblasts has also been investigated, although, based on overexpression of non-localising transcripts from heterologous promoters, it has been suggested that this process is not required for asymmetric Insc protein targeting or Insc function (Knoblich et al., 1999; Tio et al., 1999). It is not known if the localisation of endogenously expressed *insc* mRNA transcripts is required to support Insc activity.

The role of apical *wg* mRNA localisation in blastoderm embryos and epithelial cells has been previously studied, and based on mistargeting of *wg* transcripts in these cells it has suggested that *wg* localisation is required to augment Wg signalling (Simmonds et al., 2001). Similar transcript mistargeting experiments suggest that apical *crb* mRNA localisation is not required for Crb localisation or function (Ulli Tepass, personal communication). However, it is not known whether disrupting the localisation of endogenously expressed *wg* and *crb* has any effect on targeting their protein products or their activities.

In this chapter, I describe the effects on apical targeting and activity of Insc, Wg and Crb proteins when the localisation of their mRNA transcripts is disrupted in *egl* and *BicD* mutants.

3.2 Results

3.2.1 Reduced apical protein targeting in *egl* and *BicD* mutant neuroblasts

3.2.1.1 Reduced apical Insc localisation in neuroblasts

To test if *insc* mRNA localisation contributes to protein targeting in the neuroblast, I examined Insc protein in *egl* and *BicD* mutants. Insc localises as an apical crescent in all wild-type metaphase neuroblasts (Kraut and Campos-Ortega, 1996; Kraut et al., 1996); the apical enrichment is strong in 80% of neuroblasts and weak in the rest (Figure 3.1A, B, K). By contrast, apical Insc localisation is completely lost in 11% (Figure 3.1C, K) and weak in 44% of *egl* metaphase neuroblasts ($P<0.01$; Figure 3.1K). Defects are also seen in *BicD* mutant embryos, where complete loss and reduction of Insc enrichment occurs in 7% and 49% of metaphase neuroblasts, respectively ($P<0.01$; Figure 3.1K). These results suggest that *insc* mRNA localisation is required for efficient Insc protein targeting.

3.2.1.2 Egl does not transport Insc protein directly

It is conceivable that the defects in Insc protein localisation in *egl* and *BicD* mutant neuroblasts reflect an additional role for the Egl/BicD/dynein transport complex in translocating the protein directly. However, this does not appear to be case, as the efficiency of localisation of Insc protein encoded by ectopically expressed non-localising *insc* transcripts (Figure 3.1J) is indistinguishable in wild-type and *egl* mutant epithelial cells (Figure 3.1G, H; 10 embryos scored for each genotype), where the Egl/BicD/dynein machinery is normally active (see Chapter 2).

Figure 3.1 Apical Insc and Par6 protein localisation is disrupted in *egl* and *BicD* mutant neuroblasts.

(A-C) Examples of different Insc protein distributions in metaphase neuroblasts of stage 9-10 wild-type, *egl* or *BicD* embryos. Arrowheads indicate apical enrichment of Insc. The frequency at which each type of Insc protein distribution is observed in wild-type, *egl* or *BicD* neuroblasts is shown in **(K)**. **(D-F)** Examples of different Par6 distributions in metaphase neuroblasts and epithelial cells of stage 9-10 wild-type, *egl* or *BicD* embryos. Arrowheads indicate apical enrichment of Par6. Arrows show comparable Par6 apical localisation in epithelial cells of a wild-type embryo **(D)** and an *egl* mutant embryo **(F)**. The frequency at which each type of Par6 distribution is observed in wild-type, *egl* or *BicD* neuroblasts is shown in **(K)**. Categorisation of protein localisation in neuroblasts was based on the following criteria: localised (strong apical protein localisation); weak (reduced levels of apical protein, sometimes also detectable throughout the cytoplasm); unlocalised (no apical enrichment; protein detected throughout the cytoplasm). **(G, H)** Arrows indicate apical cytoplasm of epithelial cells showing a similar degree of apical enrichment of ectopically expressed Insc, from a hs-inducible transgene (*hs-insc*) lacking the signals required for *insc* localisation, in **(G)** wild-type or **(H)** *egl* mutant embryos. Levels of apical Insc protein enrichment in *hs-insc*; *egl* mutant neuroblasts and in *egl* mutants simply subjected to heat-shock treatment (egl hs) are shown in **(K)**. **(I)** Insc protein is not detected apically in epithelial cells (arrowhead) of *egl* mutant embryos that have been subjected to heat-shock. **(J)** *hs-insc* transcripts (red) are unlocalised in wild-type epithelial cells. Nuclear envelope is labelled in green. Dashed circles indicate the location of representative neuroblasts. Number of metaphase neuroblasts scored is shown above bars. Scale bar = 20μm (A-H); 30μm (I, J).

Figure 3.1

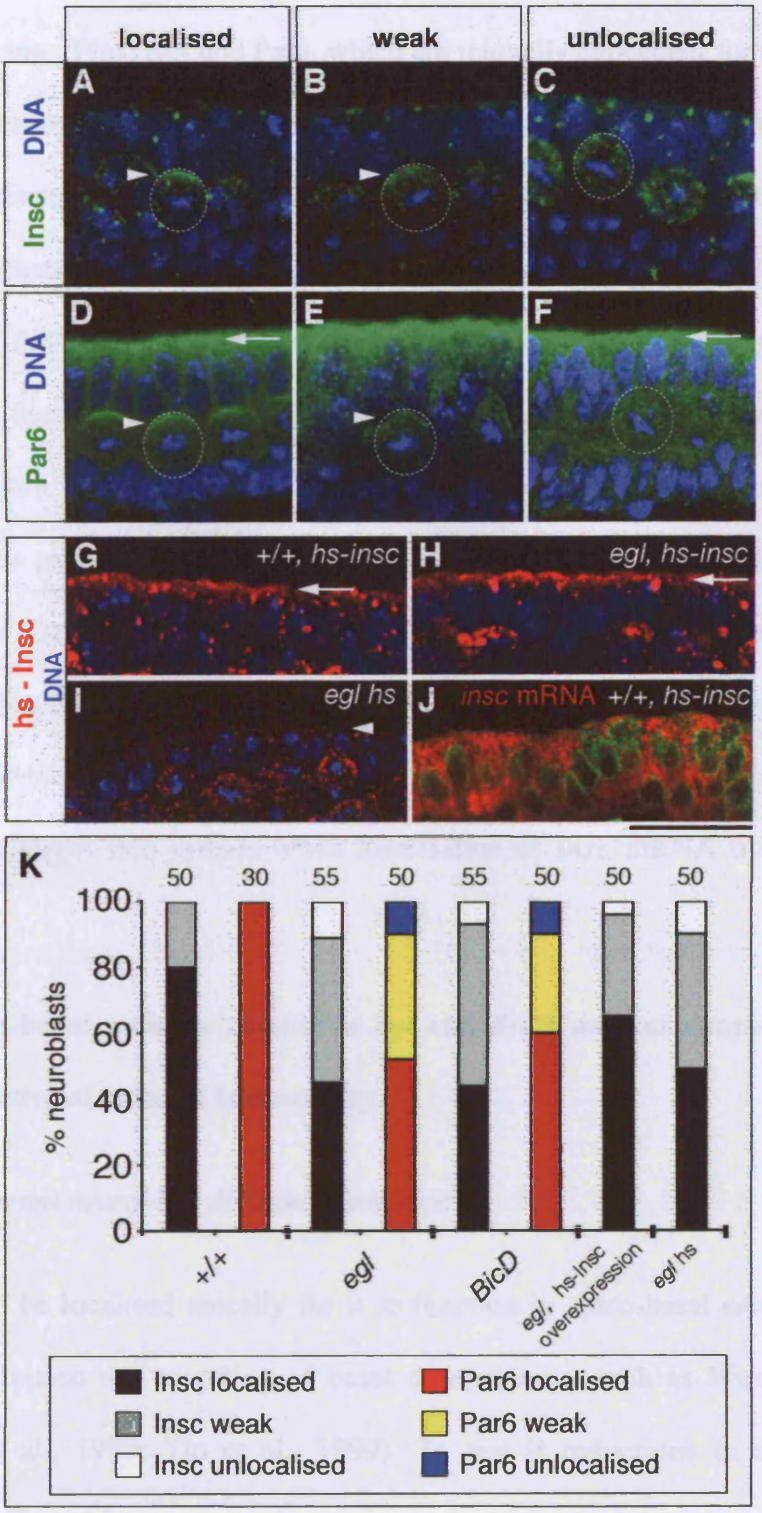
localised
weak
unlocalised
A
B
C
Insc
DNA
D
E
F
Par6
DNA
G
+/+, hs-insc
H
egl, hs-insc
hs - Insc
DNA
I
egl hs
J
insc mRNA
+/+, hs-insc
K
50
30
55
50
55
50
50
50
100
80
60
40
20
0
% neuroblasts
+/+
egl
BicD
egl, hs-Insc overexpression
egl hs
Insc localised
Insc weak
Insc unlocalised
Par6 localised
Par6 weak
Par6 unlocalised

3.2.1.3 Reduced apical Par6 localisation in neuroblasts

Apico-basal polarity in mitotic neuroblasts is marked by an apical protein complex that includes Insc, Pins, Baz and Par6, which are mutually dependent for their apical localisation during mitosis (see section 1.3.2.1). To examine whether defects in Insc localisation disrupts other apical complex members, I analysed the distribution of Par6 in metaphase neuroblasts. In *egl* and *BicD* mutant neuroblasts, defects in Par6 (Figure 3.1E, F, K) and Insc localisation occur at similar frequencies (Figure 3.1K). Furthermore, the inability to target Par6 protein efficiently in neuroblasts does not appear to result from deficiencies in Par6 localisation that are inherited from epithelial cells prior to delamination as this seems unaffected in epithelial cells of either *egl* or *BicD* mutants (Figure 3.1D, F; 20 embryos examined for each genotype). Thus, disruption of apical Par6 enrichment occurs specifically in neuroblasts, after the onset of *insc* expression, suggesting that it results from a failure to efficiently target Insc protein when localisation of *insc* mRNA transcripts is perturbed.

3.2.2 Apico-basal polarity defects in *egl* and *BicD* mutant neuroblasts are indicative of reduced Insc activity

3.2.2.1 Aberrant neuroblast division orientation

Insc needs to be localised apically for it to function in apico-basal orientation of neuroblast division and targeting of basal determinants, such as Mira and Pros (Knoblich et al., 1999; Tio et al., 1999). To test if reductions in apical Insc localisation affected Insc activity, I examined whether any of these processes were disrupted in *egl* and *BicD* mutant embryos. In wild-type anaphase and telophase

neuroblasts, all cell divisions are orientated within 45° of the apico-basal axis (Figure 3.2A, G). By contrast, 12% of anaphase and telophase neuroblast mitoses are more than 45° off-axis in *insc* homozygous mutant embryos (Figure 3.2C, G). A similar frequency of neuroblast division misorientation is seen in *egl* and *BicD* mutant embryos (12% and 13%, respectively; Figure 3.2B, G), suggesting that Insc activity is markedly reduced in neuroblasts where *insc* transcript localisation is perturbed.

3.2.2.2 Disruption of basal Mira targeting

Further evidence of reduced Insc function in *egl* and *BicD* mutant neuroblasts comes from examination of Mira protein, which responds to *insc* activity by localising in basal crescents that underlie the basal spindle pole (referred to as a 'coupled' Mira crescent and mitotic spindle pole; (Kraut et al., 1996). All Mira crescents are coupled in wild-type metaphase neuroblasts (Figure 3.2D, H) but, in homozygous $insc^{22}$ neuroblasts, Mira forms crescents that are often incorrectly localised with respect to the mitotic spindle pole ('uncoupled'; 28%; Figure 3.2E, H; (Kraut et al., 1996). Mira crescents are also uncoupled in *egl* (15%) and *BicD* mutants (16%), although, as in *insc* mutants (Schober et al., 1999), telophase rescue correctly segregates Mira into future GMCs in *egl* and *BicD* neuroblasts (Figure 3.2A-C).

Interestingly, *insc*/+ embryos exhibit similar phenotypes to *egl* and *BicD* mutant neuroblasts; 13% of neuroblasts in *insc*/+ embryos are misoriented (Figure 3.2G), and 19% of Mira crescents are uncoupled (Figure 3.2H). This unexpected haplo-insufficiency provides further evidence that the effects of delocalising *insc* transcripts are to reduce apical Insc activity.

Figure 3.2 Defects in apico-basal polarity and metaphase spindle length in *egl*, *BicD* and *insc* mutant neuroblasts.

Examples of neuroblasts in stage 8-11 wild-type, *egl* or *BicD* mutant and $insc^{22}$ homozygous mutant embryos co-stained with anti-Mira and anti-Centrosomin. Dashed circles indicate the location of representative neuroblasts. Arrowheads indicate position of centrosomes. **(A-C)** Telophase neuroblasts showing normal division orientation along the apico-basal axis in **(A)** wild-type embryos, whereas divisions are often misoriented in **(B)** *egl* or *BicD* mutants and **(C)** $insc^{22}$ homozygous mutants. Mira segregates correctly into future GMCs at telophase in *egl* or *BicD*, and $insc^{22}$ mutants (Schober et al., 1999). **(G)** Quantification of division orientation of telophase neuroblasts in wild-type, *egl*, *BicD* and $insc^{22}$ mutant embryos. Each sector of the quadrant corresponds to an angle of 22.5° and vertical axis represents the apico-basal axis of the embryo. Values indicate % of telophase neuroblasts dividing at these angles and n=number of neuroblasts scored. **(D-F)** Metaphase neuroblasts showing examples of relationships between the Mira crescent and the basal centrosome. **(D)** coupled: basal Mira crescent underlying the basal centrosome. **(E)** uncoupled: basal Mira crescent not underlying either centrosome. **(F)** cortical: Mira localised to the entire cell cortex. The frequency at which each Mira localisation phenotype is observed in wild-type, *egl*, *BicD* and $insc^{22}$ mutant embryos is shown in **(H)**. The position of the centrosomes in **(D)** illustrates the length of a wild-type metaphase spindle. Positions of centrosomes in **(E)** and **(F)** illustrate shortened metaphase spindles seen frequently in *egl*, *BicD* and $insc^{22}$ mutant embryos. **(I)** Mean metaphase spindle lengths in wild-type, *egl*, *BicD*, $insc^{22}$, heat-shocked (hs) wild-type (+/+ hs) embryos and *hs-insc; egl* mutant embryos. Spindle lengths are represented as a ratio of the neuroblast cell diameter. Error bars indicate standard error of the mean. ***, P=value is significantly different ($P<0.001$) compared to wild-type or as indicated otherwise. Number of neuroblasts scored is shown above bars. Scale bar in **(F)** = 35 μm (A-C); 15 μm (D-F).

Figure 3.2

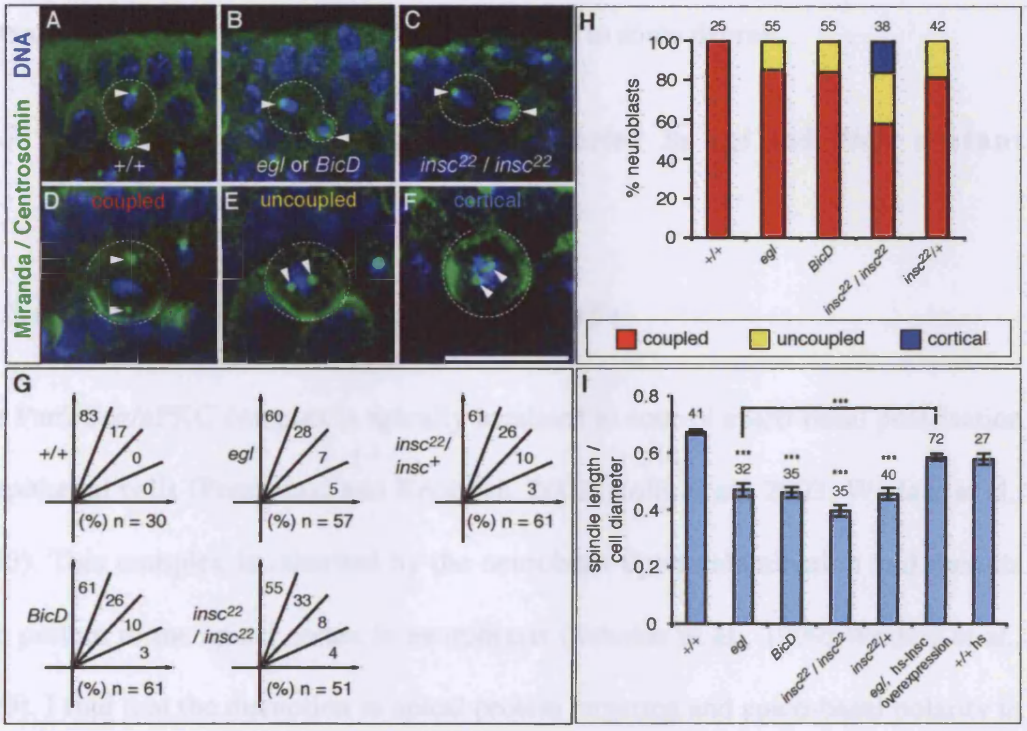
A
B
C
D
E
F
H
I
G
DNA
Miranda / Centrosomin
+/+
egl or BicD
insc22 / insc22
coupled
uncoupled
cortical
% neuroblasts
25
55
55
38
42
+/+
egl
BicD
insc22 / insc22
insc22/+
coupled
uncoupled
cortical
spindle length / cell diameter
41
32
35
35
40
72
27
egl
BicD
insc22 / insc22
insc22/+
egl, hs-Insc overexpression
+/+ hs
+/+
83
17
0
0
(%) n = 30
egl
60
28
7
5
(%) n = 57
insc22/ insc+
61
26
10
3
(%) n = 61
BicD
61
26
10
3
(%) n = 61
insc22 / insc22
55
33
8
4
(%) n = 51

Insc activity is not lost completely in *egl* and *BicD* embryos because I never see a stronger Mira phenotype found in homozygous but not heterozygous *insc* embryos, in which Mira protein is localised around the entire cell cortex (cortical; 16%; Figure 3.2F, H; (Kraut et al., 1996). This shows that *egl* and *BicD* mutant neuroblasts retain some Insc activity, consistent with the fact that the majority of neuroblasts, in these mutants, exhibit apical enrichment of Insc protein to some degree.

3.2.3 Apico-basal polarity appears unaffected in *egl* and *BicD* mutant epithelial cells.

3.2.3.1 Par6 and Baz localisation in epithelial cells

The Par6/Baz/aPKC complex is apically localised to control apico-basal polarisation of epithelial cells (Petronczki and Knoblich, 2001; Rolls et al., 2003; Wodarz et al., 2000). This complex is inherited by the neuroblast upon delamination and recruits Insc protein to the apical cortex in neuroblasts (Schober et al., 1999; Wodarz et al., 2000). I find that the disruption to apical protein targeting and apico-basal polarity in neuroblasts is not inherited from epithelial cells prior to delamination. Apical Par6 (section 3.2.1.3; Figure 3.1D, F) and Baz (Figure 3.3) localisation is unaffected in epithelial cells of either *egl* or *BicD* mutants. Therefore, it appears that aberrant apico-basal polarisation occurs specifically in the neuroblast, suggesting that it results from a failure to efficiently target Insc protein when localisation of *insc* mRNA transcripts is disrupted.

Figure 3.3 Normal apico-basal polarisation of *egl* and *BicD* mutant epithelial cells.

Stage 8-11 wild-type, *egl* and *BicD* mutant embryos co-stained with antibodies against Crb (red) and Baz (green). DNA is labelled in blue. Crb (arrowheads) and Baz (arrows) localise to the apical cell cortex in epithelial cells in wild-type, *egl* and *BicD* embryos. 20 embryos of each genotype were scored for Crb and Baz localisation in epithelial cells. Scale bar = 25μm.

Figure 3.3

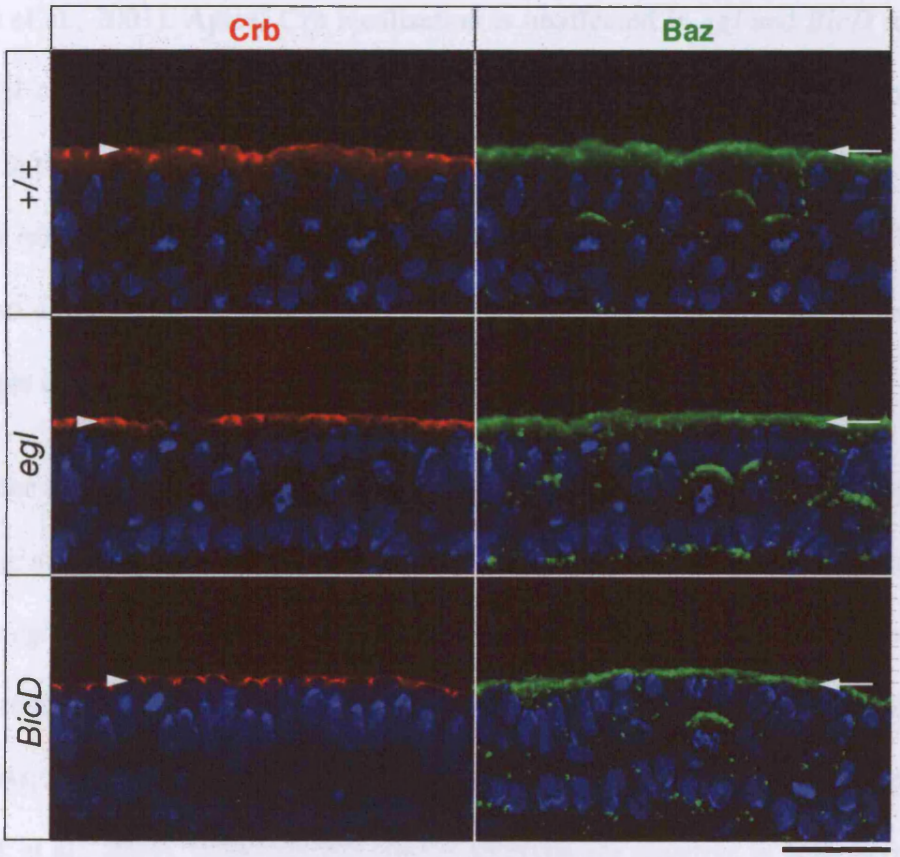

3.2.3.2 Crb localisation and function in epithelial cells

The *crb* gene is also required to direct apico-basal polarisation of epithelial cells (Tepass et al., 2001). Apical Crb localisation is unaffected in *egl* and *BicD* mutant epithelial cells (Figure 3.3) providing further evidence that apico-basal polarity defects in these mutant embryos are specific to the neuroblast. In chapter 2, I show that *crb* mRNA localisation is disrupted in *egl* and *BicD* mutant embryos (Figure 2.9), indicating that asymmetric localisation of endogenously expressed *crb* transcripts is not required to target Crb protein in epithelial cells.

To further investigate the requirement of *crb* mRNA localisation in supporting Crb targeting and activity, I performed genetic interaction experiments to determine whether *egl* mutants embryos were sensitive to *crb* gene dosage. In embryos from *egl* mutant mothers, apical localisation of pair-rule genes is also abolished (Bullock et al., 2004); e.g. *ftz,* Figure 3.4E, F), but segmentation is only slightly impaired (Bullock et al., 2004). However, *egl* mutant embryos are sensitive to heterozygosity for pair-rule genes, suggesting that the apical localisation of pair-rule mRNA transcripts enhances their activity (Bullock et al., 2004). In similar genetic interaction experiments, I find that *egl* mutant embryos are not sensitive to reductions in *crb* gene dosage. Thus, crb^{11A2}/+ 1st instar larvae from *egl* mutant mothers do not display any increase in cuticular defects compared to control larvae from a reciprocal cross and there is no significant increase in the proportion of larvae displaying absence of larval cuticle (Table 3.1). Taken together, these data indicate that *crb* mRNA localisation does not significantly enhance Crb protein localisation or Crb activity with respect to the polarisation of embryonic epithelial cells.

Figure 3.4 Metaphase spindle lengths are unaffected in *egl* mutant syncytial blastoderm embryos.

(A-D) Tangential views of the surface of wild-type and *egl* mutant syncytial blastoderm embryos during mitosis, stained to visualise centrosomes (green) and DNA (blue) along with **(A, B)** the cell cortex (red; anti-phosphotyrosine) or **(C, D)** mitotic spindles (red; anti-β-Tubulin). At metaphase, similar spindle lengths are observed between wild-type and *egl* mutant embryos. 30 embryos of each genotype were examined. **(E)** *ftz* mRNA transcripts localise to the apical cytoplasm in wild-type syncytial blastoderm embryos (arrow). **(F)** *ftz* mRNA localisation is disrupted in *egl* mutant blastoderm embryos and *ftz* is detected in the basal cytoplasm (arrowhead; 10/10 cycle 14 blastoderm embryos). Scale bar = 100μm (A-D); 50μm (E, F).

Figure 3.4

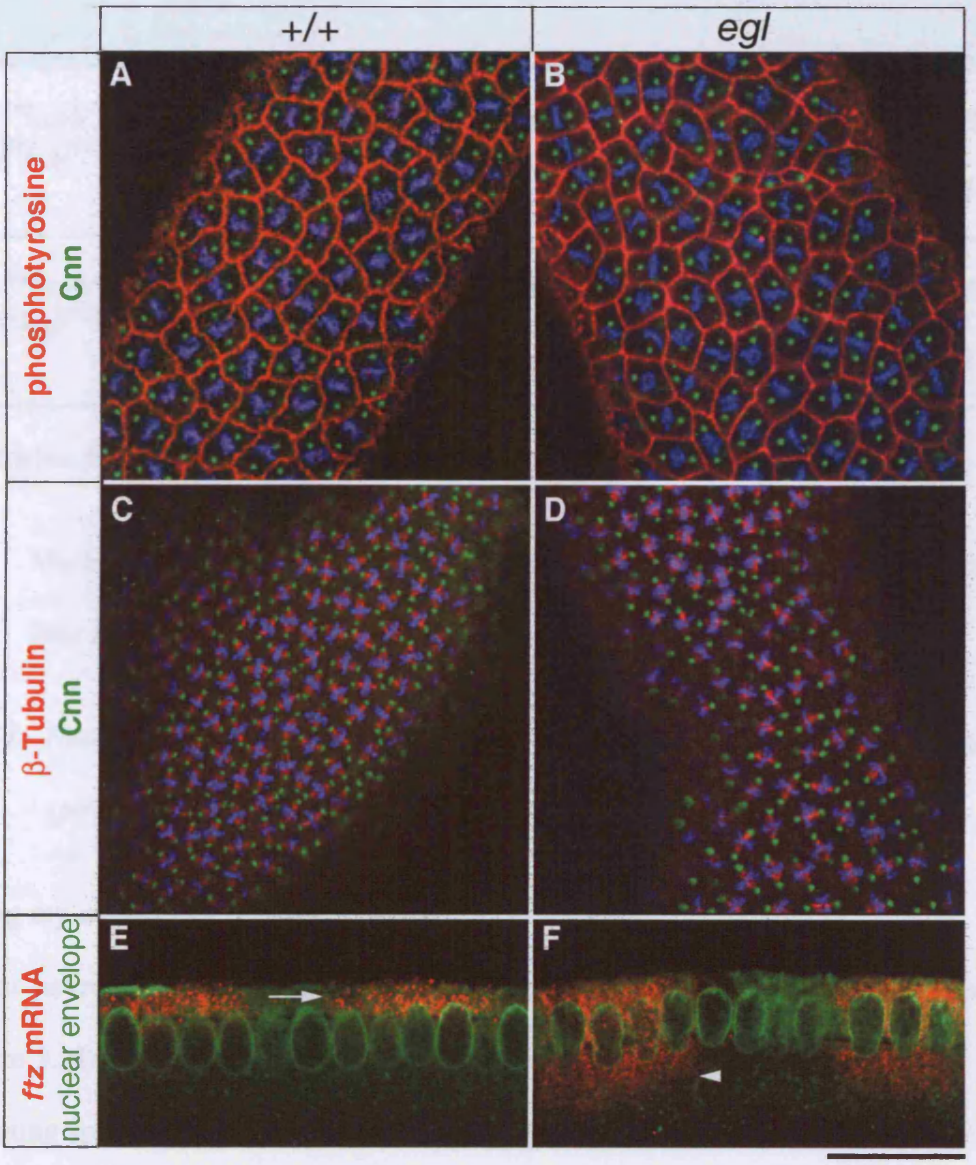
+/+
egl
A
B
C
D
E
F
phosphotyrosine
Cnn
β-Tubulin
Cnn
ftz mRNA
nuclear envelope

Table 3.1 Analysis of cuticle patterning in heterozygous *crb* mutant 1st instar larvae

crb^{11A2}/crb^{+} (M) x egl^{3e}/egl^{WU50} (F)	Normal patterning	100	92%
	Patches of cuticle or denticle missing	9	8%
crb^{11A2}/crb^{+} (F) x egl^{3e}/egl^{WU50} (M)	Normal patterning	183	96%
	Patches of cuticle or denticle missing	7	4%

M = males, F = females. This difference in not statistically significant P = 0.1109.

3.2.4 Metaphase spindle length in neuroblasts is controlled by dose-dependent Insc activity

3.2.4.1 Neuroblasts in egl, BicD *and* insc *mutants have shortened metaphase spindles*

During my analysis of *egl* and *BicD* embryos, I observed that the mitotic spindles in mutant neuroblasts are an average of 30% shorter than in wild-type neuroblasts (Figure 3.2I). This effect is unlikely to be due to a direct role of Egl and BicD in regulating spindle length, because metaphase spindles are not overly affected in *egl* mutant blastoderm embryos (Figure 3.4A-D), whereas pair-rule mRNA localisation is severely disrupted (Bullock et al., 2004); e.g. *ftz*, Figure 3.4E, F). Rather, this defect in *egl* and *BicD* mutant neuroblasts appears to reflect a previously unreported requirement for Insc function in augmenting spindle length at metaphase, as $insc^{22}$ homozygous mutant neuroblasts display a more severe shortening of the metaphase

spindle than *egl* and *BicD* mutants (average spindle length reduced by 41% compared to wild-type; Figure 3.2F, I).

Defects in spindle length are also observed in neuroblasts of $insc^{22}$/+ embryos (average spindle length reduced by 32%; Figure 3.2I) indicating that metaphase spindle length is controlled by dose-dependent Insc activity. Similar effects on metaphase spindle length are observed in an independent *insc* allele ($insc^{P72}$; Appendix A).

Spindle asymmetry in *egl* and *BicD* and *insc* mutant neuroblasts is restored by telophase, leading to the production of unequal sized daughter cells (Figure 3.5; (Cai et al., 2003). The transience of this defect in spindle length indicates that the shortened metaphase spindles are not due to widespread disruption of spindle assembly or microtubule integrity, consistent with normal microtubule distribution observed in *egl* and *BicD* mutant interphase neuroblasts and epithelial cells (Figure 2.10). No differences in neuroblast cell diameter or cell shape were observed between wild-type, *egl*, *BicD* or *insc* mutant embryos (Table 3.2), indicating that defects in normalised spindle length are not due to irregular neuroblast morphology.

Figure 3.5 Asymmetric mitotic spindles at telophase in wild-type, ***egl*** and ***BicD*** mutant neuroblasts.

(A) Examples of telophase neuroblasts from wild-type and ***egl*** mutant embryos co-stained for Miranda and Centrosomin. DNA is shown in blue. Horizontal and vertical white lines indicate approximate position of cleavage plane and mitotic spindle axis, respectively. Dashed circles indicate the outline of representative telophase neuroblasts. **(B)** Quantitative analysis of spindle asymmetry in telophase neuroblasts. Values are calculated as described. **(C)** Bar graph indicates spindle asymmetry in telophase neuroblasts in wild-type, ***egl*** and ***BicD*** mutant embryos. 25 telophase neuroblasts were scored for each genotype. Error bars indicate standard error of the mean. Scale bar in **(A)** = 10μm.

Figure 3.5

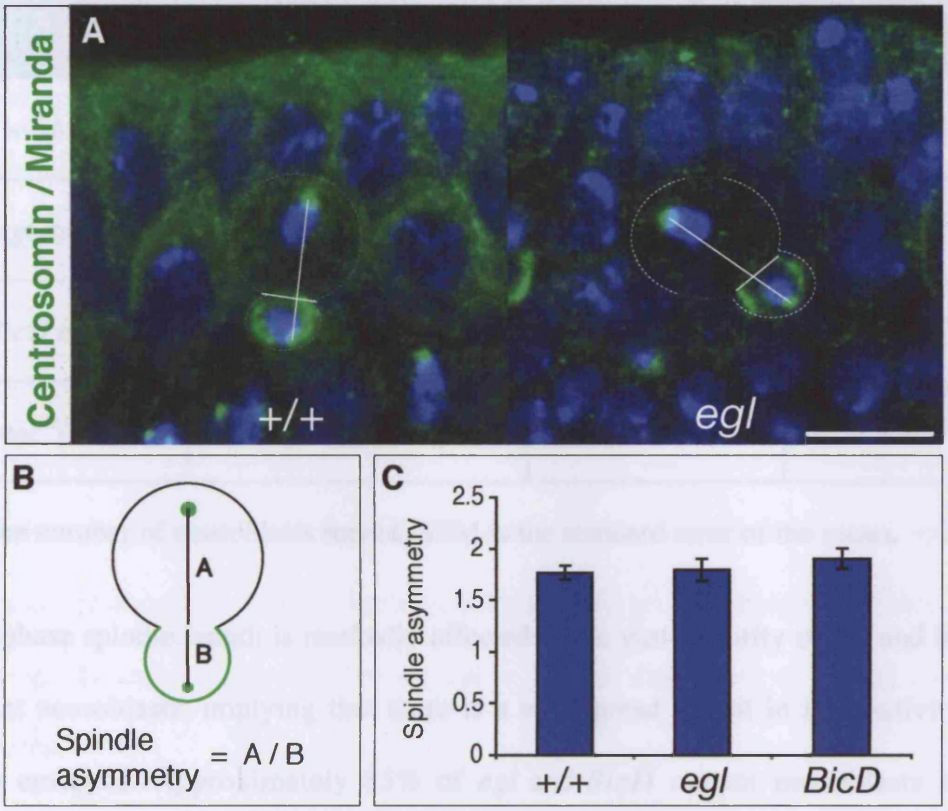
A
Centrosomin / Miranda
+/+
egl
B
A
B
Spindle asymmetry = A / B
C
Spindle asymmetry
2.5
2
1.5
1
0.5
0
+/+
egl
BicD

Table 3.2 Neuroblast cell diameters are unaffected in stage 8-10 *egl*, *BicD* and *insc* mutant embryos

wild-type	11.44	0.194	41
egl mutant	11.47	0.177	32
BicD mutant	10.91	0.195	35
$insc^{22}/insc^{22}$	10.93	0.183	35

n is the number of neuroblasts scored. SEM is the standard error of the mean.

Metaphase spindle length is markedly affected in the vast majority of *egl* and *BicD* mutant neuroblasts, implying that there is a widespread deficit in Insc activity in these embryos. Approximately 85% of *egl* and *BicD* mutant neuroblasts have metaphase spindles that are shorter than the shortest observed wild-type spindle, indicating that *insc* activity is reduced even in those cells where Insc protein appears strongly enriched apically by immunostaining (~45%, Figure 3.1K). My analysis of *egl, BicD* and *insc*/+ mutant embryos shows that levels of apically localised Insc are critical for activity, and thus it seems likely that disrupting *insc* mRNA localisation reduces the efficiency of apical Insc protein targeting in all neuroblasts.

To show that polarity and spindle length defects were not due to differences in genetic background, I performed control experiments and find that neuroblasts in

embryos produced by egl^{3e}/+ and egl^{WU50}/+ flies do not display shortened metaphase spindles (Appendix A).

3.2.4.2 *Overexpression of Insc augments metaphase spindle length in* egl *mutant embryos*

Further experiments indicate that reductions in Insc activity cause metaphase spindle shortening in *egl* and *BicD* mutants. Overexpression of Insc, using a heat-shock inducible promoter, can significantly augment spindle lengths in *egl* mutant neuroblasts, producing metaphase spindles that are similar in length to those in neuroblasts in heat-shocked wild-type embryos (Figure 3.2I). Shortened spindles are still observed in *egl* mutant embryos that are simply subjected to the heat-shock treatment (Appendix A). These data, together with unaltered metaphase spindle length in *egl* mutant blastoderm embryos (Figure 3.4), provide further evidence that shortened metaphase spindles are not due to a more direct role of Egl in spindle dynamics.

Metaphase spindle length is not increased by overexpression of Insc in wild-type neuroblasts, compared to heat-shocked wild-type embryos (Appendix A), possibly because there are physical limitations on the maximum length of metaphase spindles in neuroblasts.

Heat-shock treatment drives *insc* expression throughout the embryo. For example, Insc is enriched in the apical cytoplasm in epithelial cells, outside the PNR, in both wild-type and *egl* mutant embryos (Figure 3.1G, H). Heat-shock induced overexpression of Insc partially rescues apical levels of Insc protein in *egl* mutant neuroblasts. Strong apical Insc enrichment is detected in 61% of metaphase

neuroblasts in *egl* mutant embryos that overexpress Insc, compared to 45% ($P<0.05$) of metaphase neuroblasts in *egl* mutant embryos that have been subjected to heat-shock treatment (Figure 3.1K). This data indicates that increased levels of apically localised Insc protein may be responsible for the observed rescue of metaphase spindle length defects in *egl* mutant neuroblasts.

3.2.4.3 Testing the function of insc *mRNA localisation by genetic interaction experiments*

Disruption of neuroblast division orientation, basal Mira targeting and metaphase spindle length strongly suggests that Insc activity is reduced in *egl* and *BicD* mutant neuroblasts due to a requirement for apical transport of endogenous *insc* transcripts for efficient Insc protein localisation. To test this idea, I performed genetic interaction experiments to determine whether *egl* mutants are sensitive to reductions in *insc* gene dosage.

Embryos with one functional copy of *insc* and laid by egl^{3e}/egl^{WU50} mutant mothers display significantly shortened metaphase spindle length neuroblasts compared to heterozygous $insc^{22}$ mutant control embryos ($P<0.05$; Table 3.3). However, this difference in spindle length appears to be due to differences in genetic background, as *insc*/+ embryos laid by wild-type mothers also have shorter metaphase spindles in neuroblasts compared to embryos from a reciprocal cross ($P<0.05$; Table 3.3). Therefore, I am unable to provide more evidence, using genetic interaction experiments, that reductions in apical Insc activity in neuroblasts are due directly to the loss of *insc* mRNA localisation.

Table 3.3 Metaphase spindle length analysis to test genetic interaction between *insc* and *egl.*

egl^{3e}/egl^{WU50} mothers x $insc^{22}/insc^{+}$ males	0.458	0.0122	36
$insc^{22}/insc^{+}$ mothers x egl^{3e}/egl^{WU50} males	0.494	0.0102	51
wild-type mothers x $insc^{22}/insc^{+}$ males	0.433	0.0175	38
$insc^{22}/insc^{+}$ mothers x *wild-type* males	0.508	0.0191	32

For each cross, the zygotic genotype of scored embryos is $insc^{22}/insc^{+}$. n is the number of neuroblasts scored. SEM is the standard error of the mean.

3.2.5 Examination of Insc protein levels in *egl* mutant embryos.

Recent work has provided evidence that Egl has additional functions that are independent of microtubules (section 1.2.1.4; (Huynh and St Johnston, 2000; Navarro et al., 2004), which may involve regulation of translation. Therefore, I attempted to test whether defects in the efficiency of Insc translation contributed to the observed reduction in Insc activity in neuroblasts in *egl* mutant embryos.

Despite trying many conditions, I have been unable to detect Insc protein specifically using the available anti-Insc antibodies, as these antibodies recognise multiple bands on Western blots (Figure 3.6). Insc has been reported to migrate as a band of

approximately 100kDa on Western blots (Irion et al., 2004; Li et al., 1997). To determine if any of the bands corresponded to Insc, lysates from embryos in which Insc has been overexpressed, under the control of a heat-shock inducible promoter (*hs-insc*), were Western blotted. None of the bands were enhanced when Insc protein is highly overexpressed (Figure 3.6), although overexpressed Insc can be readily detected in embryos by immunohistochemistry (Figure 3.1G, H). Therefore, the specific Insc band could not be distinguished by Western blotting of extracts from embryos that overexpress Insc protein.

I also tested whether decreases in the strength of any band could be detected in a lysate from embryos produced by an *insc* heterozygous mutant stock. However, none of the bands recognised by the anti-Insc antibody was decreased, compared to lysates from wild-type embryos (Figure 3.6). One band in this blot, migrating at around 100kDa is weakened. However, this appears to be due to unequal loading as other bands exhibit a similar decrease (arrowheads, Figure 3.6). Therefore, in my hands, Insc cannot be detected specifically on Western blots, making it impossible to assess whether there are differences in Insc protein levels between wild-type and *egl* mutant embryos. Nonetheless, no overt difference in the strength of any band was observed between stage-matched wild-type and *egl* mutant embryos (Figure 3.6). However, I am unable to rule out that the reduced Insc protein activity is due to decreased Insc protein levels in *egl* mutant embryos.

Figure 3.6 Insc protein levels cannot be determined by Western blotting.

Example of an Insc Western blot. Amount of protein loaded in each lane corresponded to lysate extracted from 10 embryos, at embryonic stages 8-11. Lysates were from: wild-type embryos subjected to heat-shock treatment (hs +/+); embryos overexpressing Insc under the control of a heat-shock inducible promoter (hs Insc); non-heat-shocked wild-type embryos (+/+) and embryos produced by an *insc*/+ mutant stock. Extracts from stage-matched wild-type and *egl* mutant embryos were also Western blotted with the Insc antibody (see methods for details of stage matching). Relative molecular weights are indicated on the left (kDa). Arrowheads indicate weakened bands in the *insc*/+ lane, which appears to be due to unequal loading.

Figure 3.6

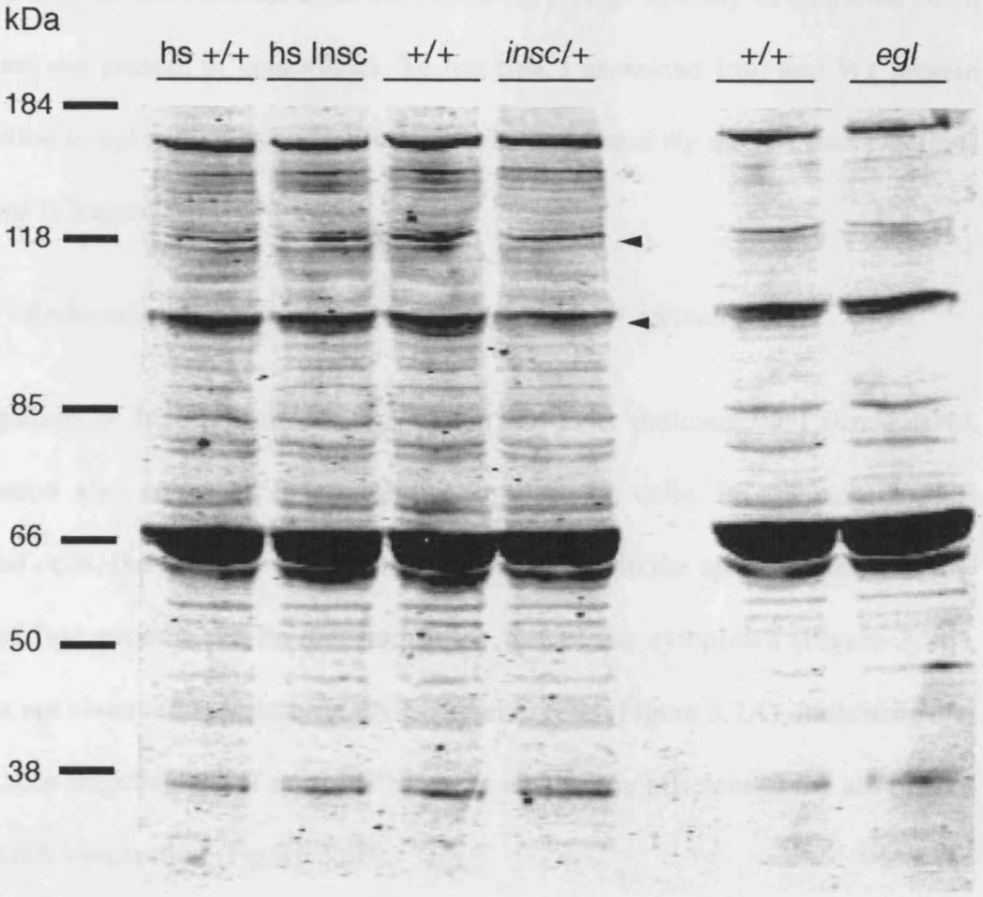

3.2.6 Reduced apical Insc and Wg targeting in *egl* mutants epithelial cells

In this chapter, I have provided evidence that mRNA localisation acts to enhance protein targeting in neuroblasts. However, in epithelial cells the localisation of *crb* mRNAs does not appear to be important for Crb targeting. One possible explanation is that additional mechanisms exist for localising protein apically in epithelial cells, which are not present in neuroblasts. To test this, I examined Insc and Wg protein localisation in *egl* mutant epithelial cells, in which *insc* and *wg* mRNA localisation is abolished (Chapter 2).

3.2.6.1 Reduced apical Insc protein localisation in PNR epithelial cells

Investigation of Insc protein localisation in the PNR indicates that *insc* mRNA localisation also enhances Insc targeting in epithelial cells. In *egl* mutant PNR epithelial cells, the majority of Insc protein is localised to the apical cortex, but low levels of Insc protein can be detected in the rest of the cytoplasm (Figure 3.7B), which is not observed in wild-type PNR epithelial cells (Figure 3.7A), indicating that Insc protein targeting in *egl* mutant PNR cells is not fully efficient in the absence of *insc* mRNA localisation (Figure 2.6B).

Figure 3.7 Apical Insc targeting is disrupted in *egl* mutant PNR epithelial cells.

Examples of PNR epithelial cells in stage 8-11 wild-type and *egl* mutant embryos stained for Insc protein and DNA. Insc is enriched at the apical cell cortex in PNR epithelial cells in both wild-type and *egl* mutant embryos (arrows). Insc protein is often detected at low levels in the rest of the cytoplasm in *egl* mutant embryos (arrowheads; 8/10 embryos) but not in wild-type embryos (10/10 embryos). Scale bar = 15μm.

Figure 3.7

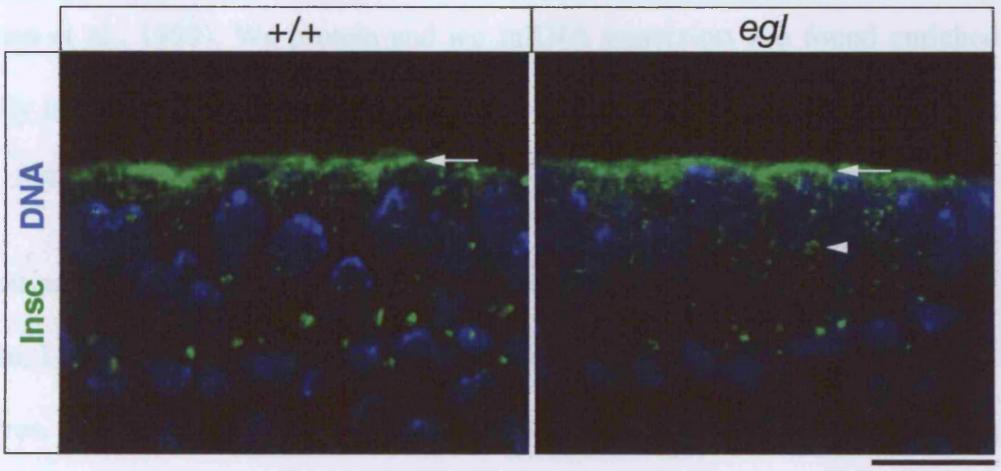

3.2.6.2 Disruption of Wg localisation, but not activity, in epithelial cells

Wg is a secreted glycoprotein, and activates signalling cascades in neighbouring epithelial cells in the *Drosophila* embryo to control embryonic patterning (Wodarz and Nusse, 1998). As a secreted protein, Wg is directed to the apical cytoplasm within specialised vesicles (Ikonen and Simons, 1998; Simons and Ikonen, 1997; Yeaman et al., 1999). Wg protein and *wg* mRNA transcripts are found enriched apically in epithelial cells (Figure 2.6A, 3.8A; (Baker, 1987; Baker, 1988; Gonzalez et al., 1991).

To test whether localisation of endogenous *wg* mRNA is required to target Wg protein, I examined Wg distribution in epithelial cells and neuroblasts in *egl* mutant embryos, in which *wg* mRNA localisation is abolished (Figure 2.8). Wg protein is enriched apically in wild-type epithelial cells, although Wg can also be detected at low levels throughout the cell (Figure 3.8A). In *egl* mutant epithelial cells, the apical concentration of Wg protein is reduced, resulting in higher levels of Wg throughout the epithelial cell (Figure 3.8B), suggesting that *wg* mRNA localisation is required for efficient apical targeting of Wg protein.

I performed genetic interaction experiments to determine whether *egl* mutant embryos were sensitive to *wg* gene dosage. No significant increase in the frequency of cuticular patterning defects was observed in wg^{CX4}/wg^{+} 1st instar larvae from *egl* mutant mothers compared to heterozygous *wg* mutant larvae generated from a reciprocal cross (wg^{CX4}/wg^{+} females crossed with egl^{3e}/egl^{WU50} males; Table 3.4). This data suggests that the apical localisation of *wg* mRNA and Wg protein is not

absolutely required to support Wg signalling with respect to patterning of the *Drosophila* embryo.

Table 3.4 Analysis of cuticle patterning in heterozygous *wg* mutant 1st instar larvae

wg^{CX4}/wg^{+}	Normal patterning	154	94.5%
(from egl^{3e}/egl^{WU50} mothers)	Patches of cuticle or denticle missing / fused denticle belts	9	5.5%
wg^{CX4}/wg^{+}	Normal patterning	271	97.8%
(from wg^{CX4}/wg^{+} mothers)	Patches of cuticle or denticle missing / fused denticle belts	6	2.2%

This difference is not statistically significant, P = 0.099. n =number of larvae scored.

Figure 3.8 Apical Wg targeting is disrupted in *egl* mutant epithelial cells.

Examples of *wg* expressing epithelial cells in stage 8-11 wild-type and *egl* mutant embryos stained for Wg protein and DNA. **(A)** Wg is enriched apically in wild-type epithelial cells (30/30) and neuroblasts (arrows), although low levels of Wg are detected throughout the cell (arrowhead). **(B)** Apical enrichment of Wg is reduced in *egl* mutant epithelial cells (26/30) and Wg protein can be detected at higher levels basally (arrowhead). Scale bar = 15μm.

Figure 3.8

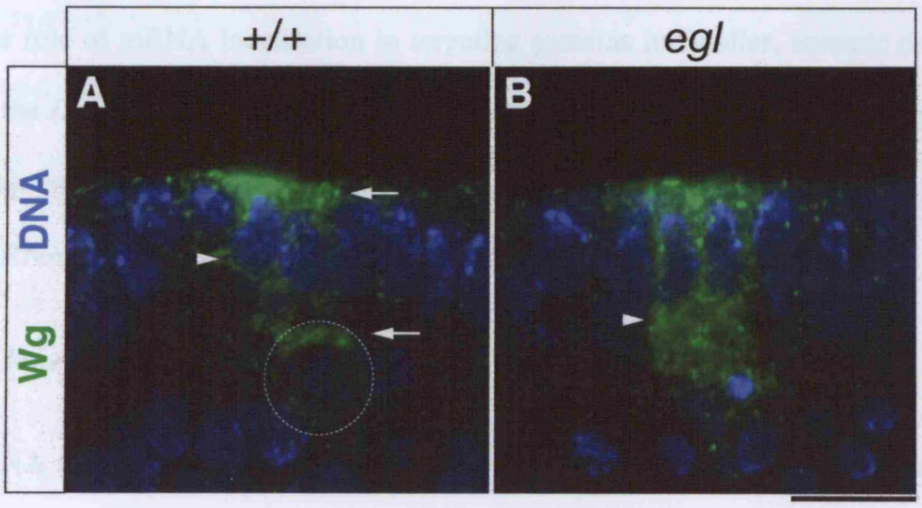

3.3 Discussion

3.3.1 mRNA localisation enhances protein targeting in somatic cells in the *Drosophila* embryo

During *Drosophila* oogenesis and in blastoderm embryos, the localisation of mRNAs has been shown to be required for efficient targeting and function of their protein products (Bashirullah et al., 1998; Bullock et al., 2004). However, little is known about the role of mRNA localisation in targeting proteins in smaller, somatic cells types in the *Drosophila* embryo. To investigate this, I have examined Insc, Crb and Wg protein localisation in neuroblasts and epithelial cells in *egl* and *BicD* mutants, in which mRNA localisation is disrupted.

3.3.1.1 Neuroblasts

insc mRNA transcripts localise apically in *Drosophila* embryonic neuroblasts and epithelial cells (Knirr et al., 1997; Li et al., 1997), but to date the function and developmental significance of this localisation has been unclear. In this chapter, I show that in *egl* and *BicD* mutants, where endogenous *insc* mRNA localisation is perturbed, the efficiency of Insc protein targeting in neuroblasts and PNR epithelial cells is also disrupted, suggesting that localisation of *insc* transcripts to the apical cytoplasm boosts the efficiency of Insc protein targeting in these cells. Insc protein does not appear to be localised apically by Egl directly (section 3.2.1.2), providing further evidence that *insc* mRNA localisation acts to enhance Insc targeting. Therefore, mRNA localisation may be a general mechanism that promotes efficient targeting of proteins to their sites of activity in a wide range of somatic cell types in *Drosophila*.

Despite the severe defects in asymmetric *insc* mRNA localisation in *egl* and *BicD* mutants, the majority of neuroblasts (~90%) display some enrichment of Insc protein apically (Figure 3.1K), and only weak reductions in efficiency of Insc localisation are detected in *egl* mutant PNR epithelial cells (Figure 3.7). This suggests that additional, Egl/BicD-independent mechanisms are used to target Insc protein apically. This conclusion is also supported by the ability of truncated non-localising *insc* transcripts to direct expression of apically enriched Insc protein in epithelial cells and neuroblasts (Figure 3.1G, H; (Knoblich et al., 1999; Tio et al., 1999). In the absence of *insc* mRNA localisation, Insc protein localisation to the apical cell cortex may occur by diffusion and anchorage to other apically localised factors, including Baz and Pins, with which it can associate *in vivo* (Schaefer et al., 2000; Schober et al., 1999; Wodarz et al., 1999; Yu et al., 2000).

In *egl* and *BicD* mutant neuroblasts, disruption of Insc and Par6 localisation occurs at similar frequencies, consistent with their previously known interdependence for apical localization in mitotic neuroblasts (Petronczki and Knoblich, 2001). Neuroblasts lacking apical Par6 are still able to localise Insc (Rolls et al., 2003), suggesting that disruption of Par6 localisation in *egl* and *BicD* mutants results from reduced efficiency of apical Insc targeting. Par6 localisation defects in mutant neuroblasts cannot be due to a role of Egl and BicD in the localisation of *par6* mRNA, as these transcripts are not asymmetrically localised in wild-type neuroblasts (Petronczki and Knoblich, 2001).

By enhancing apical Insc targeting, *insc* mRNA localisation in neuroblasts may be an important step in re-establishing apico-basal polarity following cell division. During telophase, Insc and other apical complex members are delocalised from the apical

neuroblast cortex (Kraut et al., 1996; Petronczki and Knoblich, 2001; Schober et al., 1999; Wodarz et al., 2000; Wodarz et al., 1999). At the start of the next cell cycle these proteins need to be relocalised to maintain correctly oriented divisions and segregation of cell fate determinants. The cue for apical localisation at the start of the next mitosis is not known, yet, recent reports suggest that the apical cortex is still marked during telophase by the apical localisation of factors, such as Cornetto (Bulgheresi et al., 2001). In addition, *insc* mRNA localisation during interphase may act to target apical production of Insc protein in neuroblasts for rapid re-establishment of the apical complex and apico-basal polarity.

3.3.1.2 Epithelial cells

Asymmetric mRNA localisation also enhances protein targeting in epithelial cells in *Drosophila* embryos. For example, I find that Insc localisation is partially reduced in *egl* mutant PNR epithelial cells, where *insc* mRNA localisation is abolished. This partial disruption of Insc localisation is similar to that observed in *egl* mutant neuroblasts, suggesting that similar mechanisms exist in both cell types to target Insc protein apically when *insc* mRNA localisation is perturbed.

Apical localisation of Wg protein in epithelial cells appears to be very sensitive to delocalisation of *wg* mRNA transcripts (Figure 3.8). I find that Wg is distributed evenly throughout *egl* mutant epithelial cells, suggesting that *wg* mRNA localisation is required to target Wg apically. This is supported by the observation that Wg protein, encoded by non-localising *wg* transcripts, is also evenly distributed throughout epithelial cells (Simmonds et al., 2001). These results also argue against the possibility that Egl participates in dynein-based transport of Wg containing

vesicles, which may also have contributed to the defects in Wg protein targeting in *egl* mutant embryos.

Wg signalling controls segmentation of the Drosophila embryo (reviewed in Wodarz and Nusse, 1998). In *egl* mutant embryos, segmentation is only slightly impaired (Bullock et al., 2004), indicating that sufficient Wg signalling occurs to correctly pattern *egl* mutant embryos, in which apical enrichment of *wg* mRNA and Wg protein is disrupted (Figure 2.8, 3.8). Surprisingly, I also find that patterning phenotypes caused by heterozygosity of *wg* are not enhanced significantly in embryos from *egl* mutant mothers, suggesting that neither apical localisation of *wg* transcripts nor Wg protein in epithelial cells is required to augment Wg signalling in the embryonic epithelium. These experiments do not address the consequence of completely blocking *wg* transcript localisation, as *wg* transcripts and Wg protein are present throughout the cell (Figure 3.8). For example, mistargeting of *wg* transcripts to basal regions of the epithelial cell cytoplasm results in embryonic patterning defects (Simmonds et al., 2001).

In contrast to targeting of Insc and Wg protein, I find that Crb localisation is unaffected in *egl* and *BicD* mutant epithelial cells (Figure 3.3), indicating that apical Crb targeting is not dependent on the localisation of endogenous *crb* mRNA transcripts. This also provides further evidence that epithelial apico-basal polarity is normal in these mutants. Other studies have found that Crb targeting is unaffected in epithelial cells expressing *crb* transgenes that target *crb* mRNA transcripts throughout the cytoplasm or to basal-lateral cytoplasmic regions (Ulli Tepass, personal communication). Furthermore, *egl* mutant embryos are not sensitive to reductions in *crb* gene dose (Table 3.1), suggesting that apical targeting of Crb and

Crb activity in epithelial cells of *egl* and *BicD* mutants is efficient when *crb* mRNA localisation is disrupted.

As a transmembrane protein, apical Crb trafficking is most likely to occur via directed movement of specialised vesicles (Ikonen and Simons, 1998; Simons and Ikonen, 1997; Yeaman et al., 1999), following translation on Rough Endoplasmic Reticulum (ER). In blastoderm embryos, the ER resident chaperone BiP is present throughout the cytoplasm but is more concentrated apically (Lecuit and Wieschaus, 2000). This distribution of the ER is likely to be maintained after blastoderm cellularisation and formation of the peripheral epithelial cell layer. Therefore, Crb may be translated throughout the cytoplasm and transported apically within vesicles, which is able to provide efficient apical targeting of Crb protein in the absence of *crb* mRNA localisation. However, *crb* transcript localisation may enhance Crb translation apically, as the majority of ER appears to be in the apical cytoplasm, or it may represent a requirement for *crb* mRNA localisation in supporting Crb function in other polarised cell types in *Drosophila*.

Similarly, apical Par6 (Figure 3.1) and Baz (Figure 3.3) localisation in epithelial cells does not appear to be affected in *egl* and *BicD* mutant embryos, indicating that disruption of apical Par6 protein localisation occurs only in neuroblasts in these mutants (Figure 3.1). This is consistent with the requirement for Insc in maintaining the apical complex during mitosis (Yu et al., 2000). In mammalian epithelial cells, Par6 is able to directly bind to Sdt, which recruits it to the membrane by simultaneous binding to the Crb homologue, Crb3 (Hurd et al., 2003). Therefore, efficient apical Par6 localisation in *egl* and *BicD* mutant epithelial cells is likely to occur via association with Sdt and Crb.

3.3.2 *insc* mRNA localisation augments apical Insc activity in mitotic neuroblasts

3.3.2.1 Apico-basal polarity

Consistent with reductions in apical Insc localisation, I observe defects in apico-basal polarity and basal Mira targeting in mitotic neuroblasts in *egl* and *BicD* mutants (Figure 3.2), suggesting that apical *insc* mRNA localisation augments apical Insc activity by enhancing Insc protein targeting. These polarity defects are only of partial penetrance, presumably due to the fact that the majority of neuroblasts (~90%) exhibit some apical enrichment of Insc. Nevertheless, the fact that *egl* and *BicD* mutants exhibit polarity defects at similar frequencies to *insc*/+ embryos, provides further evidence that the effect of delocalising *insc* transcripts is to reduce apical Insc activity.

I cannot rule out that defects in the efficiency of Insc translation contribute to the observed reduction in Insc activity (section 3.2.5). I have attempted western blots for Insc, but I am unable to detect Insc protein specifically using the available anti-Insc antibodies. However, in *egl* mutants, levels of protein encoded by other Egl/BicD/dynein mRNA cargoes (pair-rule transcripts) are not altered, arguing against a general role for Egl or apical mRNA localisation in translational regulation (Simon Bullock, personal communication).

It is also possible that an inability to localise other mRNA transcripts, and maybe other cargoes, required for apical complex assembly and/or stability results in defects in apical protein targeting and apico-basal polarity in *egl* and *BicD* mutants. For example, *baz* transcripts are known to localise apically in neuroblasts, which may

help to target Baz protein to the apical complex. It remains to be tested whether *baz* mRNA localisation is also disrupted in *egl* and *BicD* mutants.

3.3.2.2 Metaphase spindle length

I find that metaphase spindle length in neuroblasts is controlled by dose-dependent Insc activity. Metaphase spindle lengths are reduced by 41% in *insc* homozygous mutant neuroblasts and by 32% in *insc*/+ mutant neuroblasts (Figure 3.2). In *egl* and *BicD* mutants, spindle length is reduced by approximately 30% (Figure 3.2). This similarity in the extent of spindle shortening between *egl, BicD* and *insc*/+ mutants, provides further evidence that disrupting *insc* mRNA localisation reduces apical Insc activity.

The rescue of shortened spindles in *egl* mutant neuroblasts, by heat-shock induced overexpression of Insc (Figure 3.2), indicates that Insc acts to control spindle length at metaphase. Indeed, the defects in spindle length are transient, with spindle asymmetry being restored at telophase (Figure 3.5), suggesting that shortened metaphase spindles do not represent a requirement for Egl and BicD in spindle assembly or dynamics or microtubule integrity.

It is unclear how apical Insc activity controls spindle length in metaphase neuroblasts. Insc probably orients mitotic spindles along the apico-basal axis, by regulating cortical attachment of astral microtubules and anchorage of the apical centrosome to direct a 90° spindle reorientation in mitotic neuroblasts and epithelial cells (Bulgheresi et al., 2001; Kaltschmidt et al., 2000; Kraut et al., 1996). Thus, metaphase spindles may be shorter in embryos with reduced *insc* activity (Figure 3.2I) because levels of apical Insc help to determine the strength or number of

interactions between astral microtubules and the cell cortex, thus reducing the pulling forces that attract the apical centrosome.

It appears that both the apical and basal halves of the metaphase spindle are shortened when Insc activity is reduced (*e.g.* Figure 3.2F). Therefore, additional factors must be influencing the length of the central spindle when Insc activity is compromised. Reduced apical pulling forces may be transmitted through the central mitotic spindle by motors that act to pull both the apical and basal centrosomes together. For example, KinC, a minus-end-directed spindle kinesin in yeast, has been found to apply forces that counteract spindle pole separation during anaphase (reviewed in (Wittmann et al., 2001).

Alternatively, the activity of the apical complex may be required for the localisation of factors to the basal neuroblast cortex that enhance the attachment of astral microtubules basally. It is not clear what this basal factor may be, although, Mira appears to have the ability to bind to microtubules as it is found to localise to mitotic spindles and centrosomes when cortical binding is inhibited (Albertson and Doe, 2003; Barros et al., 2003). Shortened metaphase spindles have not been described in *mira* mutant neuroblasts, yet, neuroblast mitotic spindles are often misoriented in mutants for the Myosin VI motor *jag*, which exhibit disruption in basal Mira localisation, but not apical Insc localisation (Petritsch et al., 2003), suggesting that attachment of microtubules to basal Mira may be important in regulating spindle alignment in neuroblasts. However, disruption of spindle orientation may also reflect a role for Myosins in the control of this process (Guo and Kemphues, 1996).

In conclusion, I have provided evidence that the localisation of *insc* transcripts acts with other mechanisms of Insc protein targeting to ensure maximum Insc and apical complex activities, which are crucial for accurate establishment of apico-basal polarity and control of metaphase spindle length in mitotic neuroblasts. My results indicate that Egl/BicD/dynein-dependent mRNA localisation may be employed to target proteins, and generate cellular polarity in a wide-range of small, somatic cell-types.

CHAPTER 4: INVESTIGATING THE MECHANISM OF APICAL *MIRANDA* mRNA LOCALISATION IN *DROSOPHILA* NEUROBLASTS

4.1 Introduction

In Chapter 2, I show that the Egl/BicD/dynein mRNA localisation machinery mediates apical localisation of *insc* transcripts in neuroblasts. In addition to *insc* transcripts, *mira* and *pros* mRNAs also localise apically in neuroblasts. Interestingly, *mira* transcripts are apically localised throughout the cell cycle (Schuldt et al., 1998), whereas, *insc* and *pros* transcripts localise apically only in interphase neuroblasts, suggesting that additional anchorage mechanisms retain *mira* apically during mitosis. During mitosis, Stau and Mira mediate relocation of *pros* mRNA to the basal cortex (Broadus et al., 1998; Li et al., 1997; Matsuzaki et al., 1998; Schuldt et al., 1998). However, the mechanism by which *mira* and *pros* transcripts are localised to the apical cytoplasm in neuroblasts is unknown.

In this chapter, I present preliminary data that focuses on the mechanism of apical *mira* localisation in neuroblasts, which I have attempted to elucidate by RNA injection, *in situ* analysis and by comparison with the localisation characteristics of *pros* mRNA.

Figure 4.1 Apical localisation of *mira* mRNA transcripts in epithelial cells and neuroblasts.

mira mRNA transcripts localise to the apical cytoplasm in neuroblasts and epithelial cells (arrowheads) in wild-type embryos. Scale bar = 15μm.

Figure 4.1

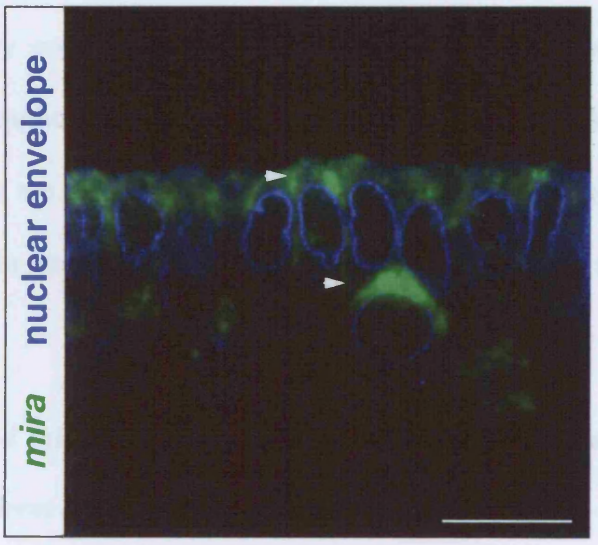

4.2 Results

4.2.1 Investigating the requirement for the Egl/BicD/dynein machinery in apical *mira* mRNA localisation

mira mRNA transcripts are found localised to the apical cytoplasm in neuroblasts and epithelial cells (Figure 4.1), where the Egl/BicD/dynein complex is active (Chapter 2). By contrast to localised *insc* mRNA, apical *mira* localisation is maintained throughout the cell cycle (Schuldt et al., 1998). One possibility is that *mira* transcripts are transported to the apical cytoplasm during interphase, by the Egl/BicD/dynein complex, and then anchored apically by a separate mechanism during mitosis.

4.2.1.1 Injected mira *and* pros *transcripts do not localise apically in syncytial blastoderm embryos*

To test if the Egl/BicD/dynein mRNA transport machinery can mediate localisation of *mira* and *pros* mRNAs, I injected these transcripts into syncytial blastoderm embryos. Injected *insc* transcripts accumulate apically of the peripheral nuclei within 5 minutes (85% of embryos; Figure 4.2A, 2.2C), whereas *mira* and *pros* transcripts fail to localise apically 5 min after injection (Figure 4.2B, C). Injected *mira* transcripts are not localised even after 20 min (Figure 4.2D), showing that failure to localise is not because of slow or inefficient RNA transport, which appears to be the case for injected *crb* (section 2.2.5.4, Figure 2.9) and *osk* RNAs (Bullock and Ish-Horowicz, 2001). These results suggest that *mira* and *pros* RNAs are not recognised and transported apically by the Egl/BicD/dynein mRNA localisation machinery.

Figure 4.2 Injected *mira* and *pros* transcripts do not localise apically in syncytial blastoderm embryos.

(A) *insc* RNAs localise apically within 5 min of injection into blastoderm embryos (arrowhead), whereas injected **(B)** *mira* (15/15 embryos) and **(C)** *pros* (30/30 embryos) transcripts do not localise apically after 5 min and remain within the basal cytoplasm. **(D)** *mira* RNAs and **(D')** control, non-localising *pins* RNAs are not enriched in the apical cytoplasm, 20 min after injection into blastoderm embryos. Merged images are shown in **(D")**. Scale bar = 50μm.

Figure 4.2

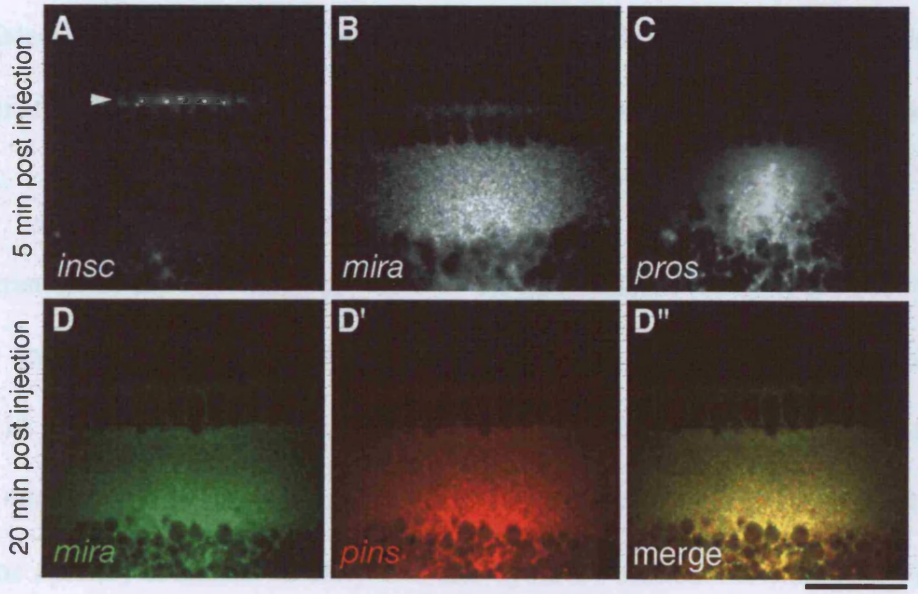
A
B
C
insc
mira
pros
5 min post injection
D
D'
D"
mira
pins
merge
20 min post injection

4.2.1.2 Endogenous mira *transcripts are localised apically in syncytial blastoderm embryos*

The failure of injected *pros* and *mira* RNAs to localise in the injection assay may be because specific factors that mediate their localisation in neuroblasts are not present in blastoderm embryos. Alternatively, *mira* and *pros* mRNAs may need to be associated with specific nuclear factors for localisation. I tested these possibilities by examination of *mira* and *pros* transcripts that are transcribed in the blastoderm nuclei.

mira transcripts are maternally provided to the early embryo (Shen et al., 1997), but newly transcribed, nascent *mira* transcripts can be detected in blastoderm nuclei at cycle 13 (Figure 4.3A), indicating the onset of zygotic *mira* transcription at this stage. *mira* mRNA is detected in the apical cytoplasm at cycle 13 (Figure 4.3A), and remains apically localised in early and late cycle 14 blastoderm embryos (Figure 4.3B, C), suggesting that factors required for apical *mira* localisation are expressed in blastoderm embryos.

Localised *ftz* transcripts appear to occupy the entire apical cytoplasm in blastoderm embryos (Figure 4.3C). By contrast, *mira* transcripts exhibit a different localisation pattern: they are concentrated close to the edge of the blastoderm nuclei and do not extend to the edge of the embryo (Figure 4.3C). This difference in localisation patterns of *mira* and *ftz* mRNA transcripts suggests that they are retained or anchored in the apical cytoplasm by different mechanisms.

Figure 4.3 Endogenously expressed *mira* mRNAs localise apically in syncytial blastoderm embryos.

(A-C) Distribution of *mira* and *ftz* mRNA transcripts in wild-type syncytial blastoderm embryos. Nuclear envelope is labelled in blue. Merged images are shown on the right. **(A)** Zygotic *mira* expression is detected in cycle 13 blastoderm embryos by the presence of newly transcribed *mira* transcripts within blastoderm nuclei (arrowhead). *mira* and *ftz* mRNAs are enriched in the apical cytoplasm at this stage. **(B)** Apical localisation of *mira* and *ftz* is detected in early cycle 14 blastoderm embryos and both transcripts appear to occupy the entire apical cytoplasm. Notice that the striped pattern of *ftz* is resolved at this stage. **(C)** Apical *mira* and *ftz* localisation is maintained in late cycle 14 blastoderm embryos. At this stage, localised *mira* transcripts are more closely associated with the apical edge of the blastoderm nuclei, whereas *ftz* occupies the entire apical cytoplasm (indicated by brackets). *mira* and *ftz* mRNA localisation was examined in at least 10 blastoderm embryos at each stage. Similar distributions of *mira* and *ftz* transcripts are observed using Fast Red and tyramide detection methods. Scale bar = 50μm.

Figure 4.3

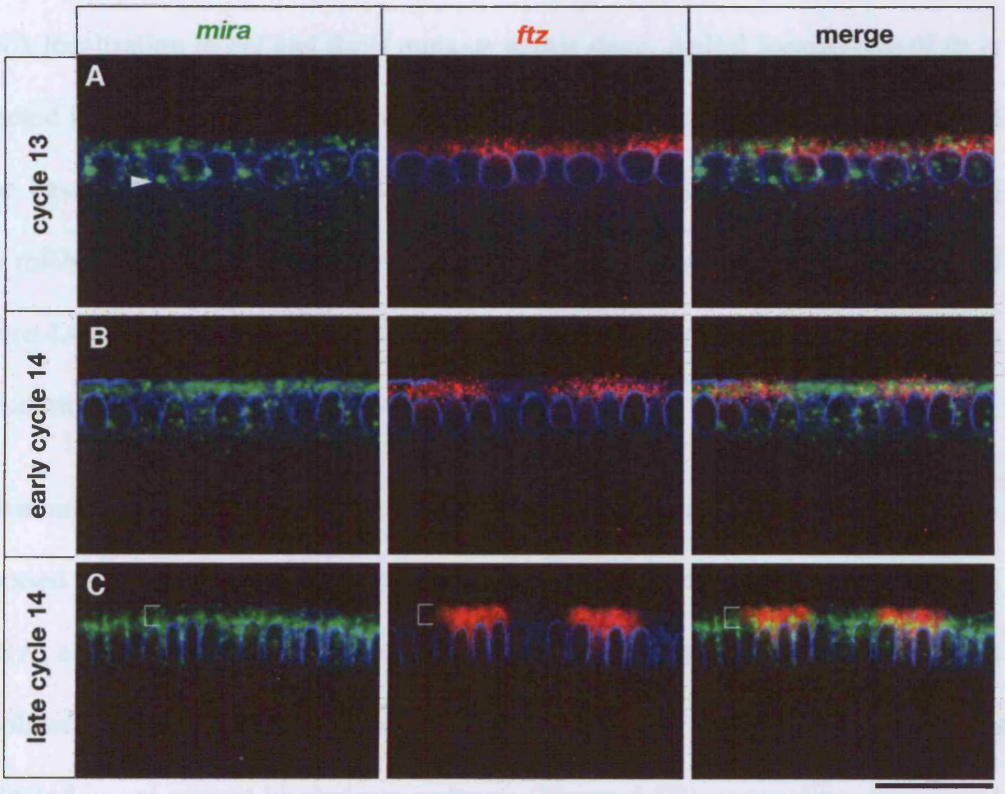

4.2.1.3 Apical localisation of mira *mRNA transcripts in blastoderm embryos does not require Egl and BicD*

I next tested whether the Egl/BicD/dynein machinery is required to transport *mira* transcripts to the apical cytoplasm in blastoderm embryos, by examining *mira* mRNA localisation in *egl* and *BicD* mutants at this stage. Apical localisation of *ftz* is disrupted in *egl* and *BicD* mutant blastoderm embryos and *ftz* transcripts are detected in the basal cytoplasm (Figure 4.4A, B; (Bullock et al., 2004). By contrast, apical *mira* mRNA localisation is unaffected in *egl* and *BicD* mutant blastoderm embryos (Figure 4.4A, B). These results indicate that *mira* transcripts are localised apically in blastoderm embryos, independently of Egl and BicD.

To examine the localisation of *pros* transcripts in blastoderm embryos, I ectopically expressed *pros* under the control of a heat-shock inducible promoter. Similar to *mira* mRNA, ectopically expressed *pros* transcripts are also enriched in the apical cytoplasm in wild-type embryos (Figure 4.5A). *pros* mRNA localisation is unaffected in *egl* mutant blastoderm embryos (Figure 4.5B), suggesting, that apical *pros* transcripts localisation in blastoderm embryos and neuroblasts is also independent of the Egl/BicD/dynein machinery.

Figure 4.4 Apical *mira* mRNA localisation in syncytial blastoderm embryos does not require Egl and BicD.

(A, B) Distribution of *mira* and *ftz* mRNA transcripts in early cycle 14, *egl* and *BicD* mutant syncytial blastoderm embryos. Nuclear envelope is labelled in blue. Merged images are shown on the right. **(A)** Apical *ftz* localisation is disrupted in *egl* mutants, and *ftz* transcripts are detected in the basal cytoplasm (arrowhead). *mira* mRNAs localise apically. **(B)** *ftz* localisation is partially disrupted in *BicD* mutant embryos with *ftz* transcripts enriched apically but also detectable in the basal cytoplasm (arrowhead). Apical *mira* mRNA localisation is normal in *BicD* mutants. These distributions of *mira* and *ftz* mRNAs were observed in 100% of n=10 early cycle 14 blastoderm embryos for each genotype. Scale bar = 30μm.

Figure 4.4

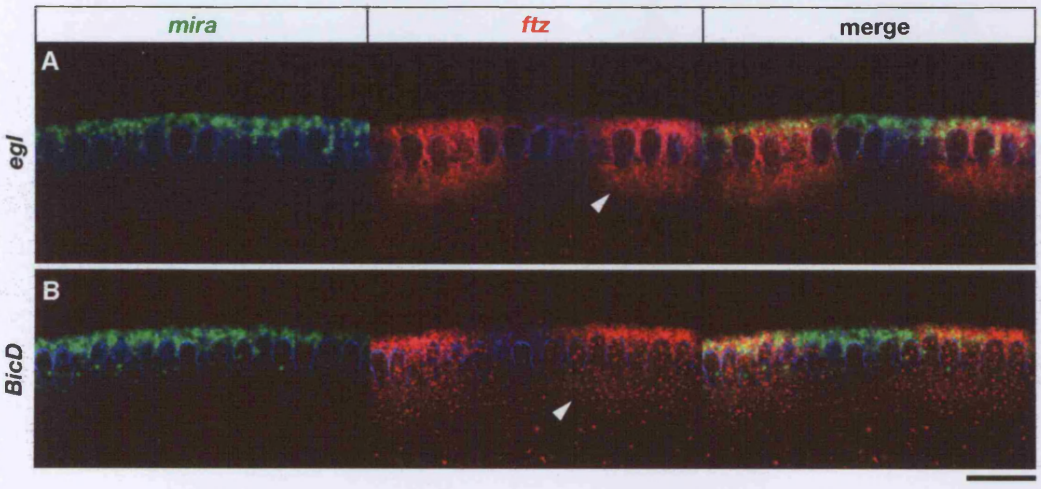

Figure 4.5 Misexpressed *pros* transcripts are enriched apically in wild-type and *egl* mutant blastoderm embryos.

Ectopically expressed *pros* transcripts produced by a heat-shock inducible *pros* transgene *(hs-pros)* are enriched in the apical cytoplasm (arrowheads) in **(A)** wild-type and **(B)** *egl* mutant blastoderm embryos. Scale bar = 30μm.

Figure 4.5

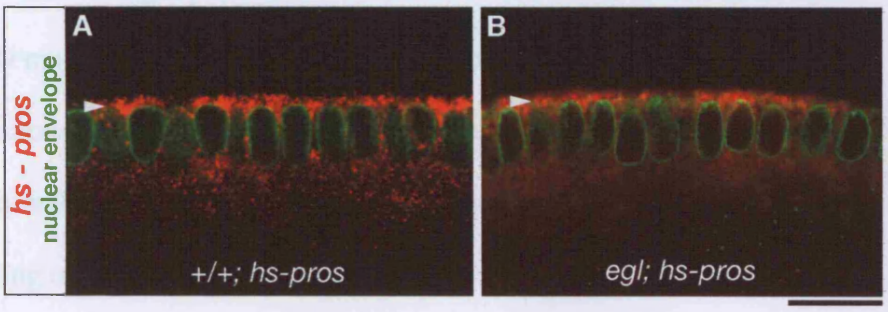

4.2.1.4 Apical localisation of mira *is unaffected in* egl *and* BicD *mutant neuroblasts*

Next I tested whether the Egl/BicD/dynein machinery was required for apical *mira* mRNA localisation in neuroblasts. In wild type embryos, *mira* mRNA is localised exclusively to the apical cytoplasm in 76% of neuroblasts (localised; n=50; Figure 4.6A, D) and exhibits a slightly broader distribution in the rest (broad; Figure 4.6B, D). *egl* and *BicD* mutant neuroblasts exhibit similar *mira* mRNA localisation patterns (Figure 4.6D), showing that *mira* localisation in neuroblasts is independent of the Egl/BicD/dynein mRNA transport machinery and that additional mechanisms exist for apical targeting of *mira* mRNA transcripts.

In occasional *egl* and *BicD* mutant neuroblasts, *mira* is localised asymmetrically but not at the apical cytoplasm (mislocalised; Figure 4.6C, D). This may occur as a result of disruptions in neuroblast apico-basal polarity in *egl* and *BicD* mutants (Chapter 3). These results also indicate that *mira* transcripts retain the ability to localise asymmetrically when Egl and BicD function is compromised.

4.2.2 Investigating the requirement for Stau in apical *mira* mRNA localisation

4.2.2.1 Injected mira *and* pros *transcripts associate with endogenous Stau*

My results show that *mira* and *pros* transcripts behave similarly upon injection, and following transcription in wild-type and *egl* mutant blastoderm embryos, indicating that they are asymmetrically targeted by mechanisms other than the Egl/BicD/dynein mRNA transport machinery. Previous work has shown that injected *bcd* and *pros* RNAs can specifically associate with Stau protein in blastoderm embryos (Ferrandon et al., 1994; Schuldt et al., 1998) and that Stau is required for *bcd* localisation in oocytes, and basal localisation of *pros* in mitotic neuroblasts (Broadus et al., 1998; Li

Figure 4.6 Apical *mira* mRNA localisation in neuroblasts is independent of Egl and BicD.

(A-C) Examples of different *mira* mRNA distributions in neuroblasts of stage 9-10 wild-type, *egl* and *BicD* embryos: **(A)** localised (*mira* mRNA exclusively at the apical cytoplasm); **(B)** broad (*mira* transcripts apical but extending to lateral cytoplasmic regions (arrowhead)); **(C)** mislocalised (asymmetric distribution of *mira* transcripts, but not to apical cytoplasm). The frequency at which each type of *mira* mRNA distribution is observed in wild-type, *egl* or *BicD* embryos is shown in **(D)**. Neuroblasts displaying broad and mislocalised distributions of *mira* mRNA transcripts were distributed randomly throughout the sets of embryos that were studied and were not found predominantly in a subset of embryos. Scale bar = 25 μm.

Figure 4.6

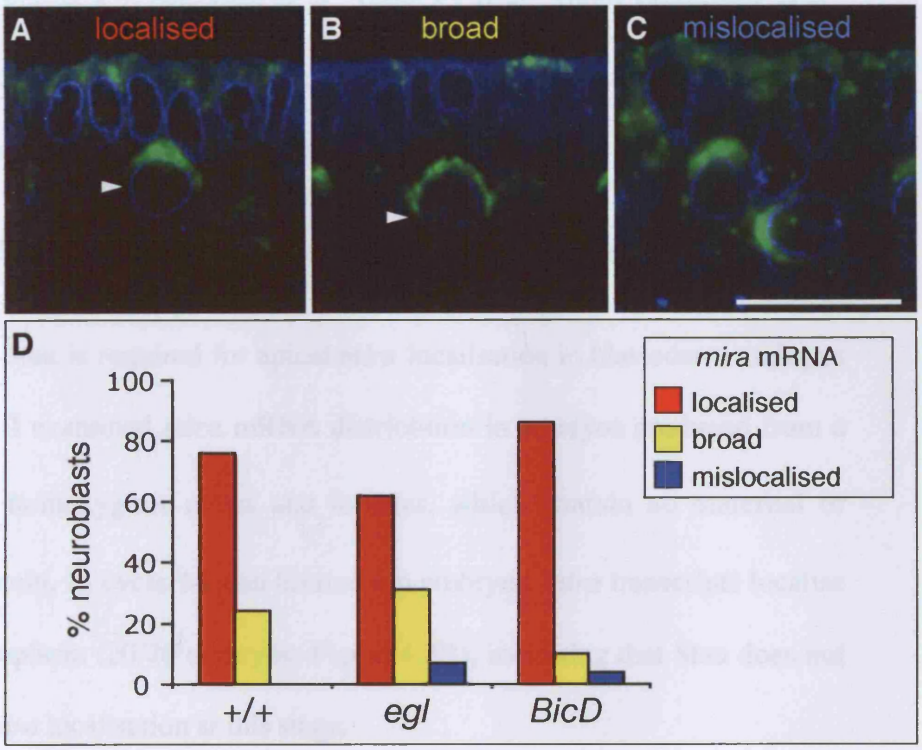
A localised
B broad
C mislocalised
D
% neuroblasts
100
80
60
40
20
0
+/+
egl
BicD
mira mRNA
localised
broad
mislocalised

et al., 1997; Matsuzaki et al., 1998; Schuldt et al., 1998). In interphase neuroblasts, Stau is localised to the apical cell cortex, and I find that endogenous Stau protein can associate with injected *mira* and *pros* transcripts in blastoderm embryos. This leads to an enrichment of Stau protein in the basal cytoplasm at the sites of *mira* and *pros* RNA injection (Figure 4.7; (Broadus et al., 1998; Li et al., 1997; Matsuzaki et al., 1998; Schuldt et al., 1998). These data suggest that Stau can bind and mediate apical localisation of these transcripts in interphase neuroblasts.

4.2.2.2 Apical localisation of mira *transcripts does not require* Stau

To test whether Stau is required for apical *mira* localisation in blastoderm embryos and neuroblasts, I examined *mira* mRNA distribution in embryos produced from a cross of $stau^{D3}$ homozygous males and females, which contain no maternal or zygotic Stau protein. In cycle 14 *stau* blastoderm embryos, *mira* transcripts localise to the apical cytoplasm (20/20 embryos; Figure 4.8B), indicating that Stau does not mediate apical *mira* localisation at this stage.

As described in section 4.2.1.2, *mira* is apically localised in cycle 14 wild-type blastoderm embryos, although *mira* is also detected between the blastoderm nuclei (Figure 4.8A). Stau protein exhibits a similar distribution and is enriched on membranes that invaginate between the blastoderm nuclei during cellularisation (Figure 4.8C). *mira* transcripts are no longer detected between the blastoderm nuclei in *stau* mutants at similar stages (Figure 4.8B), suggesting that endogenous *mira* transcripts can associate with Stau and direct some aspects of *mira* localisation in the embryo.

Figure 4.7 Injected *mira* and *pros* transcripts associate with endogenous Stau in blastoderm embryos.

(A) Injected *mira* transcripts associate with **(A')** endogenous Stau protein in blastoderm embryos (8/8 embryos) and Stau becomes enriched basally above the site of *mira* RNA injection (arrowheads). **(B)** Injected *pros* transcripts associate with **(B')** endogenous Stau protein above the site of *pros* RNA injection (arrows; 5/5 embryos; Schuldt, 1997) **(A", B")** Merged images of (A, A') and (B, B'), respectively. Scale bar = 50μm.

Figure 4.7

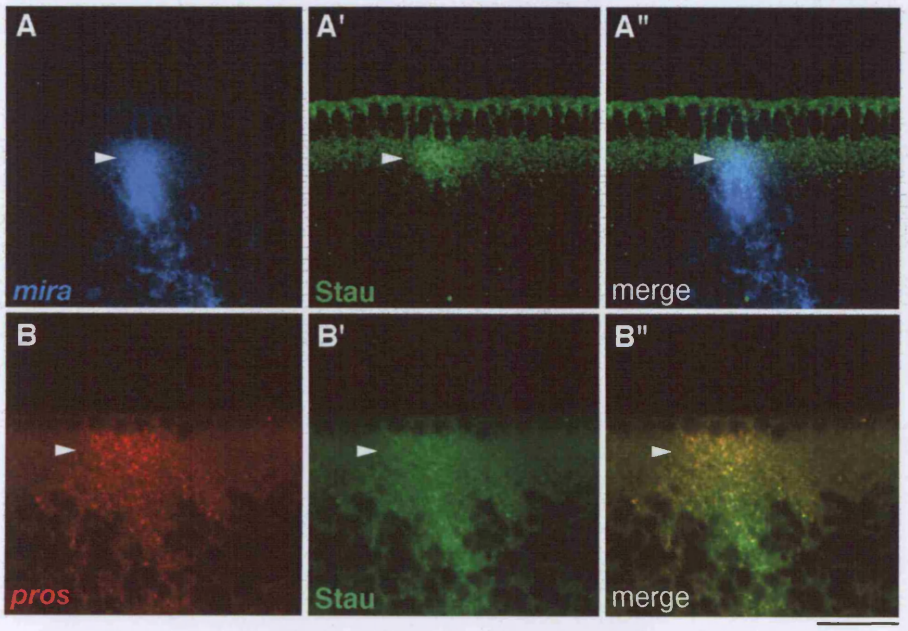

Figure 4.8 Apical *mira* mRNA localisation does not require Stau.

(A) *mira* transcripts are localised to the apical cytoplasm (arrowhead) and are also enriched between the blastoderm nuclei (arrow) in wild-type, cycle 14 blastoderm embryos. **(B)** *mira* transcripts are localised to the apical cytoplasm (arrowhead), but not between blastoderm nuclei, in *stau* cycle 14 blastoderm embryos **(C)** Stau protein (red) is enriched between blastoderm nuclei (arrow) in wild-type, cycle 14 blastoderm embryos and **(D)** around the cortex of metaphase neuroblasts. Dashed circle indicates the outline of representative neuroblast. DNA is stained in blue in (C, D). **(E, F)** Apical localisation of *mira* transcripts is also indistinguishable between **(E)** wild-type and **(F)** *stau* mutant neuroblasts (arrowheads). Nuclear envelope is labelled in blue in all panels except (C, D).

Figure 4.8

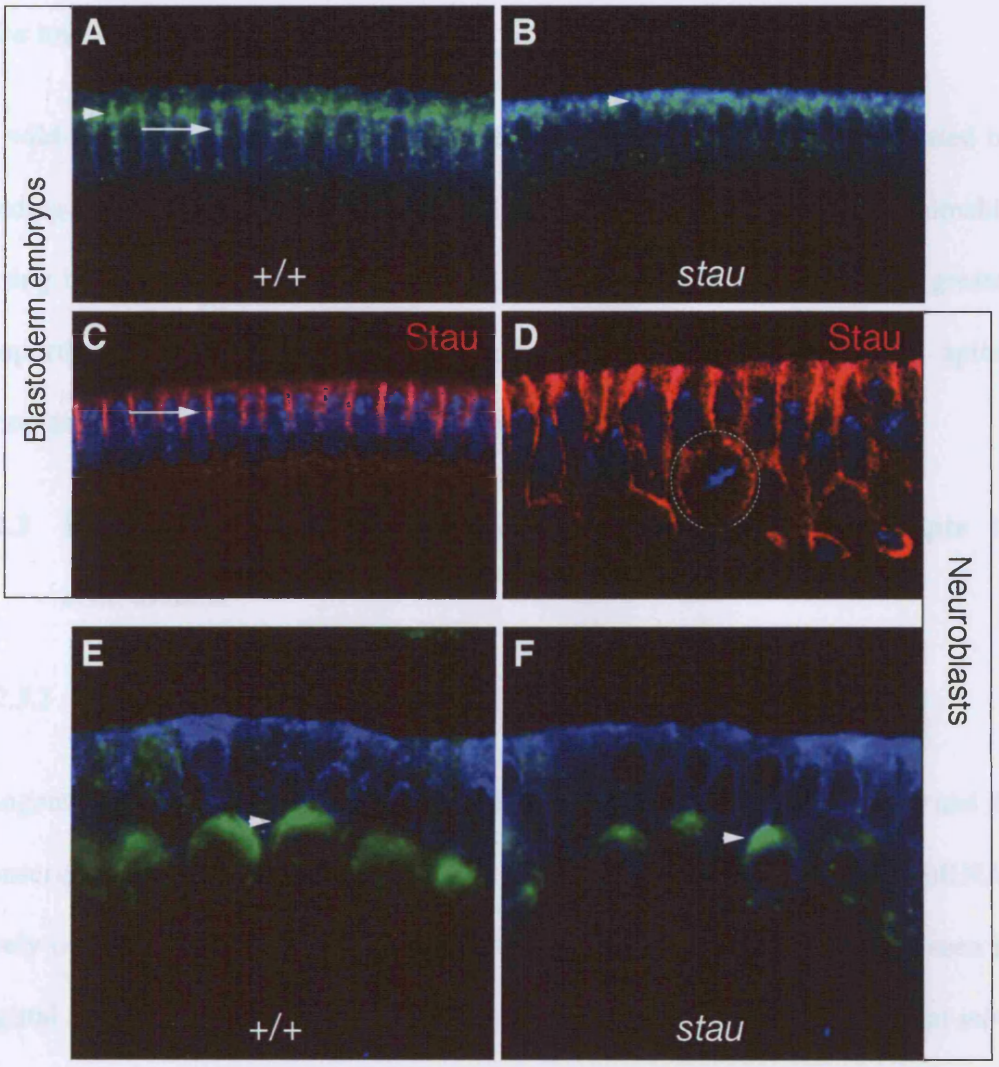
A
B
+/+
stau
C
Stau
D
Stau
Blastoderm embryos
Neuroblasts
E
F
+/+
stau

I tested whether Stau mediates *mira* localisation in neuroblasts. *mira* is localised exclusively to the apical cytoplasm, in 93% (n=30) of *stau* mutant neuroblasts (Figure 4.8F), with the rest exhibiting a broader distribution, as seen in wild-type neuroblasts (Figure 4.6B), indicating that Stau does not mediate apical localisation of *mira* transcripts in neuroblasts.

In wild-type neuroblasts, broadly distributed *mira* localisation may be mediated by binding to Stau, which is found all around the cell cortex at metaphase, presumably during its basal translocation (Figure 4.8D). As a result, in *stau* mutants a greater proportion of neuroblasts exhibit *mira* localisation specifically to the apical cytoplasm, rather than a broader distribution around the cell cortex.

4.2.3 Evidence for apical localisation of *mira* mRNA transcripts to centrosomes

4.2.3.1 Comparison of localised mira *and* ftz *mRNAs in blastoderm embryos*

Tangential views of cycle 14 blastoderm embryos show that localised *mira* and *ftz* transcripts occupy distinct regions within the apical cytoplasm, and these mRNAs rarely overlap (Figure 4.9A). This difference in localisation pattern is also seen in sagittal cross sections of the apical cytoplasm (Figure 4.9B) and suggests that *mira* and *ftz* transcripts are retained in the apical cytoplasm by different mechanisms and by association with distinct apical factors.

Apically localised pair-rule transcripts are excluded from the apical centrosomes and pericentriolar matrix (PCM) in blastoderm embryos (Simon Bullock, Ilan Davis and Renald Delanoue, personal communications). My observation that pair-rule and *mira* mRNAs localise to distinct regions in the apical cytoplasm raises the intriguing

Figure 4.9 *ftz* and *mira* transcripts localise to distinct regions of the apical cytoplasm in blastoderm embryos.

(A) Sagittal cross-section of a blastoderm embryo showing localisation of *mira* (green) and *ftz* (red) mRNAs to the apical cytoplasm. In merged image (bottom panel) *ftz* and *mira* transcripts are mostly distinct and only occasional overlap (yellow). **(B)** Tangential view of the surface of a blastoderm embryo within stripe of *ftz* (red) expression. *mira* transcripts (green) appear mostly separated from *ftz* transcripts with occasional overlap (yellow). In these images, the contrast has been adjusted to focus on areas where *ftz* and *mira* mRNA localisation is strongest. Scale bar = 30μm (A); 50μm (B).

Figure 4.9

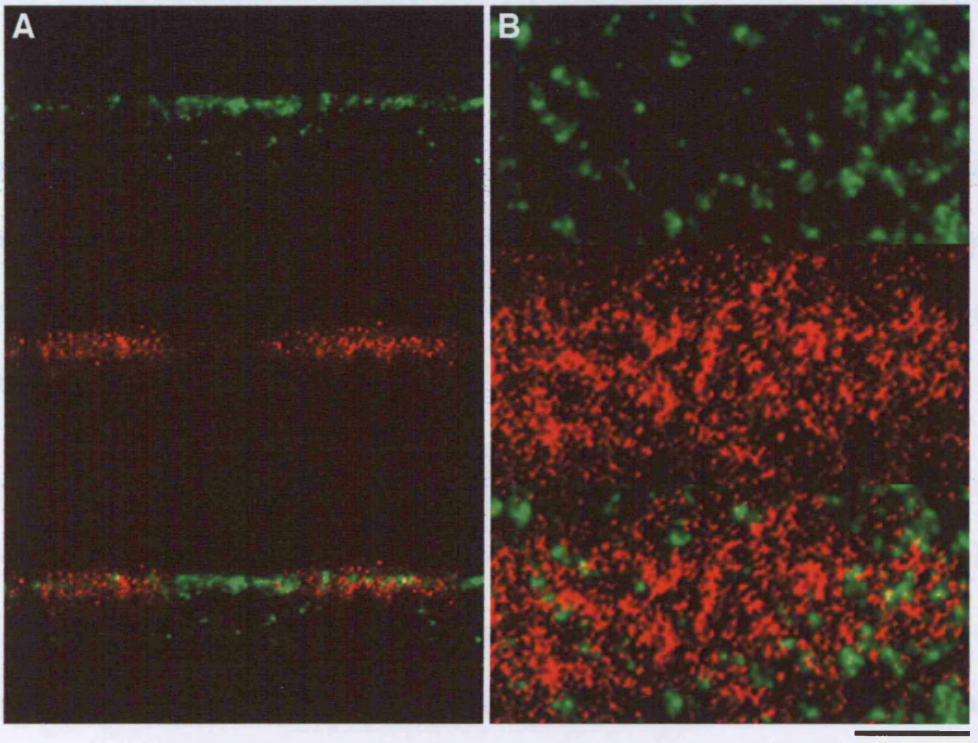

possibility that *mira* transcripts are maintained apically in blastoderm embryos by direct association with components of the centrosome or PCM. I tested this by comparing the distributions of *mira* mRNA transcripts and the centrosome associated proteins Cnn and γ-Tubulin.

4.2.3.2 mira *transcripts co-localise with γ-Tubulin, but not Cnn, in blastoderm embryos*

Cnn is a component of the PCM (Megraw et al., 2001). *mira* mRNAs do not co-localise with apical Cnn in blastoderm embryos (Figure 4.10A), suggesting that apical *mira* mRNA localisation is not maintained by association with the PCM or Cnn.

By contrast, it appears that *mira* transcripts frequently co-localise with apical γ-Tubulin in blastoderm embryos (Figure 4.10B), suggesting that *mira* is anchored in the apical cytoplasm, in these cells and in neuroblasts, by the γ-TuRC located at microtubule minus ends. Consistent with the localisation of γ-TuRCs to microtubule minus-ends, γ-Tubulin appears concentrated at apical centrosomes, but is also detected throughout the apical cytoplasm. *mira* transcripts that do not localise to the centrosome may be associated with free γ-TuRCs that are formed within the cytoplasm, before recruitment to microtubules minus-ends (Blagden and Glover, 2003; Moritz et al., 2000). This is preliminary data, and more detailed analysis will be needed to determine the extent of the co-localisation of *mira* transcripts with γ-Tubulin and other components of the γ-TuRC, such as Dgrip75.

Figure 4.10 ***mira*** transcripts co-localise with γ-Tubulin, but not Centrosomin, in blastoderm embryos.

(A, B) Sagittal cross sections of the cytoplasm of cycle 14 blastoderm embryos showing apically localised *mira* transcripts (green) together with an immunostaining for **(A)** the PCM with anti-Centrosomin (red) and **(B)** the γ-TuRC with anti-γ-Tubulin (red). Merged images are shown at the bottom. Arrowheads indicate examples of co-localised *mira* mRNA and γ-Tubulin. Scale bar = 30μm.

Figure 4.10

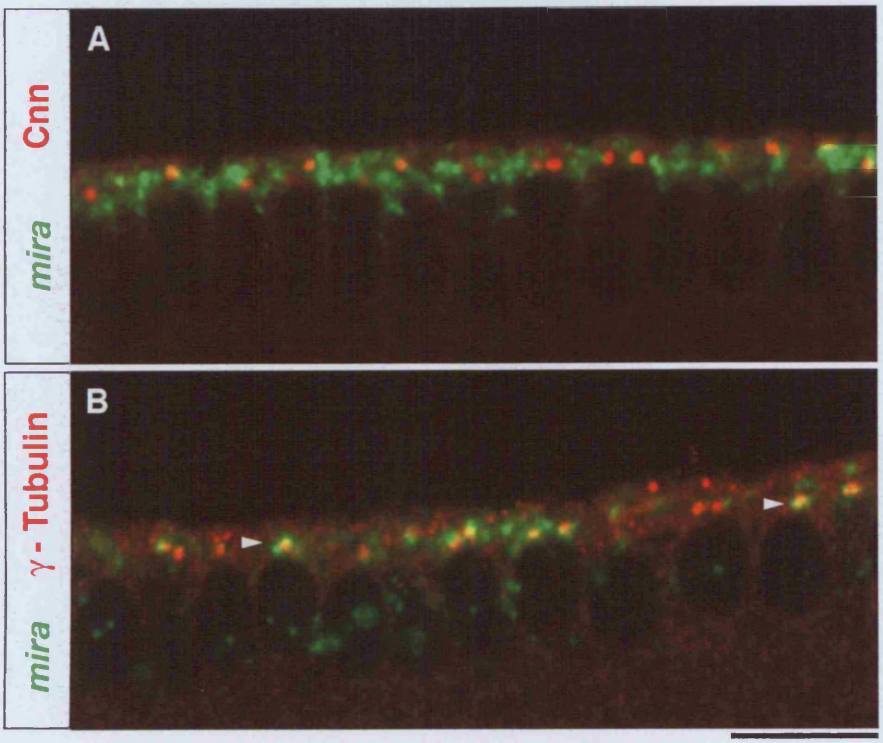

4.3 Discussion

4.3.1 A novel mechanism for mRNA localisation in *Drosophila* embryos

In *Drosophila* embryos, known mechanisms for asymmetric mRNA localisation involve Egl/BicD/dynein mediated transport of pair-rule and *wg* mRNAs along microtubules (Bullock and Ish-Horowicz, 2001; Wilkie and Davis, 2001); Chapter 2) or Stau/Mira dependent segregation of *pros* mRNAs to specific daughter cells by localisation to the cell cortex (Broadus et al., 1998; Li et al., 1997; Matsuzaki et al., 1998; Schuldt et al., 1998). In this chapter, I have shown that *mira* mRNAs are localised apically in blastoderm embryos and neuroblasts independently of Egl, BicD and Stau, demonstrating the presence of a novel mechanism for mRNA localisation in the *Drosophila* embryo.

Stau is not required for localisation of *mira* to the apical cytoplasm in neuroblasts and blastoderm embryos. However, Stau can direct some aspects of *mira* localisation in the embryo, for example, the enrichment of *mira* transcripts between cycle 14 blastoderm nuclei. Therefore, Stau may act to target *mira* transcripts asymmetrically in other cell types, such as neurons (Kohrmann et al., 1999).

The failure of *mira* and *pros* transcripts to localise in the blastoderm injection assay suggests that they are unable to be transported from the cytoplasm towards microtubule minus-ends. However, only *mira* and *pros* 3'UTRs were injected in these experiments. Therefore, I cannot rule out that there are signals within the remainder of the *mira* and *pros* transcripts that are required for transport apically in blastoderm embryos. This seems unlikely for *pros,* as the 3'UTR is sufficient to mediate *pros* mRNA localisation in the neuroblast (Li et al., 1997). Alternatively,

injected and endogenous *mira* and *pros* transcripts may fold differently *in vivo*, such that the former cannot be efficiently recognised by transport complexes in the blastoderm embryo, which appears to be the case for injected *osk* transcripts (Bullock and Ish-Horowicz, 2001).

Interestingly, *mira* and *pros* transcripts are able to localise apically in the blastoderm when expressed by the blastoderm nuclei, suggesting that nuclear factors may be required for efficient localisation of *mira* and *pros* mRNAs. This could be tested by incubation of these RNAs with nuclear extract prior to injection into the blastoderm embryo. Also, the localisation of endogenous *mira* and *pros* could be examined in mutants for nuclear factors that are known to be involved in mRNA localisation.

Studies to date have shown that mechanisms that mediate mRNA localisation in *Drosophila* embryos require multiple components that are conserved from oogenesis to early neurogenesis (Chapter 1, 2). Here, I present preliminary evidence that *mira* mRNA and γ-Tubulin are co-localised apically in blastoderm embryos (Figure 4.9). Recent studies show that the γ-TuRC components, γ-Tub37C and Dgrip75, are essential for the maintenance of *bcd* mRNA at the anterior pole of the oocyte after stage 10, indicating that this complex mediates mRNA anchorage (Schnorrer et al., 2002). Furthermore, the γ-TuRC is located specifically at the tips of microtubule minus-ends within the PCM (Moritz et al., 1995), suggesting that this complex may mediate anchorage of *mira* mRNAs at apically localised centrosomes in blastoderm embryos and neuroblasts.

In mollusc embryos, asymmetric segregation of mRNA transcripts at cell division occurs by localisation of mRNAs to specific centrosomes (Lambert and Nagy, 2002).

A similar mechanism may exist to retain *mira* specifically in the apical neuroblast at cell division. However, further analysis into the extent of *mira* and γ-Tubulin colocalisation is required. It would also be of interest to examine the localisation pattern of γ-TuRC components in neuroblasts and test whether apical *mira* localisation is disrupted in *γTub37C* and *Dgrip75* mutant embryos (Schnorrer et al., 2002).

It is unclear whether *mira* transcripts are actually transported apically, or whether they simply diffuse before being anchored. The co-localisation of *mira* and γ-Tubulin suggests that *mira* may be transported to microtubule minus-ends. The requirement for the dynein motor complex could be examined by analysis of *mira* localisation in neuroblasts that overexpress Dmn, in which *insc* mRNA localisation is partially disrupted (Chapter 2). It is important to determine the role of the microtubule cytoskeleton in *mira* localisation, which could also be tested by injection of the microtubule depolymerising compound, Colcemid, into blastoderm embryos (Wilkie and Davis, 2001).

Another factor required for localisation and maintenance of *bcd* at the oocyte anterior pole is Sww (St Johnston et al., 1989; Stephenson et al., 1988). Sww could be tested for an involvement in asymmetric *mira* mRNA localisation. Indeed, Sww is able to bind the γ-TuRC and is found localised to centrosomes (Schnorrer et al., 2002) and also interacts with Dlc (Schnorrer et al., 2000). Therefore, Sww may mediate dynein-dependent transport of *mira* and other mRNAs towards the minus-ends of microtubules in blastoderm embryos and neuroblasts. Sww is present in embryos until stage 11 (Hegde and Stephenson, 1993). Further work could determine whether

Sww is asymmetrically distributed in blastoderm embryos and neuroblasts, and if *mira* mRNA localisation is disrupted in *sww* mutant embryos.

4.3.2 Possible functions of *mira* mRNA localisation in neuroblasts

Localisation of Mira protein to the basal neuroblast cortex directs the segregation of Stau/Pros cargoes into the basal GMC at mitosis. By contrast, Mira is localised to the apical cell cortex in interphase neuroblasts (Fuerstenberg et al., 1998; Ikeshima-Kataoka et al., 1997; Shen et al., 1997). Therefore, apical localisation of *mira* mRNA transcripts in neuroblasts is probably required for localised translation of Mira protein at the apical cell cortex at interphase, where it may be required to associate with Stau/Pros and the Myosin motors, Jag and Zip, which mediate basal Mira/Stau/Pros relocation at mitosis (Barros et al., 2003; Petritsch et al., 2003). Mira protein is not detected apically during mitosis, which suggests that *mira* transcripts are translationally repressed during these stages of the cell cycle.

Maintenance of apical *mira* mRNA localisation during mitosis indicates that the neuroblast apical cell cortex is still specified following the delocalisation of the apical complex components at anaphase/telophase (section 1.3.2.1). Mira and Stau bind each other (Schuldt et al., 1998; Shen et al., 1998) and both are able to interact with Insc (Li et al., 1997; Shen et al., 1998). Therefore, apical translation of Mira protein, late in mitosis or early in interphase, may help to anchor Insc at the apical cortex and promote rapid re-establishment of the apical complex to direct a correctly oriented asymmetric cell division.

Apical localisation of *mira* mRNA throughout the cell cycle would also ensure that *mira* transcripts are retained in the apical neuroblast and restricted from entering the GMC. The exact role of apical *mira* mRNA localisation is not understood. Following segregation into the GMC, Mira is rapidly degraded at the GMC cortex and its protein/mRNA cargoes are released into the cytoplasm. Rapid degradation of Mira appears to be important for activation of the GMC cell fate. For example, some truncated mutant Mira proteins are degraded more slowly than the wild-type protein, which delays cargo release, resulting in a failure to activate specific gene expression in GMCs (Fuerstenberg et al., 1998; Ikeshima-Kataoka et al., 1997; Shen et al., 1997). Therefore, restriction of *mira* mRNA transcripts in the apical neuroblast may be required to limit the levels of Mira that are segregated into the GMC, thereby ensuring rapid Mira degradation and sufficient levels of Pros activity. The discovery of factors required for asymmetric *mira* mRNA localisation in neuroblasts, or *mira* mRNA mistargeting experiments, will allow a more detailed study into the function of this process.

In this chapter, I have presented preliminary results suggesting that apical localisation of *mira* mRNA transcripts is mediated by the γ-TuRC, thereby providing evidence for a novel mechanism for mRNA localisation during *Drosophila* embryogenesis. Therefore, it seems that multiple mechanisms exist during *Drosophila* embryogenesis to achieve specific accumulation of mRNA transcripts in a wide range of cell types and at different stages of the cell cycle.

CHAPTER 5: CONCLUDING REMARKS

In this thesis, I have described my investigations into the mechanisms and function of mRNA localisation, in the generation of cell polarity in somatic cells in the *Drosophila* embryo. My PhD project began with an interest into the generality of the Egl/BicD/dynein mRNA transport machinery. As described in Chapter 2, this complex is active in many cell types in *Drosophila*, and mediates the localisation of several different mRNA transcripts in egg chambers, blastoderm embryos, epithelial cells and neuroblasts.

These results indicate that this is a general machinery for mRNA localisation in *Drosophila*. As also described in the introduction, not all asymmetrically localising mRNAs utilise the Egl/BicD/dynein complex and I provide preliminary evidence, in Chapter 4, that a novel mechanism exists to localise *mira* transcripts in *Drosophila* embryos. In Chapter 3, I show that the function of mRNA localisation in *Drosophila* embryonic epithelial cells and neuroblasts is to enhance the efficiency of asymmetric protein targeting in these cells.

It is not known what factor(s) actually associates directly with the localisation signals of mRNA cargoes of the Egl/BicD/dynein complex. Egl contains an RNase D domain ((Moser et al., 1997), making it best candidate for a role in mRNA binding, although this remains to be demonstrated. Therefore, it is possible that there are other components of the Egl/BicD/dynein complex that are required for mRNA localisation, providing the basis for screens to identify other members of this complex. The generality of the Egl/BicD/dynein complex may allow the discovery of new components of this mRNA localisation machinery. For example, genetic screens

could be performed *in vitro* using dsRNAi on polarised *Drosophila* cell lines. Identifying new members of the Egl/BicD/dynein complex may lead to a better understanding of how the kinetics of this machinery is regulated, or even provide insights into the specificity of mRNA recognition.

In Chapter 4, I describe preliminary evidence that *mira* localisation is mediated by the γ-Tubulin Ring Complex, indicating that multiple mechanisms exist to mediate mRNA localisation in the *Drosophila* embryo. Further work will be required to identify the factors responsible for *mira* mRNA localisation in neuroblasts and blastoderm embryos, in particular the requirement for microtubules and γ-TuRC components in this process. In turn, this would allow investigations into the function of apical *mira* localisation, in targeting of Mira protein at different stages of the cell cycle in neuroblasts.

Apical localisation of *mira* transcripts is observed throughout the cell cycle in neuroblasts ((Schuldt et al., 1998)), suggesting that *mira* localisation is maintained by anchorage in the apical cytoplasm. Therefore, the study of *mira* mRNA localisation could lead to a better understanding into the mechanistic basis of mRNA anchorage in *Drosophila*. Furthermore, the mapping of the *mira* mRNA localisation signal may shed light on the structures of *cis*-acting signals that mediate specificity for distinct mRNA localisation machineries.

Known localisation signals do not appear to have any obvious similarities in their primary sequences, but some are able to form secondary structures, such as stem-loops (Bullock et al., 2003; Gonzalez et al., 1999b; Serano and Cohen, 1995). Higher order RNA structure may also be important for RNA recognition (Bullock et al.,

2003; Macdonald and Kerr, 1998). The specific motifs that mediate recognition by the Egl/BicD/dynein machinery are not known. However, detailed analysis of the *K10* localisation signal, which forms a 44 nucleotide stem-loop structure, suggests that localisation of *K10* by Egl/BicD/dynein requires specific nucleotides in non-base-paired regions or 'bulges' within the stem (Inbal Ringel, unpublished observations; Hermann and Patel, 2000). Further analysis should provide exciting new information into the basis of mRNA recognition, by protein complexes, at the nucleotide level.

As discussed in Chapter 3, mRNA localisation in somatic cells in the *Drosophila* embryo is required for efficient targeting of proteins, and the establishment of cell polarity. Particularly, I show that the apical localisation of *insc* mRNA is required to enhance apical Insc targeting and activity, in controlling apico-basal polarity and metaphase spindle length in neuroblasts. Shortened metaphase spindles in *insc* mutants, probably represents a requirement for Insc in mediating attachment of astral microtubules to the apical neuroblast cortex. However, the mechanism by which this is achieved is unknown. It would therefore be of interest to identify binding partners of Insc that are able to interact with microtubules to regulate cortical spindle attachment.

In neuroblasts with reduced Insc function, both apical and basal halves of metaphase spindle lengths are shortened (Figure 3.2). Therefore, additional factors appear to control spindle length basally, in response to Insc activity. Mira may play a role in microtubule attachment at the basal cortex (section 3.3.2.2), which could be tested by examination of spindle lengths in *mira* mutant neuroblasts. In a similar manner to Insc, factors that promote cortical attachment of microtubules are likely to control

spindle orientation, positioning and length. Using fluorescently labelled centrosomes as a visible marker, genetic screens could be performed, to identify genes involved in the regulation of these processes in *Drosophila* neuroblasts, early *C. elegans* embryos and vertebrate neural stem-cells.

The research described in this thesis, provides interesting new insight into the mechanisms and function of mRNA localisation in *Drosophila*. Many genes have been implicated in the different aspects of mRNA targeting, including transport, anchorage and translational control. Further analysis of these factors in *Drosophila* will reveal the exact nature of these molecular pathways in the control of asymmetric mRNA localisation.

CHAPTER 6: MATERIALS AND METHODS

6.1 Fly Culture

6.1.1 Alleles

Wild-type flies are of the strain Oregon-R. The genotype of *egl* mutant females is egl^{3e}/egl^{WU50}; egl^{3e} is a hypomorphic allele (Navarro et al., 2004) and egl^{WU50} is a null allele (Schupbach and Wieschaus, 1989) (both gifts from Ruth Lehmann). egl^{3e}/egl^{WU50} females were mated with wild-type males to obtain *egl* mutant embryos. The genotype of *BicD* mutant females is $P\{BicD^{HA40}\}$; $BicD^{R26}/Df(2L)TW119$. $BicD^{R26}$ is a weak dominant-negative allele (Mohler and Wieschaus, 1986). $P\{BicD^{HA40}\}$ is a transgene which expresses 12% as much BicD as the wild-type gene (6% of diploid production) (Oh et al., 2000) and *Df(2L)TW119* uncovers the *BicD* locus. *BicD* mutant females were mated with $BicD^{R26}/BicD^{+}$ males to obtain *BicD* mutant embryos. $insc^{22}$ (Cai et al., 2001) and $insc^{P72}$ (Kraut and Campos-Ortega, 1996) are both null alleles (gifts from Jürgen Knoblich). The $insc^{22}$ and $insc^{P72}$ mutations are balanced over *CyO ftz-lacZ* so that progeny could be genotyped on the basis of β-galactosidase expression. $stau^{D3}$ is a null allele (St Johnston et al., 1991) and was a gift from Ilan Davis. crb^{11A2} and wg^{CX4} are reported to be amorphic alleles (Bilder et al., 2003; Baker, 1987).

6.1.2 Misexpression experiments

UAS-inscNMyc flies (Knoblich et al., 1999; a gift from Jürgen Knoblich) were crossed with *h-Gal4* flies to produce a striped pattern of *inscNMyc* misexpression in stage 8-10 embryos, using the UAS-Gal4 system (Brand and Perrimon, 1993).

Overexpression of Dynamitin, specifically in neuroblasts, was achieved by using the scabrous-GAL4 driver (Brand and Perrimon, 1993) to drive expression of the *UAS-GFPdDmn* transgene. *UAS-GFPdDmn* flies were described previously (Januschke et al., 2002).

K10 transcripts were misexpressed by the *hs-K10* transgene under the control of the heat-inducible, *hsp70* promoter (Karlin-Mcginness et al., 1996); stage 8-9 embryos were heat-shocked at 36.0°C for 15 min, and incubated at 25°C for 15 min before fixation.

Non-localising *insc* transcripts produced by the *hs-insc2.1* transgene (a gift from Jürgen Knoblich) were misexpressed in embryos under the control of a heat-shock inducible promoter. Stage 8-9 embryos were heat-shocked at 36.0°C for 30 min, and incubated at 25°C for 30 min before fixation. This treatment was performed before immunohistochemistry and Western blotting for Insc. Control embryos were treated identically.

pros transcripts were misexpressed in blastoderm embryos by the *hsp-pros* transgene, under the control of the *hsp70* promoter (a gift from Fumio Matsuzaki). 1.5 – 2.5 h old embryos (timings are given as hours at 25°C after egg lay) were heat-shocked at 36.0°C for 15 min, and incubated at 25°C for 15 min before fixation.

6.2 RNA injections into syncytial blastoderm embryos

6.2.1 *in vitro* synthesis of sense RNA

10μg of plasmid DNA was linearised using restriction enzymes (New England Biolabs, NEB), that leave blunt ends or 5' overhangs, to produce a template for sense

RNA synthesis. Template DNA was extracted by phenol/chloroform, precipitated with 0.3M NaOAC/EtOH and resuspended in 10µl nuclease-free water. Linearisation of template DNA was checked by agarose gel electrophoresis on a 1% TAE agarose gel against a 1kb DNA ladder (5µl; NEB).

Template DNA was transcribed in a solution containing 0.4mM ATP, 0.4mM CTP, 0.36mM UTP, 0.04mM Cy3-, Cy5- (Perkin Elmer) or Alexa-488 (Molecular Probes) UTP, 0.12mM GTP, 0.3mM 7mG(5')pppG cap analogue (Ambion), and 10U RNase inhibitor (Stratagene), using 30U T7 (Stratagene) or T3 (Roche) polymerases and 2.5µl 10x transcription buffer (Roche). The reaction mixture was made up to 25µl using nuclease free water (Ambion).

The transcription reaction was performed at 36°C for 2.5h and was then treated with 10U DNase I (Stratagene) for 1h at 36°C to remove template DNA. RNA was extracted with phenol/chloroform and spun through a mini Quick Spin G50 column (Roche) to remove unincorporated nucleotides. RNA was precipitated with 0.3M NH_4OAC/EtOH and resuspended in 3µl nuclease-free water (Ambion). The final concentration of RNA was typically between 500ng/µl and 1µg/µl. RNAs were stored at -20°C. Fluorescent RNAs typically contain 1 fluorochrome / 250 nucleotides.

The efficiency of RNA synthesis was checked by running 1/10th of the transcription reaction on a 1% TAE agarose gel. *in vitro* synthesised RNA and an RNA ladder (Molecular Probes) were incubated at 75°C for 10 min in RNA loading buffer (Molecular Probes) prior to running. Gel tanks were washed with 10% SDS, prior to pouring of the agarose gel, in order to remove nucleases.

6.2.2 Blastoderm injection assay

Wild-type flies (around one week old) were caged and induced to lay embryos on apple juice agar plates (produced by CRUK research services), by placing a little fresh yeast at the centre of the plate. Cages were kept in a closed box, in the dark, at 25°C. To synchronise egg lays, a prelay was performed for 30 min. Eggs from the prelay were discarded, fresh apple juice plates and yeast were put onto cages and a second 30min egg lay was performed. These embryos were then aged appropriately at 25°C, so that RNA was injected into mitotic cycle 13-14 blastoderm embryos (2.5 – 3 h after egg lay at 25°C).

For preparation of embryos before injection, embryos were removed from the apple juice plate using a wet paintbrush and washed with water in a wire basket. After washing, embryos were soaked in 1:1 bleach (Sodium hypochlorite; Anachem) / water for 1 min to remove the chorion and rinsed with water to wash off the bleach. Embryos were then lined up in rows on an apple juice plate so that dorsal sides were facing the same direction.

One side of a coverslip (9mm x 35mm) was covered in glue. Glue was prepared by dissolving the glue from brown packing tape, with 5ml n-heptane (AnalaR) in a 25ml glass bottle, placed on a tilting roller for about 30 min, making sure that brown covering was not removed. Aligned embryos were picked up off the apple juice plate by gently sticking them to the glued coverslip. This was followed by dehydration for 10 min in a box containing Silica Gel. Embryos were covered with 10S voltaleff oil (Atachem) prior to RNA injection.

Glass injection needles were prepared by pulling capilliary tubes on a Narashige needle puller, and broken on the edge of a glass slide, to give a tapered end of 1-2μm in diameter. RNA was pipetted into the glass injection needle, which was placed into a Leitz needle holder on a Narashige micromanipulator. Injections were performed at room temperature (RT) and typically around 50 blastoderm embryos were injected in a single experiment.

RNA was injected at a concentration of 250ng/μl. RNA was diluted in injection buffer (Anderson and Nusslein-Volhard, 1984) and spun briefly in a centrifuge to clear debris. 1μg/μl RNA was injected when addressing recruitment of Egl, BicD or Stau protein. In some experiments, anti-BicD antibody (mouse monoclonal 4C2; (Suter and Steward, 1991); a gift from Beat Suter), anti-Egl antibody (rabbit polyclonal; (Mach and Lehmann, 1997); a gift from Ruth Lehmann), anti-Orb antibody (mouse monoclonal 6H4; (Lantz et al., 1994); Developmental Studies Hybridoma Bank), or injection buffer as a negative control was injected into embryos 5-10 min before *insc* RNA injection. Antibodies were injected undiluted.

Injected embryos were fixed in n-heptane (AnalaR) saturated with formaldehyde (37% solution; AnalaR) (fix solution), 5 min or 20 min after injection of the last embryo. It takes approximately 5 min to inject 50 embryos. Voltaleff oil was removed first by rinsing with fix solution until embryos started to come away from the glue. Embryos were then washed off the glue, with fix, into a 1.5ml Eppendorf tube and fixed for 20 min.

Following fixation embryos were rinsed in heptane and dropped onto a glass slide using a plastic pasteur pipette. After evaporation of heptane, embryos were stuck to

another glass slide with double sided tape. Embryos were covered with PBS and hand peeled with a fine syringe needle to remove the vitelline membrane. For observation of injected RNAs, embryos were immediately mounted. When addressing recruitment of Egl, BicD or Stau protein, embryos were fixed for 5 min only, hand peeled, and then washed for 2 x 5 min in PBS / 0.1% Triton-X (PBST) prior to immunostaining (see below).

Embryos were mounted on glass slides. A piece of insulation tape was put onto the slide, into which a square hole was cut into the tape, which formed a chamber for the embryos. Any remaining buffer was aspirated. The samples were then covered with Citifluor (Citifluor Ltd.) and overlaid with a coverslip. Covering the edges of the coverslip with nail varnish sealed the chamber.

Table 6.1 Summary of RNAs injected into blastoderm embryos

Insc	3.27kb	Full-length	1 - 3272	Kraut and Campos-Ortega, 1996
inscΔ3'UTR	2.81kb	*insc* 5'UTR and coding sequence	1 - 2811	Subcloned from *insc* cDNA (section 6.8.3/4)
InscCDS	2.58kb	*insc* coding sequence only	232 - 2811	Subcloned from *insc* cDNA (section 6.8.3/4)
H	2.12kb	Full-length	1 - 2121	Simon Bullock
Pros	1.5kb	3'UTR only	4513 - 6019	Andrea Brand
mira3'UTR	1.3kb	3'UTR only	2238 – 3119	Cloned from genomic DNA (section 6.8.3/4)
crb (c4b4)	1.6kb	3'UTR plus 1kb coding sequence	5619 - 7219	Tepass et al. 1990
Pins	3.3kb	Full-length	1 - 3300	Fengwei Yu

6.3 Immunohistochemistry

For detection of proteins in neuroblasts and epithelial cells, stage 8-10 embryos were fixed for 12 min in heptane saturated with 4% formaldehyde in PBS (section 6.9.2) and devitellinised with methanol (AnalaR). Fixed embryos were stored in methanol at -20°C. Cycle 13-14 blastoderm embryos were treated similarly for detection of proteins at these stages. Injected embryos were fixed and devitellinised as described above (section 6.2.2).

Prior to immunostaining, embryos were rehydrated by sequential washes at RT, each for 5 min, in 75%, 50% and 25% MeOH in PBS. Embryos were then washed at RT in PBST for 3 x 5 min, then 3 x 20 min. To reduce background, a final 20 min wash at RT was performed in PBST / 2% heat-inactivated normal goat serum (HINGS) before incubation with primary antibodies.

Embryos were incubated overnight in PBST / 2% HINGS at 4°C with the following antibodies: mouse monoclonal anti-BicD 1B11 (1:10; (Suter and Steward, 1991); a gift from Beat Suter); anti-Egl (1:2000; a gift from Ruth Lehmann); rabbit polyclonal anti-DmPar6 (1:500; (Petronczki and Knoblich, 2001) and mouse monoclonal anti-EB1 (1:300; both gifts from Jürgen Knoblich); rabbit polyclonal anti-Insc (1:1000, (Tio et al., 1999), rabbit polyclonal anti-N-Mira (1:500; (Matsuzaki et al., 1998) and rabbit polyclonal anti-Baz (1:1000; (Yu et al., 2000); all three gifts from Bill Chia); mouse monoclonal anti-Wg 4D4 (1:20; from Simon Bullock); mouse anti-β-Galactosidase (1:100, Promega); mouse anti-γ-tubulin (1:20, Sigma); rabbit polyclonal anti-Stau (1:100; (Schuldt et al., 1998); a gift from Daniel St Johnston); mouse monoclonal anti-phosphotyrosine (1:20; (McCartney et al., 2001); Upstate

Biotech); mouse monoclonal anti-β-Tubulin (1:20; a gift from Giampietro Schiavo); rabbit polyclonal anti-Cnn (1:500; (Megraw et al., 2001); a gift from Thom Kaufman) and mouse monoclonal anti-Crb cq4 (1:3; Developmental Studies Hybridoma Bank).

Embryos were washed at RT for 3 x 5 min and then 3 x 20 min in PBST. To reduce background, a final 20 min wash at RT was performed in PBST / 2%HINGS before incubation with anti-mouse or anti-rabbit secondary antibodies, conjugated to Alexa-488, Alexa-594 (1:500; Molecular Probes) or Cy5 (1:200; Jackson ImmunoResearch). Embryos were incubated with secondary antibodies for 2 h at RT. DNA was stained with TO-PRO-3 iodide (Molecular Probes) diluted 1:1000 in PBST, and incubated at 4°C overnight. Embryos were washed at RT for 3 x 5 min and then 3 x 20 min in PBST prior to mounting on a glass slide in Citifluor (section 6.2.2) before confocal analysis.

6.4 *in situ* hybridisation in *Drosophila* embryos

6.4.1 *in vitro* synthesis of riboprobes

5μg of plasmid DNA was linearised using restriction enzymes (NEB) to produce a template for antisense RNA synthesis. DNA was extracted by phenol/chloroform treatment, precipitated with 0.3M NaOAC/EtOH and resuspended in 10μl nuclease-free water. Template DNA was transcribed in a solution containing digoxigenin-(DIG) or FITC-RNA labelling mix with transcription buffer (Roche), according to manufacturer's instructions, using 30U T7 (Stratagene) or T3 (Roche) polymerases, and 10U RNase inhibitor (Stratagene). The reaction mixture was made up to 100μl using RNase-free water (Ambion). The transcription reaction was performed at 36°C

for 2.5h and was then spun through a chroma spin-100 DEPC-H_20 column (Clontech) to remove unincorporated nucleotides. Antisense RNA probes were stored at -20°C.

6.4.2 *in situ* hybridisation

For detection of mRNAs, embryos were fixed, stored and rehydrated as above (section 6.3). Following dehydration, embryos were 'post-fixed' in 4% formaldehyde in PBS, before 4 x 5 min washes at RT in PBS / 0.1% Tween-20 (PBT). Embryos were washed at RT for 5 min in 1:1 hybridisation buffer (HYB; section 6.9.2) / PBT and then for 5 min in HYB only. Embryos were then incubated in HYB for 1 h at 70°C. 1µl of antisense probe was heated to 80°C for 2 min in a 200µl PCR tube, and then put on ice, before addition of the probe to 500µl of HYB, preheated to 70°C. Embryos were incubated at 70°C overnight in HYB/riboprobe mix.

Embryos were washed at 70°C: 1 x 20 min in HYB; 1 x 20 min in HYB/PBT (1:1) and 4 x 20 min in PBT. Embryos were then washed in PBT at RT for 20 min. To reduce background, a final 20 min wash at RT was performed in PBT / 2%HINGS before incubation with Alkaline Phosphatase conjugated-anti-DIG (1:1000; Roche) or anti-FITC (1:1000; Roche) antibodies for 1h at RT. Embryos were then washed 3 x 20 in PBT at RT prior to detection of transcripts. Fluorescent detection of *insc*, *insc2.1*, *inscNMyc*, *wg*, *K10*, *crb*, *ftz* and *pros* transcripts was performed using Fast Red (Roche).

6.4.3 Fast Red detection of transcripts and labelling of nuclear envelope

Embryos were washed 2 x 10 min in 0.1M Tris pH 8.0 in water/ 0.1% Tween-20. One Fast Red tablet was dissolved in 2ml 0.1M Tris pH 8.0/0.1% Tween-20 (Fast

Red solution) and passed through a 0.22μm filter. Embryos were washed quickly in 500μl Fast Red solution and then transferred to a 12-well plate in 1ml fresh Fast Red solution. Colour development was allowed to proceed for between 30 min and 3 h at RT. The reaction was stopped by 3 x 5 min washed in PBT/10mM EDTA. The nuclear envelope was then stained by overnight incubation at 4°C in Alexa 660-wheat germ agglutinin (5 μg/ml Molecular Probes) (Virtanen and Wartiovaara, 1976). Embryos were mounted in Citifluor as described above (section 6.2).

6.4.4 Double *in situ* hybridisation

For detection of *ftz* and *mira* transcripts, embryos were incubated with both *ftz* and *mira* riboprobes and washed as described above. Embryos were incubated at RT with both Horseradish Peroxidase-conjugated anti-DIG (1:1000; Roche) and Alkaline Phosphatase-conjugated anti-FITC (1:1000; Roche) antibodies and then washed 3 x 20 min PBT at RT prior to detection of mRNA transcripts. *mira* transcripts were detected using FITC-labelled tyramides diluted (1:50) in amplification buffer (NEN Life Sciences) for 10 min at RT. Embryos were then washed 3 x 10min in PBT at RT and then 2 x 10 min in 0.1M Tris pH 8.0 in water/ 0.1% Tween-20, before detection of *ftz* transcripts with Fast Red (see section 6.4.3).

6.5 Controls for *in situ* and immunohistochemistry experiments

insc riboprobe was generated from a full length *insc* cDNA as described in Kraut and Campos-Ortega, 1996. Specificity of *insc* riboprobe and anti-Insc antibody described in this thesis was determined by comparison to *β-gal* expression in embryos from the P-*lacZ* insertion line AB44 (Kraut and Campos-Ortega, 1996).

All antibodies used in experiments described in this thesis have been previously tested for immunoreactive specificity: anti-Egl (Mach and Lehmann, 1997); anti-BicD (Suter and Steward, 1991); anti-EB1 (Subramanian et al., 2003); anti-Crb (Tepass et al., 1991); anti-DmPar6 ((Petronczki and Knoblich, 2001); anti-Mira (Matsuzaki et al., 1998); anti-Cnn (Heuer et al., 1995); anti-Baz (Wodarz et al., 1999) and anti-Stau (St Johnston et al., 1991).

In wild-type embryos, all antisense *in situ* probes used gave expression patterns that were identical to previously published observations: *wg* (Baker, 1997); *crb* (Tepass et al., 1991); *mira* (Shen et al., 1997); *pros* (Schuldt et al., 1998) and *ftz* (Hafen et al., 1994). The loss of asymmetric *insc, wg, crb, K10* and *ftz* localisation in *egl* mutant embryos also provides good evidence that their *in situ* patterns are not artifactual.

6.6 Confocal microscopy

Confocal imaging was performed on a Zeiss LSM 510 using a 40X oil or water immersion lens. The standard image size was 1024 x 1024 pixels. Scale bars in all figures were calculated using LSM 510 software. Digital images were processed and arranged using the Adobe Photoshop 5.5 software.

The first 3-5 neuroblasts in each embryo at the cell-cycle stage of interest were scored for mRNA or protein distributions, to avoid bias. Multiple confocal sections were analysed per neuroblast to assess the distribution of detected proteins and mRNAs. Histograms summarising the data from *in situ* (*insc, wg* and *mira)* and antibody (Insc, Par6 and Mira) experiments show the percentage of cells, from the

total cell count, that exhibit a particular mRNA or protein distribution. All histograms were generated using Microsoft Excel software.

Confocal images were taken using similar settings in order to assess the relative apical levels of protein before categorisation according to the strength of apical Insc or Par6 enrichment: localised (strong apical protein localisation); weak (reduced levels of apical protein, sometimes also detectable in the cytoplasm); unlocalised (no apical enrichment; protein detected throughout the cytoplasm). Only embryos in which at least one neuroblast shows strong apical Insc or Par6 enrichment were scored to ensure immunostaining had worked efficiently.

The first 3-5 metaphase neuroblasts detected in each embryo were scored for spindle phenotypes, to avoid bias. Spindle lengths were measured between the centres of the two centrosomes using Zeiss LSM 510 software, and are represented as a ratio of the cell diameter. Cell diameters were measured along the axis of the mitotic spindle from the basal Mira crescent to the apical edge of the neuroblast as detected by autofluorescence. To ensure that spindle length measurements were not affected by mitotic orientation, only neuroblasts with both centrosomes in the same 2μm thick confocal section were analysed. Histograms summarising metaphase spindle length (Fig. 3.2) and telophase spindle asymmetry (Fig. 3.5) represent the mean of the values from all cells analysed. Error bars indicate the standard error of the mean, which was calculated using Microsoft Excel software. All other statistics were performed using Graphpad.com (www.graphpad.com/quickcalcs/index.cfm).

6.7 Cuticle preparation

After egg laying, yeast was removed from apple juice plate, and embryos were incubated at 25°C. Between 24-36 h after egg lay, 1st instar larvae were removed from apple juice plates using sharp forceps and were the placed on a glass slide in a drop of water. The slide was placed on a 70°C hot plate for 30 sec so that majority of the water evaporated. Larvae were then covered in Lacto-Hoyers medium (see section 6.9.2). A coverslip was placed over the top and larvae were baked in the oven at 80°C for 2-3 h.

6.8 Insc Western blotting analysis

Typically 100 embryos were homogenised in 100µl 1x NuPage LDS sample buffer (Invitrogen). Lyates were centrifuged at 13000 rpm in a tabletop centrifuge for 2 min. The supernatant was stored at -20°C.

Embryos of wild-type and *egl* mutant embryos were stage-matched as follows: embryos were placed on a glass slide under 10S voltaleff oil and viewed under a light microscope. Syncytial blastoderm stages (2.5-3h old embryos at 25°C) can be distinguished by clearing of cytoplasm around the nuclei. These embryos were selected, oil was washed off in wire baskets, and embryos were placed on apple juice plates at 25°C for 2 h.

Western blotting was performed using the Xcell *SureLock* Mini-Cell blot module (Invitrogen) and NuPage 4-12% Bis-Tris precast gels (Invitrogen) according to manufacturers instructions. Amount of protein loaded into each lane corresponded to lysate extracted from 10 embryos, at embryonic stages 8-11. 5µl of BenchMark

protein ladder (Invitrogen) was run alongside to determine molecular weight. Transfer of protein onto Hybond nitrocellulose membrane (Amersham Biosciences) was checked by staining with Ponceau-S (Amersham Biosciences) and removed by rinsing with water.

To reduce background, membrane was preblocked in 5% dried-skimmed milk powder (Marvel) in PBS / 0.2% Tween-20 (Sigma) for 1 h at RT. Rabbit anti-Insc antibody was diluted 1:5000 in 2% dried-skimmed milk powder (Marvel) in PBS / 0.2% Tween-20. Membrane was incubated in diluted anti-Insc antibody for 1 h at RT in 50ml polypropylene tubes (Falcon). Membrane was rinsed twice and washed 3 x 20 min with PBS/ 0.2% Tween-20 before blocking in 5% milk (Marvel) in PBS / 0.2% Tween-20 (Sigma) for 1 h at RT. Membrane was incubated with Infra-Red Dye (800nm)-conjugated anti-rabbit secondary antibodies (Rockland Immunochemicals) for 1h at RT, and then washed 3 x 10 min in PBS / 0.2% Tween-20 and 2 x 5 min in PBS. Western blots were imaged using LI-COR Odyssey Infrared Imager and software.

6.9 Molecular Biology

6.9.1 Transformation of competent bacteria

For transformation of *DH5α* competent bacteria (Invitrogen) with plasmid DNA, a 50µl aliquot of frozen bacteria was thawed on ice. 1µl of plasmid DNA was added, mixed gently, and the mixture was incubated on ice for 30 min. The suspension was heat shocked at 42°C for 90 sec and put back on ice for 90 sec. After addition of 0.8 ml of SOC at RT, the bacterial suspension was incubated on a shaker at 37°C for 45 min. 50µl of the bacterial solution was spread on a sterile Ampicillin (100µg/µl) /LB

agar plate, and incubated overnight at 37°C, lid side down. Blue-white selection was performed by spreading 40µl X-Gal onto Ampicillin (100µg/µl) /LB agar plates, and allowing 1 h to dry at 37°C, before plating of bacteria. Colonies were picked from plates, placed in 5ml Amp^+ LB medium and incubated on a shaker at 37°C overnight. Suspensions were centrifuged at 4000rpm in an Eppendorf floor centrifuge (5810), medium was discarded and plasmid DNA was purified using an automated version of the Qiagen mini-prep kit (CRUK Equipment Park).

6.9.2 PCR

Polymerase chain reaction (PCR; (Saiki et al., 1988) was carried out in 200µl Thermo-Tube thin walled tubes (ABgene) using a Peltier (PTC-200, DNA Engine) thermal cycler. PCR was performed using the PCR Master Mix system (Qiagen) according to manufacturer's instructions. For all PCR reactions, the thermal cycle used was: 94°C for 30sec, 52°C for 30sec and 72°C for 1min, for 30 cycles. Before the first cycle, PCR reaction was incubated at 96°C for 5 min and was cooled to 10°C after the final cycle.

6.9.3 Cloning of *inscΔ3'UTR*, *inscCDS* and *mira3'UTR*

insc and *mira* DNA sequences are available on Flybase (http://flybase.bio.indiana.edu/) and basic sequence analysis was performed using the DNA Strider software. PCR was performed using 25µl 2 x PCR Master Mix in a 50µl reaction. *inscΔ3'UTR* and *inscCDS* fragments were sub-cloned using 14ng of template DNA (full-length *insc* cDNA; (Kraut and Campos-Ortega, 1996), with 100ng of forward and reverse primers (see below). The *mira* 3'UTR was cloned from

2µl genomic DNA, extracted from adult flies (provided by Barbara Jennings), using 250ng of forward and reverse primers (see below).

6.9.4 Primers

inscΔ3'UTR: Forward primer (T3 primer) - AATTAACCCTCACTAAAGGA

Reverse primer (*inscΔ3'*) - CTAGACGAAACTCTCCTGACG

inscCDS: Forward primer (*inscCR)* – ATGTCCTTTCAGCGCAGCTACAG

Reverse primer (*inscΔ3'*) – CTAGACGAAACTCTCCTGACG

mira3'UTR Forward primer (mira5F) – GCAGTTCGCCCAATTGGAGCTG

Reverse primer (mira3R) - TGTTCCGATTCGCTCGAGGAAC

All oligos were provided by the CRUK oligonucleotide synthesis service.

PCR reactions were run on 1% TAE agarose gels and PCR product of correct size was purifed from the gel using the QIAquick gel extraction kit (Qiagen). The TOPO TA cloning kit (Invitrogen) was used for cloning of PCR fragments into the pCR 2.1-TOPO vector, according to manufacturers instructions. Plasmids were then transformed into *DH5α* competent bacteria (see section 6.8.1).

6.9.5 Sequencing

The sequencing reaction was performed in a solution containing 8.0 µl BigDye Terminator Ready Reaction mix (Applied Biosystems), 200ng template DNA, and 100ng primer and made up to a final volume of 20µl. Sequencing was performed on an ABI 3730 DNA Analyzer (Applied Biosystems) by the CRUK equipment park.

6.10 Solutions and buffers

PBS: 8g NaCl, 0.2 g KCl, 1.44 g Na_2HPO_4 and 0.24 g KH_2PO_4 are added to 800 ml distilled H_2O. The pH is adjusted to 7.4 with 1N HCl, and water added to make up to 1 l. The solution is autoclaved.

20x SSC: 175.3 g of NaCl and 88.2 g of Sodium citrate are dissolved in 800 ml water. The pH is adjusted to 7.0 with a few drops of 1N NaOH. The volume is then increased to 1 litre with water, and the solution was autoclaved.

SOB: 20g bacto-tryptone, 5g bacto-yeast extract and 0.5 g NaCl are added to 950 ml $H2O$ and dissolved. 10 ml of a 250mM KCl solution is added, and the pH adjusted to 7.0 with 5 N NaOH. The volume is adjusted to 1 litre with deionised H_2O, and autoclaved. 5 ml of a sterile solution of 2 M $MgCl_2$ is added, before aliquoting.

SOC: After the autoclaving step in SOB production, the solution is cooled, and 20 ml of a sterile solution of 1M glucose added.

LB Medium: To 950 ml of deionised H_2O, 10 g bacto-tryptone, 5 g bacto-yeast extract, and 10 g NaCl are added. The pH is raised to 7.0 with 5 N NaOH, then the volume increased to 1 l with deionised H_2O. 15g/ l of bacto-agar is added to produce LB Agar. The solution is autoclaved.

HYB: for 50 ml, mix 25ml formamide, 12.5ml 20x SSC, 50 μl Tween-20, 11.925 ml RNase-free water (Ambion), 25μl of 1.1g/l heparin, 10μl 10mg/ml E.coli tRNA.

37% fix: 37% formaldehyde / heptane (1:1), shaken for 1 min and allowed to settle for 15 min.

4% fix: Add 5ml 37% formaldehyde to 42.5ml PBS. Make up 1:1 mixture of this and n-heptane, shake for 1 min and allow 15 min to settle.

Ampicillin plates: 400 ml of LB Agar was melted in the microwave, and then cooled to 50°C. 400 μl of a 100 mg/ml ampicillin stock (dissolved in H_2O, stored at -20°C) was added, mixed and poured into petri dishes (Sterilin, 90 mm).

1x TAE gel electrophoresis buffer: 0.04 M Tris-acetate, 1mM Ethylene di-amine tetra-acetate (EDTA) (50x: 242 g Tris base, 57.1 ml glacial acetic acid, 100 ml 0.5M EDTA pH 8.0, water to make volume up to 1 l.)

PBT: 0.1% Tween-20 (Sigma) in 1x PBS.

PBST: 0.1% Triton-X100 (Sigma) in 1x PBS

Lacto-Hoyers medium: Dissolve 30g of gum arabic in 50ml of water overnight with magnetic stirring. Add 200g chloral hydrate in small amounts. When chloral hydrate has dissolved, add 20g of glycerol. Centrifuge for 30 min at 10,000g and filter the supernatant through glass wool. This solution should be made up to a 1:1 mixture with lactic acid.

Appendix A Metaphase spindle length analysis in neuroblasts

wild-type	0.672	0.009	41
egl mutant	0.470	0.022	32
BicD mutant	0.461	0.018	35
$insc^{22}/insc^{22}$	0.398	0.020	35
$insc^{22}/+$	0.456	0.021	40
$insc^{P72}/insc^{P72}$	0.449	0.018	34
$insc^{P72}/+$	0.503	0.013	42
$insc^{+}$ / $insc^{+}$. *CyO ftzLacZ*	0.576	0.011	35
egl mutant, *hs-insc*	0.585	0.011	72
Heat-shocked *egl* mutant embryos	0.490	0.017	16
wild-type, hs-insc	0.573	0.011	36

Heat-shocked *wild-type* embryos	0.577	0.019	27
egl^{3e}/ +	0.574	0.014	28
egl^{WU50}/ +	0.608	0.018	25
Dmn overexpressing neuroblasts	0.492	0.024	52

n is the number of neuroblasts scored. SEM is the standard error of the mean.

CHAPTER 7: REFERENCES

Ainger, K., Avossa, D., Morgan, F., Hill, S. J., Barry, C., Barbarese, E., and Carson, J. H. (1993). Transport and localization of exogenous myelin basic protein mRNA microinjected into oligodendrocytes. J Cell Biol *123*, 431-441.

Akam, M. (1987). The molecular basis for metameric pattern in the Drosophila embryo. Development *101*, 1-22.

Albertson, R., and Doe, C. Q. (2003). Dlg, Scrib and Lgl regulate neuroblast cell size and mitotic spindle asymmetry. Nat Cell Biol *5*, 166-170.

Anderson, K. V., and Nusslein-Volhard, C. (1984). Information for the dorsal--ventral pattern of the Drosophila embryo is stored as maternal mRNA. Nature *311*, 223-227.

Arn, E. A., Cha, B. J., Theurkauf, W. E., and Macdonald, P. M. (2003). Recognition of a bicoid mRNA localization signal by a protein complex containing Swallow, Nod, and RNA binding proteins. Dev Cell *4*, 41-51.

Ashraf, S. I., and Ip, Y. T. (2001). The Snail protein family regulates neuroblast expression of inscuteable and string, genes involved in asymmetry and cell division in Drosophila. Development *128*, 4757-4767.

Babu, K., Cai, Y., Bahri, S., Yang, X., and Chia, W. (2004). Roles of Bifocal, Homer, and F-actin in anchoring Oskar to the posterior cortex of Drosophila oocytes. Genes Dev *18*, 138-143.

Bachmann, A., Schneider, M., Theilenberg, E., Grawe, F., and Knust, E. (2001). Drosophila Stardust is a partner of Crumbs in the control of epithelial cell polarity. Nature *414*, 638-643.

Baker, N. E. (1987). Molecular cloning of sequences of *wingless*, a segment polarity gene in *Drosophila*: the spacial distribution of transcripts in embryos. Embo J *6*, 1765-1773.

Baker, N. E. (1988). Localization of transcripts from the wingless gene in whole Drosophila embryos. Development *103*, 289-298.

Bardin, A. J., Le Borgne, R., and Schweisguth, F. (2004). Asymmetric localization and function of cell-fate determinants: a fly's view. Curr Opin Neurobiol *14*, 6-14.

Barros, C. S., Phelps, C. B., and Brand, A. H. (2003). Drosophila nonmuscle myosin II promotes the asymmetric segregation of cell fate determinants by cortical exclusion rather than active transport. Dev Cell *5*, 829-840.

Bashirullah, A., Cooperstock, R. L., and Lipshitz, H. D. (1998). RNA localization in development. Annu Rev Biochem *67*, 335-394.

Bergsten, S. E., and Gavis, E. R. (1999). Role for mRNA localization in translational activation but not spatial restriction of nanos RNA. Development *126*, 659-669.

Berleth, T., Burri, M., Thoma, G., Bopp, D., Richstein, S., Frigerio, G., Noll, M., and Nusslein-Volhard, C. (1988). The role of localization of bicoid RNA in organizing the anterior pattern of the Drosophila embryo. Embo J *7*, 1749-1756.

Bernad, A., Blanco, L., Lazaro, J. M., Martin, G., and Salas, M. (1989). A conserved 3'----5' exonuclease active site in prokaryotic and eukaryotic DNA polymerases. Cell *59*, 219-228.

Berrueta, L., Kraeft, S.K., Tirnauer, J.S., Schuyler, S.C., Chen, L.B., Hill, D.E., Pellman, D., Bierer, B.E. (1998) The adenomatous polyposis coli-binding protein EB1 is associated with cytoplasmic and spindle microtubules. Proc Natl Acad Sci U S A. *95*, 10596-601

Betschinger, J., Mechtler, K., and Knoblich, J. A. (2003). The Par complex directs asymmetric cell division by phosphorylating the cytoskeletal protein Lgl. Nature *422*, 326-330.

Bilder, D., Li, M., and Perrimon, N. (2000). Cooperative regulation of cell polarity and growth by Drosophila tumor suppressors. Science *289*, 113-116.

Bilder, D., Schober, M., and Perrimon, N. (2003). Integrated activity of PDZ protein complexes regulates epithelial polarity. Nat Cell Biol *5*, 53-58.

Blagden, S. P., and Glover, D. M. (2003). Polar expeditions--provisioning the centrosome for mitosis. Nat Cell Biol *5*, 505-511.

Bobola, N., Jansen, R. P., Shin, T. H., and Nasmyth, K. (1996). Asymmetric accumulation of Ash1p in postanaphase nuclei depends on a myosin and restricts yeast mating-type switching to mother cells. Cell *84*, 699-709.

Bolivar, J., Huynh, J. R., Lopez-Schier, H., Gonzalez, C., St Johnston, D., and Gonzalez-Reyes, A. (2001). Centrosome migration into the Drosophila oocyte is

independent of BicD and egl, and of the organisation of the microtubule cytoskeleton. Development *128*, 1889-1897.

Bossing, T., Udolph, G., Doe, C. Q., and Technau, G. M. (1996). The embryonic central nervous system lineages of Drosophila melanogaster. I. Neuroblast lineages derived from the ventral half of the neuroectoderm. Dev Biol *179*, 41-64.

Brand, A. H., and Perrimon, N. (1993). Targeted gene expression as a means of altering cell fates and generating dominant phenotypes. Development *118*, 401-415.

Brendza, R. P., Serbus, L. R., Duffy, J. B., and Saxton, W. M. (2000). A function for kinesin I in the posterior transport of oskar mRNA and Staufen protein. Science *289*, 2120-2122.

Broadus, J., and Doe, C. Q. (1997). Extrinsic cues, intrinsic cues and microfilaments regulate asymmetric protein localization in Drosophila neuroblasts. Curr Biol *7*, 827-835.

Broadus, J., Fuerstenberg, S., and Doe, C. Q. (1998). Staufen-dependent localization of prospero mRNA contributes to neuroblast daughter-cell fate. Nature *391*, 792-795.

Bulgheresi, S., Kleiner, E., and Knoblich, J. A. (2001). Inscuteable-dependent apical localization of the microtubule-binding protein Cornetto suggests a role in asymmetric cell division. J Cell Sci *114*, 3655-3662.

Bullock, S. L., and Ish-Horowicz, D. (2001). Conserved signals and machinery for RNA transport in Drosophila oogenesis and embryogenesis. Nature *414*, 611-616.

Bullock, S. L., Stauber, M., Prell, A., Hughes, J. R., Ish-Horowicz, D., and Schmidt-Ott, U. (2004). Differential cytoplasmic mRNA localisation adjusts pair-rule transcription factor activity to cytoarchitecture in dipteran evolution. Development.

Bullock, S. L., Zicha, D., and Ish-Horowicz, D. (2003). The Drosophila hairy RNA localization signal modulates the kinetics of cytoplasmic mRNA transport. Embo J *22*, 2484-2494.

Burkhardt, J. K., Echeverri, C. J., Nilsson, T., and Vallee, R. B. (1997). Overexpression of the dynamitin (p50) subunit of the dynactin complex disrupts dynein-dependent maintenance of membrane organelle distribution. J Cell Biol *139*, 469-484.

Cai, Y., Chia, W., and Yang, X. (2001). A family of snail-related zinc finger proteins regulates two distinct and parallel mechanisms that mediate Drosophila neuroblast asymmetric divisions. Embo J *20*, 1704-1714.

Cai, Y., Yu, F., Lin, S., Chia, W., and Yang, X. (2003). Apical complex genes control mitotic spindle geometry and relative size of daughter cells in Drosophila neuroblast and pI asymmetric divisions. Cell *112*, 51-62.

Campos-Ortega, J. A. (1993). Early Neurogenesis in *Drosophila melanogaster*. In The Development of *Drosophila melanogaster*, M. Bate, and J. A. Campos-Ortega, eds. (Cold Spring Harbor, N.Y, Cold Spring Harbor Laboratory), pp. 1091-1130.

Campos-Ortega, J. A. (1997). Asymmetic division: dynastic intricacies of neuroblast division. Curr Biol *7*, R726-728.

Campos-Ortega, J. A., and Hartenstein, V. (1985). The embryonic development of Drosophila melanogaster (Berlin, Springer-Verlag).

Capri, M., Santoni, M. J., Thomas-Delaage, M., and Ait-Ahmed, O. (1997). Implication of a 5' coding sequence in targeting maternal mRNA to the Drosophila oocyte. Mech Dev *68*, 91-100.

Carmena, A., Murugasu-Oei, B., Menon, D., Jimenez, F., and Chia, W. (1998). Inscuteable and numb mediate asymmetric muscle progenitor cell divisions during Drosophila myogenesis. Genes Dev *12*, 304-315.

Carson, J. H., Kwon, S., and Barbarese, E. (1998). RNA trafficking in myelinating cells. Curr Opin Neurobiol *8*, 607-612.

Cha, B. J., Serbus, L. R., Koppetsch, B. S., and Theurkauf, W. E. (2002). Kinesin I-dependent cortical exclusion restricts pole plasm to the oocyte posterior. Nat Cell Biol *4*, 592-598.

Cheung, H. K., Serano, T. L., and Cohen, R. S. (1992). Evidence for a highly selective RNA transport system and its role in establishing the dorsoventral axis of the Drosophila egg. Development *114*, 653-661.

Cooley, L., and Theurkauf, W. E. (1994). Cytoskeletal functions during Drosophila oogenesis. Science *266*, 590-596.

Corral-Debrinski, M., Blugeon, C., and Jacq, C. (2000). In yeast, the 3' untranslated region or the presequence of ATM1 is required for the exclusive localization of its mRNA to the vicinity of mitochondria. Mol Cell Biol *20*, 7881-7892.

Costa, A., and Schedl, P. (2001). Conservation signals location. Nature *414*, 593-595.

Davis, I., and Ish-Horowicz, D. (1991). Apical localization of pair-rule transcripts requires 3' sequences and limits protein diffusion in the Drosophila blastoderm embryo. Cell *67*, 927-940.

Deng, W., and Lin, H. (2001). Asymmetric germ cell division and oocyte determination during Drosophila oogenesis. Int Rev Cytol *203*, 93-138.

Deshler, J. O., Highett, M. I., Abramson, T., and Schnapp, B. J. (1998). A highly conserved RNA-binding protein for cytoplasmic mRNA localization in vertebrates. Curr Biol *8*, 489-496.

Ding, D., Parkhurst, S. M., Halsell, S. R., and Lipshitz, H. D. (1993). Dynamic Hsp83 RNA localization during Drosophila oogenesis and embryogenesis. Mol Cell Biol *13*, 3773-3781.

Doe, C. Q., and Bowerman, B. (2001). Asymmetric cell division: fly neuroblast meets worm zygote. Curr Opin Cell Biol *13*, 68-75.

Doe, C. Q., Chu-LaGraff, Q., Wright, D. M., and Scott, M. P. (1991). The prospero gene specifies cell fates in the Drosophila central nervous system. Cell *65*, 451-464.

Duncan, J. E., and Warrior, R. (2002). The cytoplasmic dynein and kinesin motors have interdependent roles in patterning the Drosophila oocyte. Curr Biol *12*, 1982-1991.

Echeverri, C. J., Paschal, B. M., Vaughan, K. T., and Vallee, R. B. (1996). Molecular characterization of the 50-kD subunit of dynactin reveals function for the complex in chromosome alignment and spindle organization during mitosis. J Cell Biol *132*, 617-633.

Eckley, D. M., Gill, S. R., Melkonian, K. A., Bingham, J. B., Goodson, H. V., Heuser, J. E., and Schroer, T. A. (1999). Analysis of dynactin subcomplexes reveals a novel actin-related protein associated with the arp1 minifilament pointed end. J Cell Biol *147*, 307-320.

Ephrussi, A., Dickinson, L. K., and Lehmann, R. (1991). Oskar organizes the germ plasm and directs localization of the posterior determinant nanos. Cell *66*, 37-50.

Erdelyi, M., Michon, A. M., Guichet, A., Glotzer, J. B., and Ephrussi, A. (1995). Requirement for Drosophila cytoplasmic tropomyosin in oskar mRNA localization. Nature *377*, 524-527.

Ferrandon, D., Elphick, L., Nusslein-Volhard, C., and St Johnston, D. (1994). Staufen protein associates with the 3'UTR of bicoid mRNA to form particles that move in a microtubule-dependent manner. Cell *79*, 1221-1232.

Foe, V. E. (1989). Mitotic domains reveal early commitment of cells in Drosophila embryos. Development *107*, 1-22.

Foe, V. E., Odell, G. M., and Edgar, B. A. (1993). Mitosis and Morphogenesis in the *Drosophila* Embryo, Point and Counterpoint. In The Development of *Drosophila melanogaster*, M. Bate, and A. Martinez Arias, eds. (Cold Spring Harbor, N.Y, Cold Spring Harbor Laboratory), pp. 149-300.

Fontaine, B., and Changeux, J. P. (1989). Localization of nicotinic acetylcholine receptor alpha-subunit transcripts during myogenesis and motor endplate development in the chick. J Cell Biol *108*, 1025-1037.

Forrest, K. M., and Gavis, E. R. (2003). Live imaging of endogenous RNA reveals a diffusion and entrapment mechanism for nanos mRNA localization in Drosophila. Curr Biol *13*, 1159-1168.

Frise, E., Knoblich, J. A., Younger-Shepherd, S., Jan, L. Y., and Jan, Y. N. (1996). The Drosophila Numb protein inhibits signaling of the Notch receptor during cell-cell interaction in sensory organ lineage. Proc Natl Acad Sci U S A *93*, 11925-11932.

Fuerstenberg, S., Peng, C. Y., Alvarez-Ortiz, P., Hor, T., and Doe, C. Q. (1998). Identification of Miranda protein domains regulating asymmetric cortical localization, cargo binding, and cortical release. Mol Cell Neurosci *12*, 325-339.

Fuse, N., Hisata, K., Katzen, A. L., and Matsuzaki, F. (2003). Heterotrimeric G proteins regulate daughter cell size asymmetry in Drosophila neuroblast divisions. Curr Biol *13*, 947-954.

Gautreau, D., Cote, C. A., and Mowry, K. L. (1997). Two copies of a subelement from the Vg1 RNA localization sequence are sufficient to direct vegetal localization in Xenopus oocytes. Development *124*, 5013-5020.

Gavis, E. R., and Lehmann, R. (1992). Localization of nanos RNA controls embryonic polarity. Cell *71*, 301-313.

Giansanti, M. G., Gatti, M., and Bonaccorsi, S. (2001). The role of centrosomes and astral microtubules during asymmetric division of Drosophila neuroblasts. Development *128*, 1137-1145.

Glotzer, J. B., Saffrich, R., Glotzer, M., and Ephrussi, A. (1997). Cytoplasmic flows localize injected oskar RNA in Drosophila oocytes. Curr Biol *7*, 326-337.

Goldstein, L. S. (2001). Molecular motors: from one motor many tails to one motor many tales. Trends Cell Biol *11*, 477-482.

Gonzalez, F., Swales, L., Bejsovec, A., Skaer, H., and Martinez Arias, A. (1991). Secretion and movement of wingless protein in the epidermis of the Drosophila embryo. Mech Dev *35*, 43-54.

Gonzalez, I., Buonomo, S. B., Nasmyth, K., and von Ahsen, U. (1999a). ASH1 mRNA localization in yeast involves multiple secondary structural elements and Ash1 protein translation. Curr Biol *9*, 337-340.

Gonzalez, T. N., Sidrauski, C., Dorfler, S., and Walter, P. (1999b). Mechanism of non-spliceosomal mRNA splicing in the unfolded protein response pathway. Embo J *18*, 3119-3132.

Gonzalez-Reyes, A., Elliott, H., and St Johnston, D. (1995). Polarization of both major body axes in Drosophila by gurken-torpedo signalling. Nature *375*, 654-658.

Groisman, I., Huang, Y. S., Mendez, R., Cao, Q., Theurkauf, W., and Richter, J. D. (2000). CPEB, maskin, and cyclin B1 mRNA at the mitotic apparatus: implications for local translational control of cell division. Cell *103*, 435-447.

Gu, W., Pan, F., Zhang, H., Bassell, G. J., and Singer, R. H. (2002). A predominantly nuclear protein affecting cytoplasmic localization of beta-actin mRNA in fibroblasts and neurons. J Cell Biol *156*, 41-51.

Guo, M., Jan, L. Y., and Jan, Y. N. (1996). Control of daughter cell fates during asymmetric division: interaction of Numb and Notch. Neuron *17*, 27-41.

Guo, S., and Kemphues, K. J. (1996). A non-muscle myosin required for embryonic polarity in Caenorhabditis elegans. Nature *382*, 455-458.

Hafen, E., Kuroiwa, A., and Gehring, W. J. (1984). Spatial distribution of transcripts from the segmentation gene fushi tarazu during Drosophila embryonic development. Cell *37*, 833-841.

Hamm, H. E. (1998). The many faces of G protein signaling. J Biol Chem *273*, 669-672.

Hannan, A. J., Schevzov, G., Gunning, P., Jeffrey, P. L., and Weinberger, R. P. (1995). Intracellular localization of tropomyosin mRNA and protein is associated with development of neuronal polarity. Mol Cell Neurosci *6*, 397-412.

Hegde, J., and Stephenson, E. C. (1993). Distribution of swallow protein in egg chambers and embryos of Drosophila melanogaster. Development *119*, 457-470.

Hesketh, J. E., Campbell, G. P., and Whitelaw, P. F. (1991). c-myc mRNA in cytoskeletal-bound polysomes in fibroblasts. Biochem J *274 (Pt 2)*, 607-609.

Heuer, J.G., Li, K., and Kaufman, T.C. (1995) The Drosophila homeotic target gene centrosomin (cnn) encodes a novel centrosomal protein with leucine zippers and

maps to a genomic region required for midgut morphogenesis. Development *121*, 3861-76.

Hirata, J., Nakagoshi, H., Nabeshima, Y., and Matsuzaki, F. (1995). Asymmetric segregation of the homeodomain protein Prospero during Drosophila development. Nature *377*, 627-630.

Hong, Y., Stronach, B., Perrimon, N., Jan, L. Y., and Jan, Y. N. (2001). Drosophila Stardust interacts with Crumbs to control polarity of epithelia but not neuroblasts. Nature *414*, 634-638.

Hoogenraad, C. C., Akhmanova, A., Howell, S. A., Dortland, B. R., De Zeeuw, C. I., Willemsen, R., Visser, P., Grosveld, F., and Galjart, N. (2001). Mammalian Golgi-associated Bicaudal-D2 functions in the dynein-dynactin pathway by interacting with these complexes. Embo J *20*, 4041-4054.

Hoogenraad, C. C., Wulf, P., Schiefermeier, N., Stepanova, T., Galjart, N., Small, J. V., Grosveld, F., de Zeeuw, C. I., and Akhmanova, A. (2003). Bicaudal D induces selective dynein-mediated microtubule minus end-directed transport. Embo J *22*, 6004-6015.

Hurd, T. W., Gao, L., Roh, M. H., Macara, I. G., and Margolis, B. (2003). Direct interaction of two polarity complexes implicated in epithelial tight junction assembly. Nat Cell Biol *5*, 137-142.

Huynh, J. R., and St Johnston, D. (2000). The role of BicD, Egl, Orb and the microtubules in the restriction of meiosis to the Drosophila oocyte. Development *127*, 2785-2794.

Ikeshima-Kataoka, H., Skeath, J. B., Nabeshima, Y., Doe, C. Q., and Matsuzaki, F. (1997). Miranda directs Prospero to a daughter cell during Drosophila asymmetric divisions. Nature *390*, 625-629.

Ikonen, E., and Simons, K. (1998). Protein and lipid sorting from the trans-Golgi network to the plasma membrane in polarized cells. Semin Cell Dev Biol *9*, 503-509.

Ingham, P. W., Howard, K. R., and Ish-Horowicz, D. (1985). Transcription pattern of the *Drosophila* segmentation gene *hairy*. Nature *318*, 439-445.

Irion, U., Leptin, M., Siller, K., Fuerstenberg, S., Cai, Y., Doe, C. Q., Chia, W., and Yang, X. (2004). Abstrakt, a DEAD box protein, regulates Insc levels and asymmetric division of neural and mesodermal progenitors. Curr Biol *14*, 138-144.

Izumi, Y., Ohta, N., Itoh-Furuya, A., Fuse, N., and Matsuzaki, F. (2004). Differential functions of G protein and Baz-aPKC signaling pathways in Drosophila neuroblast asymmetric division. J Cell Biol *164*, 729-738.

Jan, Y. N., and Jan, L. Y. (2001). Asymmetric cell division in the Drosophila nervous system. Nat Rev Neurosci *2*, 772-779.

Jankovics, F., Sinka, R., Lukacsovich, T., and Erdelyi, M. (2002). MOESIN crosslinks actin and cell membrane in Drosophila oocytes and is required for OSKAR anchoring. Curr Biol *12*, 2060-2065.

Jansen, R. P. (2001). mRNA localization: message on the move. Nat Rev Mol Cell Biol *2*, 247-256.

Januschke, J., Gervais, L., Dass, S., Kaltschmidt, J. A., Lopez-Schier, H., St Johnston, D., Brand, A. H., Roth, S., and Guichet, A. (2002). Polar transport in the Drosophila oocyte requires Dynein and Kinesin I cooperation. Curr Biol *12*, 1971-1981.

Job, C., and Eberwine, J. (2001). Localization and translation of mRNA in dendrites and axons. Nat Rev Neurosci *2*, 889-898.

Johnson, K., and Wodarz, A. (2003). A genetic hierarchy controlling cell polarity. Nat Cell Biol *5*, 12-14.

Johnstone, O., and Lasko, P. (2001). Translational regulation and RNA localization in Drosophila oocytes and embryos. Annu Rev Genet *35*, 365-406.

Kaltschmidt, J. A., Davidson, C. M., Brown, N. H., and Brand, A. H. (2000). Rotation and asymmetry of the mitotic spindle direct asymmetric cell division in the developing central nervous system. Nat Cell Biol *2*, 7-12.

Karki, S., and Holzbaur, E. L. (1999). Cytoplasmic dynein and dynactin in cell division and intracellular transport. Curr Opin Cell Biol *11*, 45-53.

Karlin-Mcginness, M., Serano, T. L., and Cohen, R. S. (1996). Comparative analysis of the kinetics and dynamics of K10, bicoid, and oskar mRNA localization in the Drosophila oocyte. Dev Genet *19*, 238-248.

Kim-Ha, J., Smith, J. L., and Macdonald, P. M. (1991). oskar mRNA is localized to the posterior pole of the Drosophila oocyte. Cell *66*, 23-35.

Kimple, R. J., Willard, F. S., and Siderovski, D. P. (2002). The GoLoco motif: heralding a new tango between G protein signaling and cell division. Mol Interv *2*, 88-100.

King, R. C. (1970). Ovarian development in Drosophila melanogaster (New York ; London, Academic Press).

King, S. M. (2000). The dynein microtubule motor. Biochim Biophys Acta *1496*, 60-75.

Kislauskis, E. H., Zhu, X., and Singer, R. H. (1997). beta-Actin messenger RNA localization and protein synthesis augment cell motility. J Cell Biol *136*, 1263-1270.

Knaut, H., Pelegri, F., Bohmann, K., Schwarz, H., and Nusslein-Volhard, C. (2000). Zebrafish vasa RNA but not its protein is a component of the germ plasm and segregates asymmetrically before germline specification. J Cell Biol *149*, 875-888.

Knirr, S., Breuer, S., Paululat, A., and Renkawitz-Pohl, R. (1997). Somatic mesoderm differentiation and the development of a subset of pericardial cells depend on the not enough muscles (nem) locus, which contains the inscuteable gene and the intron located gene, skittles. Mech Dev *67*, 69-81.

Knoblich, J. A. (2001). Asymmetric cell division during animal development. Nat Rev Mol Cell Biol *2*, 11-20.

Knoblich, J. A., Jan, L. Y., and Jan, Y. N. (1995). Asymmetric segregation of Numb and Prospero during cell division. Nature *377*, 624-627.

Knoblich, J. A., Jan, L. Y., and Jan, Y. N. (1997). The N terminus of the Drosophila Numb protein directs membrane association and actin-dependent asymmetric localization. Proc Natl Acad Sci U S A *94*, 13005-13010.

Knoblich, J. A., Jan, L. Y., and Jan, Y. N. (1999). Deletion analysis of the Drosophila Inscuteable protein reveals domains for cortical localization and asymmetric localization. Curr Biol *9*, 155-158.

Kohrmann, M., Luo, M., Kaether, C., DesGroseillers, L., Dotti, C. G., and Kiebler, M. A. (1999). Microtubule-dependent recruitment of Staufen-green fluorescent protein into large RNA-containing granules and subsequent dendritic transport in living hippocampal neurons. Mol Biol Cell *10*, 2945-2953.

Kraut, R., and Campos-Ortega, J. A. (1996). inscuteable, a neural precursor gene of Drosophila, encodes a candidate for a cytoskeleton adaptor protein. Dev Biol *174*, 65-81.

Kraut, R., Chia, W., Jan, L. Y., Jan, Y. N., and Knoblich, J. A. (1996). Role of inscuteable in orienting asymmetric cell divisions in Drosophila. Nature *383*, 50-55.

Kuchinke, U., Grawe, F., and Knust, E. (1998). Control of spindle orientation in Drosophila by the Par-3-related PDZ-domain protein Bazooka. Curr Biol *8*, 1357-1365.

Lall, S., Francis-Lang, H., Flament, A., Norvell, A., Schupbach, T., and Ish-Horowicz, D. (1999). Squid hnRNP protein promotes apical cytoplasmic transport and localization of Drosophila pair-rule transcripts. Cell *98*, 171-180.

Lambert, J. D., and Nagy, L. M. (2002). Asymmetric inheritance of centrosomally localized mRNAs during embryonic cleavages. Nature *420*, 682-686.

LaMonte, B. H., Wallace, K. E., Holloway, B. A., Shelly, S. S., Ascano, J., Tokito, M., Van Winkle, T., Howland, D. S., and Holzbaur, E. L. (2002). Disruption of dynein/dynactin inhibits axonal transport in motor neurons causing late-onset progressive degeneration. Neuron *34*, 715-727.

Lantz, V., Ambrosio, L., and Schedl, P. (1992). The Drosophila orb gene is predicted to encode sex-specific germline RNA-binding proteins and has localized transcripts in ovaries and early embryos. Development *115*, 75-88.

Lantz, V., Chang, J. S., Horabin, J. I., Bopp, D., and Schedl, P. (1994). The Drosophila orb RNA-binding protein is required for the formation of the egg chamber and establishment of polarity. Genes Dev *8*, 598-613.

Lasko, P. (1999). RNA sorting in Drosophila oocytes and embryos. Faseb J *13*, 421-433.

Latham, V. M., Yu, E. H., Tullio, A. N., Adelstein, R. S., and Singer, R. H. (2001). A Rho-dependent signaling pathway operating through myosin localizes beta-actin mRNA in fibroblasts. Curr Biol *11*, 1010-1016.

Lawrence, J. B., and Singer, R. H. (1986). Intracellular localization of messenger RNAs for cytoskeletal proteins. Cell *45*, 407-415.

Lecuit, T., and Wieschaus, E. (2000). Polarized insertion of new membrane from a cytoplasmic reservoir during cleavage of the Drosophila embryo. J Cell Biol *150*, 849-860.

Levadoux, M., Mahon, C., Beattie, J. H., Wallace, H. M., and Hesketh, J. E. (1999). Nuclear import of metallothionein requires its mRNA to be associated with the perinuclear cytoskeleton. J Biol Chem *274*, 34961-34966.

Li, P., Yang, X., Wasser, M., Cai, Y., and Chia, W. (1997). Inscuteable and Staufen mediate asymmetric localization and segregation of prospero RNA during Drosophila neuroblast cell divisions. Cell *90*, 437-447.

Lipshitz, H. D., and Smibert, C. A. (2000). Mechanisms of RNA localization and translational regulation. Curr Opin Genet Dev *10*, 476-488.

Litman, P., Barg, J., Rindzoonski, L., and Ginzburg, I. (1993). Subcellular localization of tau mRNA in differentiating neuronal cell culture: implications for neuronal polarity. Neuron *10*, 627-638.

Long, R. M., Gu, W., Meng, X., Gonsalvez, G., Singer, R. H., and Chartrand, P. (2001). An exclusively nuclear RNA-binding protein affects asymmetric localization of ASH1 mRNA and Ash1p in yeast. J Cell Biol *153*, 307-318.

Long, R. M., Singer, R. H., Meng, X., Gonzalez, I., Nasmyth, K., and Jansen, R. P. (1997). Mating type switching in yeast controlled by asymmetric localization of ASH1 mRNA. Science *277*, 383-387.

Lopez de Heredia, M., and Jansen, R. P. (2004). mRNA localization and the cytoskeleton. Curr Opin Cell Biol *16*, 80-85.

Lu, B., Ackerman, L., Jan, L. Y., and Jan, Y. N. (1999). Modes of protein movement that lead to the asymmetric localization of partner of Numb during Drosophila neuroblast division. Mol Cell *4*, 883-891.

Lu, B., Roegiers, F., Jan, L. Y., and Jan, Y. N. (2001). Adherens junctions inhibit asymmetric division in the Drosophila epithelium. Nature *409*, 522-525.

Lyczak, R., Gomes, J. E., and Bowerman, B. (2002). Heads or tails: cell polarity and axis formation in the early Caenorhabditis elegans embryo. Dev Cell *3*, 157-166.

MacDonald, P. M. (1990). bicoid mRNA localization signal: phylogenetic conservation of function and RNA secondary structure. Development *110*, 161-171.

Macdonald, P. M., Ingham, P., and Struhl, G. (1986). Isolation, structure, and expression of even-skipped: a second pair-rule gene of Drosophila containing a homeo box. Cell *47*, 721-734.

Macdonald, P. M., and Kerr, K. (1998). Mutational analysis of an RNA recognition element that mediates localization of bicoid mRNA. Mol Cell Biol *18*, 3788-3795.

Macdonald, P. M., and Struhl, G. (1988). cis-acting sequences responsible for anterior localization of bicoid mRNA in Drosophila embryos. Nature *336*, 595-598.

Mach, J. M., and Lehmann, R. (1997). An Egalitarian-BicaudalD complex is essential for oocyte specification and axis determination in Drosophila. Genes Dev *11*, 423-435.

Mahone, M., Saffman, E. E., and Lasko, P. F. (1995). Localized Bicaudal-C RNA encodes a protein containing a KH domain, the RNA binding motif of FMR1. Embo J *14*, 2043-2055.

Mallardo, M., Deitinghoff, A., Muller, J., Goetze, B., Macchi, P., Peters, C., and Kiebler, M. A. (2003). Isolation and characterization of Staufen-containing

ribonucleoprotein particles from rat brain. Proc Natl Acad Sci U S A *100*, 2100-2105.

Matsuzaki, F., Ohshiro, T., Ikeshima-Kataoka, H., and Izumi, H. (1998). miranda localizes staufen and prospero asymmetrically in mitotic neuroblasts and epithelial cells in early Drosophila embryogenesis. Development *125*, 4089-4098.

Mazumdar, A., and Mazumdar, M. (2002). How one becomes many: blastoderm cellularization in Drosophila melanogaster. Bioessays *24*, 1012-1022.

McCartney, B. M., McEwen, D. G., Grevengoed, E., Maddox, P., Bejsovec, A., and Peifer, M. (2001). Drosophila APC2 and Armadillo participate in tethering mitotic spindles to cortical actin. Nat Cell Biol *3*, 933-938.

McGrail, M., and Hays, T. S. (1997). The microtubule motor cytoplasmic dynein is required for spindle orientation during germline cell divisions and oocyte differentiation in Drosophila. Development *124*, 2409-2419.

Megraw, T. L., Kao, L. R., and Kaufman, T. C. (2001). Zygotic development without functional mitotic centrosomes. Curr Biol *11*, 116-120.

Merdes, A., Ramyar, K., Vechio, J. D., and Cleveland, D. W. (1996). A complex of NuMA and cytoplasmic dynein is essential for mitotic spindle assembly. Cell *87*, 447-458.

Mohler, J., and Wieschaus, E. F. (1986). Dominant maternal-effect mutations of Drosophila melanogaster causing the production of double-abdomen embryos. Genetics *112*, 803-822.

Moritz, M., and Agard, D. A. (2001). Gamma-tubulin complexes and microtubule nucleation. Curr Opin Struct Biol *11*, 174-181.

Moritz, M., Braunfeld, M. B., Guenebaut, V., Heuser, J., and Agard, D. A. (2000). Structure of the gamma-tubulin ring complex: a template for microtubule nucleation. Nat Cell Biol *2*, 365-370.

Moritz, M., Braunfeld, M. B., Sedat, J. W., Alberts, B., and Agard, D. A. (1995). Microtubule nucleation by gamma-tubulin-containing rings in the centrosome. Nature *378*, 638-640.

Morris, E. J., and Fulton, A. B. (1994). Rearrangement of mRNAs for costamere proteins during costamere development in cultured skeletal muscle from chicken. J Cell Sci *107 (Pt 3)*, 377-386.

Moser, M. J., Holley, W. R., Chatterjee, A., and Mian, I. S. (1997). The proofreading domain of Escherichia coli DNA polymerase I and other DNA and/or RNA exonuclease domains. Nucleic Acids Res *25*, 5110-5118.

Muller, H. A., and Wieschaus, E. (1996). armadillo, bazooka, and stardust are critical for early stages in formation of the zonula adherens and maintenance of the polarized blastoderm epithelium in Drosophila. J Cell Biol *134*, 149-163.

Nakamura, M., Zhou, X.Z., and Lu, K.P. (2001) Critical role for the EB1 and APC interaction in the regulation of microtubule polymerization. Curr Biol *11*, 1062-7.

Navarro, C., Puthalakath, H., Adams, J. M., Strasser, A., and Lehmann, R. (2004). Egalitarian binds dynein light chain to establish oocyte polarity and maintain oocyte fate. Nat Cell Biol *6*, 427-435.

Neuman-Silberberg, F. S., and Schupbach, T. (1993). The Drosophila dorsoventral patterning gene gurken produces a dorsally localized RNA and encodes a TGF alpha-like protein. Cell *75*, 165-174.

Nishimura, T., Kato, K., Yamaguchi, T., Fukata, Y., Ohno, S., and Kaibuchi, K. (2004). Role of the PAR-3-KIF3 complex in the establishment of neuronal polarity. Nat Cell Biol *6*, 328-334.

Norvell, A., Kelley, R. L., Wehr, K., and Schupbach, T. (1999). Specific isoforms of squid, a Drosophila hnRNP, perform distinct roles in Gurken localization during oogenesis. Genes Dev *13*, 864-876.

Nusslein-Volhard, C., and Wieschaus, E. (1980). Mutations affecting segment number and polarity in Drosophila. Nature *287*, 795-801.

Oh, J., Baksa, K., and Steward, R. (2000). Functional domains of the Drosophila bicaudal-D protein. Genetics *154*, 713-724.

Oh, J., and Steward, R. (2001). Bicaudal-D is essential for egg chamber formation and cytoskeletal organization in drosophila oogenesis. Dev Biol *232*, 91-104.

Ohshiro, T., Yagami, T., Zhang, C., and Matsuzaki, F. (2000). Role of cortical tumour-suppressor proteins in asymmetric division of Drosophila neuroblast. Nature *408*, 593-596.

Oleynikov, Y., and Singer, R. H. (2003). Real-time visualization of ZBP1 association with beta-actin mRNA during transcription and localization. Curr Biol *13*, 199-207.

Pankratz, M. J., and Jackle, H. (1993). Blastoderm Segmentation. In The Development of Drosophila melanogaster, M. Bate, and A. Martinez Arias, eds. (Cold Spring Harbor, N.Y, Cold Spring Harbor Laboratory), pp. 467-516.

Pankratz, M. J., Seifert, E., Gerwin, N., Billi, B., Nauber, U., and Jackle, H. (1990). Gradients of Kruppel and knirps gene products direct pair-rule gene stripe patterning in the posterior region of the Drosophila embryo. Cell *61*, 309-317.

Parmentier, M. L., Woods, D., Greig, S., Phan, P. G., Radovic, A., Bryant, P., and O'Kane, C. J. (2000). Rapsynoid/partner of inscuteable controls asymmetric division of larval neuroblasts in Drosophila. J Neurosci *20*, RC84.

Pearson, B. J., and Doe, C. Q. (2003). Regulation of neuroblast competence in Drosophila. Nature *425*, 624-628.

Peng, C. Y., Manning, L., Albertson, R., and Doe, C. Q. (2000). The tumour-suppressor genes lgl and dlg regulate basal protein targeting in Drosophila neuroblasts. Nature *408*, 596-600.

Petritsch, C., Tavosanis, G., Turck, C. W., Jan, L. Y., and Jan, Y. N. (2003). The Drosophila myosin VI Jaguar is required for basal protein targeting and correct spindle orientation in mitotic neuroblasts. Dev Cell *4*, 273-281.

Petronczki, M., and Knoblich, J. A. (2001). DmPAR-6 directs epithelial polarity and asymmetric cell division of neuroblasts in Drosophila. Nat Cell Biol *3*, 43-49.

Prakash, N., Fehr, S., Mohr, E., and Richter, D. (1997). Dendritic localization of rat vasopressin mRNA: ultrastructural analysis and mapping of targeting elements. Eur J Neurosci *9*, 523-532.

Ran, B., Bopp, R., and Suter, B. (1994). Null alleles reveal novel requirements for Bic-D during Drosophila oogenesis and zygotic development. Development *120*, 1233-1242.

Rebagliati, M. R., Weeks, D. L., Harvey, R. P., and Melton, D. A. (1985). Identification and cloning of localized maternal RNAs from Xenopus eggs. Cell *42*, 769-777.

Rolls, M. M., Albertson, R., Shih, H. P., Lee, C. Y., and Doe, C. Q. (2003). Drosophila aPKC regulates cell polarity and cell proliferation in neuroblasts and epithelia. J Cell Biol *163*, 1089-1098.

Rongo, C., Gavis, E. R., and Lehmann, R. (1995). Localization of oskar RNA regulates oskar translation and requires Oskar protein. Development *121*, 2737-2746.

Ross, A. F., Oleynikov, Y., Kislauskis, E. H., Taneja, K. L., and Singer, R. H. (1997). Characterization of a beta-actin mRNA zipcode-binding protein. Mol Cell Biol *17*, 2158-2165.

Roth, S., Neuman-Silberberg, F. S., Barcelo, G., and Schupbach, T. (1995). cornichon and the EGF receptor signaling process are necessary for both anterior-posterior and dorsal-ventral pattern formation in Drosophila. Cell *81*, 967-978.

Roychowdhury, S., Panda, D., Wilson, L., and Rasenick, M. M. (1999). G protein alpha subunits activate tubulin GTPase and modulate microtubule polymerization dynamics. J Biol Chem *274*, 13485-13490.

Saiki, R. K., Gelfand, D. H., Stoffel, S., Scharf, S. J., Higuchi, R., Horn, G. T., Mullis, K. B., and Erlich, H. A. (1988). Primer-directed enzymatic amplification of DNA with a thermostable DNA polymerase. Science *239*, 487-491.

Salles, F. J., Lieberfarb, M. E., Wreden, C., Gergen, J. P., and Strickland, S. (1994). Coordinate initiation of Drosophila development by regulated polyadenylation of maternal messenger RNAs. Science *266*, 1996-1999.

Schaefer, M., Petronczki, M., Dorner, D., Forte, M., and Knoblich, J. A. (2001). Heterotrimeric G proteins direct two modes of asymmetric cell division in the Drosophila nervous system. Cell *107*, 183-194.

Schaefer, M., Shevchenko, A., and Knoblich, J. A. (2000). A protein complex containing Inscuteable and the Galpha-binding protein Pins orients asymmetric cell divisions in Drosophila. Curr Biol *10*, 353-362.

Schmidt, H., Rickert, C., Bossing, T., Vef, O., Urban, J., and Technau, G. M. (1997). The embryonic central nervous system lineages of Drosophila melanogaster. II. Neuroblast lineages derived from the dorsal part of the neuroectoderm. Dev Biol *189*, 186-204.

Schneider, S. Q., and Bowerman, B. (2003). Cell polarity and the cytoskeleton in the Caenorhabditis elegans zygote. Annu Rev Genet *37*, 221-249.

Schnorrer, F., Bohmann, K., and Nusslein-Volhard, C. (2000). The molecular motor dynein is involved in targeting swallow and bicoid RNA to the anterior pole of Drosophila oocytes. Nat Cell Biol *2*, 185-190.

Schnorrer, F., Luschnig, S., Koch, I., and Nusslein-Volhard, C. (2002). Gamma-tubulin37C and gamma-tubulin ring complex protein 75 are essential for bicoid RNA localization during drosophila oogenesis. Dev Cell *3*, 685-696.

Schober, M., Schaefer, M., and Knoblich, J. A. (1999). Bazooka recruits Inscuteable to orient asymmetric cell divisions in Drosophila neuroblasts. Nature *402*, 548-551.

Schuldt, A. J., Adams, J. H., Davidson, C. M., Micklem, D. R., Haseloff, J., St Johnston, D., and Brand, A. H. (1998). Miranda mediates asymmetric protein and RNA localization in the developing nervous system. Genes Dev *12*, 1847-1857.

Schupbach, T., and Wieschaus, E. (1986). Germline autonomy of maternal-effect mutations altering the embryonic body pattern of Drosophila. Dev Biol *113*, 443-448.

Schupbach, T., and Wieschaus, E. (1989). Female sterile mutations on the second chromosome of Drosophila melanogaster. I. Maternal effect mutations. Genetics *121*, 101-117.

Serano, T. L., Cheung, H. K., Frank, L. H., and Cohen, R. S. (1994). P element transformation vectors for studying Drosophila melanogaster oogenesis and early embryogenesis. Gene *138*, 181-186.

Serano, T. L., and Cohen, R. S. (1995). A small predicted stem-loop structure mediates oocyte localization of Drosophila K10 mRNA. Development *121*, 3809-3818.

Shen, C. P., Jan, L. Y., and Jan, Y. N. (1997). Miranda is required for the asymmetric localization of Prospero during mitosis in Drosophila. Cell *90*, 449-458.

Shen, C. P., Knoblich, J. A., Chan, Y. M., Jiang, M. M., Jan, L. Y., and Jan, Y. N. (1998). Miranda as a multidomain adapter linking apically localized Inscuteable and basally localized Staufen and Prospero during asymmetric cell division in Drosophila. Genes Dev *12*, 1837-1846.

Shepard, K. A., Gerber, A. P., Jambhekar, A., Takizawa, P. A., Brown, P. O., Herschlag, D., DeRisi, J. L., and Vale, R. D. (2003). Widespread cytoplasmic mRNA transport in yeast: identification of 22 bud-localized transcripts using DNA microarray analysis. Proc Natl Acad Sci U S A *100*, 11429-11434.

Shestakova, E. A., Singer, R. H., and Condeelis, J. (2001). The physiological significance of beta -actin mRNA localization in determining cell polarity and directional motility. Proc Natl Acad Sci U S A *98*, 7045-7050.

Siderovski, D. P., Diverse-Pierluissi, M., and De Vries, L. (1999). The GoLoco motif: a Galphai/o binding motif and potential guanine-nucleotide exchange factor. Trends Biochem Sci *24*, 340-341.

Sil, A., and Herskowitz, I. (1996). Identification of asymmetrically localized determinant, Ash1p, required for lineage-specific transcription of the yeast HO gene. Cell *84*, 711-722.

Simmonds, A. J., dosSantos, G., Livne-Bar, I., and Krause, H. M. (2001). Apical localization of wingless transcripts is required for wingless signaling. Cell *105*, 197-207.

Simons, K., and Ikonen, E. (1997). Functional rafts in cell membranes. Nature *387*, 569-572.

Skeath, J. B. (1999). At the nexus between pattern formation and cell-type specification: the generation of individual neuroblast fates in the Drosophila embryonic central nervous system. Bioessays *21*, 922-931.

Smith, D. S., Niethammer, M., Ayala, R., Zhou, Y., Gambello, M. J., Wynshaw-Boris, A., and Tsai, L. H. (2000). Regulation of cytoplasmic dynein behaviour and microtubule organization by mammalian Lis1. Nat Cell Biol *2*, 767-775.

Sotillos, S., Diaz-Meco, M. T., Caminero, E., Moscat, J., and Campuzano, S. (2004). DaPKC-dependent phosphorylation of Crumbs is required for epithelial cell polarity in Drosophila. J Cell Biol *166*, 549-557.

Spana, E. P., and Doe, C. Q. (1995). The prospero transcription factor is asymmetrically localized to the cell cortex during neuroblast mitosis in Drosophila. Development *121*, 3187-3195.

Spradling, A. C. (1993). Developmental Genetics of Oogenesis. In The Development of *Drosophila melanogaster*, M. Bate, and A. Martinez Arias, eds. (Cold Spring Harbor, N.Y, Cold Spring Harbor Laboratory), pp. 1-70.

St Johnston, D., Beuchle, D., and Nusslein-Volhard, C. (1991). Staufen, a gene required to localize maternal RNAs in the Drosophila egg. Cell *66*, 51-63.

St Johnston, D., Brown, N. H., Gall, J. G., and Jantsch, M. (1992). A conserved double-stranded RNA-binding domain. Proc Natl Acad Sci U S A *89*, 10979-10983.

St Johnston, D., Driever, W., Berleth, T., Richstein, S., and Nusslein-Volhard, C. (1989). Multiple steps in the localization of bicoid RNA to the anterior pole of the Drosophila oocyte. Development *107 Suppl*, 13-19.

St Johnston, D., and Nusslein-Volhard, C. (1992). The origin of pattern and polarity in the Drosophila embryo. Cell *68*, 201-219.

Stephenson, E. C., Chao, Y. C., and Fackenthal, J. D. (1988). Molecular analysis of the swallow gene of Drosophila melanogaster. Genes Dev *2*, 1655-1665.

Strand, D., Unger, S., Corvi, R., Hartenstein, K., Schenkel, H., Kalmes, A., Merdes, G., Neumann, B., Krieg-Schneider, F., Coy, J. F., and et al. (1995). A human homologue of the Drosophila tumour suppressor gene l(2)gl maps to 17p11.2-12 and codes for a cytoskeletal protein that associates with nonmuscle myosin II heavy chain. Oncogene *11*, 291-301.

Subramanian, A., Prokop, A., Yamamoto, M., Sugimura, K., Uemura, T., Betschinger, J., Knoblich, J.A., Volk, T. (2003). Shortstop recruits EB1/APC1 and promotes microtubule assembly at the muscle-tendon junction. Curr Biol. 13, 1086-95.

Sullivan, W., and Theurkauf, W. E. (1995). The cytoskeleton and morphogenesis of the early Drosophila embryo. Curr Opin Cell Biol *7*, 18-22.

Sulston, J. E., Schierenberg, E., White, J. G., and Thomson, J. N. (1983). The embryonic cell lineage of the nematode Caenorhabditis elegans. Dev Biol *100*, 64-119.

Sundell, C. L., and Singer, R. H. (1991). Requirement of microfilaments in sorting of actin messenger RNA. Science *253*, 1275-1277.

Suter, B., Romberg, L. M., and Steward, R. (1989). Bicaudal-D, a Drosophila gene involved in developmental asymmetry: localized transcript accumulation in ovaries

and sequence similarity to myosin heavy chain tail domains. Genes Dev *3*, 1957-1968.

Suter, B., and Steward, R. (1991). Requirement for phosphorylation and localization of the Bicaudal-D protein in Drosophila oocyte differentiation. Cell *67*, 917-926.

Tai, C. Y., Dujardin, D. L., Faulkner, N. E., and Vallee, R. B. (2002). Role of dynein, dynactin, and CLIP-170 interactions in LIS1 kinetochore function. J Cell Biol *156*, 959-968.

Takizawa, P. A., Sil, A., Swedlow, J. R., Herskowitz, I., and Vale, R. D. (1997). Actin-dependent localization of an RNA encoding a cell-fate determinant in yeast. Nature *389*, 90-93.

Tanentzapf, G., and Tepass, U. (2003). Interactions between the crumbs, lethal giant larvae and bazooka pathways in epithelial polarization. Nat Cell Biol *5*, 46-52.

Tekotte, H., and Davis, I. (2002). Intracellular mRNA localization: motors move messages. Trends Genet *18*, 636-642.

Tepass, U., Tanentzapf, G., Ward, R., and Fehon, R. (2001). Epithelial cell polarity and cell junctions in Drosophila. Annu Rev Genet *35*, 747-784.

Tepass, U., Theres, C., and Knust, E. (1990). crumbs encodes an EGF-like protein expressed on apical membranes of Drosophila epithelial cells and required for organization of epithelia. Cell *61*, 787-799.

Theurkauf, W. E. (1994). Microtubules and cytoplasm organization during Drosophila oogenesis. Dev Biol *165*, 352-360.

Theurkauf, W. E., Alberts, B. M., Jan, Y. N., and Jongens, T. A. (1993). A central role for microtubules in the differentiation of Drosophila oocytes. Development *118*, 1169-1180.

Thio, G. L., Ray, R. P., Barcelo, G., and Schupbach, T. (2000). Localization of gurken RNA in Drosophila oogenesis requires elements in the 5' and 3' regions of the transcript. Dev Biol *221*, 435-446.

Tio, M., Udolph, G., Yang, X., and Chia, W. (2001). cdc2 links the Drosophila cell cycle and asymmetric division machineries. Nature *409*, 1063-1067.

Tio, M., Zavortink, M., Yang, X., and Chia, W. (1999). A functional analysis of inscuteable and its roles during Drosophila asymmetric cell divisions. J Cell Sci *112 (Pt 10)*, 1541-1551.

Vaessin, H., Grell, E., Wolff, E., Bier, E., Jan, L. Y., and Jan, Y. N. (1991). prospero is expressed in neuronal precursors and encodes a nuclear protein that is involved in the control of axonal outgrowth in Drosophila. Cell *67*, 941-953.

Virtanen, I., and Wartiovaara, J. (1976). Lectin receptor sites on rat liver cell nuclear membranes. J Cell Sci *22*, 335-344.

Wang, C., and Lehmann, R. (1991). Nanos is the localized posterior determinant in Drosophila. Cell *66*, 637-647.

Wang, N., Yan, K., and Rasenick, M. M. (1990). Tubulin binds specifically to the signal-transducing proteins, Gs alpha and Gi alpha 1. J Biol Chem *265*, 1239-1242.

Wharton, R. P., and Struhl, G. (1989). Structure of the Drosophila BicaudalD protein and its role in localizing the the posterior determinant nanos. Cell *59*, 881-892.

Wiese, C., and Zheng, Y. (2000). A new function for the gamma-tubulin ring complex as a microtubule minus-end cap. Nat Cell Biol *2*, 358-364.

Wilkie, G. S., and Davis, I. (2001). Drosophila wingless and pair-rule transcripts localize apically by dynein-mediated transport of RNA particles. Cell *105*, 209-219.

Wittmann, T., Hyman, A., and Desai, A. (2001). The spindle: a dynamic assembly of microtubules and motors. Nat Cell Biol *3*, E28-34.

Wodarz, A. (2002). Establishing cell polarity in development. Nat Cell Biol *4*, E39-44.

Wodarz, A., and Huttner, W. B. (2003). Asymmetric cell division during neurogenesis in Drosophila and vertebrates. Mech Dev *120*, 1297-1309.

Wodarz, A., and Nusse, R. (1998). Mechanisms of Wnt signaling in development. Annu Rev Cell Dev Biol *14*, 59-88.

Wodarz, A., Ramrath, A., Grimm, A., and Knust, E. (2000). Drosophila atypical protein kinase C associates with Bazooka and controls polarity of epithelia and neuroblasts. J Cell Biol *150*, 1361-1374.

Wodarz, A., Ramrath, A., Kuchinke, U., and Knust, E. (1999). Bazooka provides an apical cue for Inscuteable localization in Drosophila neuroblasts. Nature *402*, 544-547.

Yeaman, C., Grindstaff, K. K., Hansen, M. D., and Nelson, W. J. (1999). Cell polarity: Versatile scaffolds keep things in place. Curr Biol *9*, R515-517.

Yisraeli, J. K., Sokol, S., and Melton, D. A. (1990). A two-step model for the localization of maternal mRNA in Xenopus oocytes: involvement of microtubules and microfilaments in the translocation and anchoring of Vg1 mRNA. Development *108*, 289-298.

Yoon, C., Kawakami, K., and Hopkins, N. (1997). Zebrafish vasa homologue RNA is localized to the cleavage planes of 2- and 4-cell-stage embryos and is expressed in the primordial germ cells. Development *124*, 3157-3165.

Yu, F., Cai, Y., Kaushik, R., Yang, X., and Chia, W. (2003). Distinct roles of Galphai and Gbeta13F subunits of the heterotrimeric G protein complex in the mediation of Drosophila neuroblast asymmetric divisions. J Cell Biol *162*, 623-633.

Yu, F., Morin, X., Cai, Y., Yang, X., and Chia, W. (2000). Analysis of partner of inscuteable, a novel player of Drosophila asymmetric divisions, reveals two distinct steps in inscuteable apical localization. Cell *100*, 399-409.